ผลของทรายและพอตเทอรีสโตนต่อสมบัติทางกายภาพของเนื้อดินเทอราคอตตา

นายประพันธ์ อังอติชาติ

วิทยานิพนธ์นี้เป็นส่วนหนึ่งของการศึกษาตามหลักสูตรปริญญาวิทยาศาสตรดุษฎีบัณฑิต
สาขาวิชาวัสดุศาสตร์ ภาควิชาวัสดุศาสตร์
คณะวิทยาศาสตร์ จุฬาลงกรณ์มหาวิทยาลัย
ปีการศึกษา 2550

EFFECTS OF SAND AND POTTERY STONE ON PHYSICAL PROPERTIES OF TERRA COTTA BODY

Mr. Prapun Aungatichart

A Dissertation Submitted in Partial Fulfillment of the Requirements

for the Degree of Doctor of Science Program in Materials Science

Department of Materials Science

Faculty of Science

Chulalongkorn University

Academic year 2007

Thesis Title	EFFECTS OF SAND AND POTTERY STONE ON PHYSICAL PROPERTIES OF TERRA COTTA BODY
By	Mr. Prapun Aungatichart
Field of Study	Materials Science
Thesis Advisor	Professor Shigetaka Wada, Ph.D.
Thesis Co-advisor	Assistant Professor Sirithan Jiemsirilers, Ph.D.

Accepted by the Faculty of Science, Chulalongkorn University in Partial Fulfillment of the Requirements for the Doctoral Degree

…….. Dean of the Faculty of Science
(Professor Supot Hannongbua, Ph.D.)

THESIS COMMITTEE

…….. Chairman
(Associate Professor Saowaroj Chuayjuljit)

…….. Thesis Advisor
(Professor Shigetaka Wada, Ph.D.)

…….. Thesis Co-advisor
(Assistant Professor Sirithan Jiemsirilers, Ph.D.)

…….. External Member
(Pavadee Aungkavattana, Ph.D.)

…….. Member
(Associate Professor Supatra Jinawath, Ph.D.)

…….. Member
(Associate Professor Danai Arayaphong)

…….. Member
(Thanakorn Wasanapiarnpong, Ph.D.)

ประพันธ์ อังอติชาติ : ผลของทรายและพอตเทอรีสโตนต่อสมบัติทางกายภาพของเนื้อดินเทอราคอตตา. (EFFECTS OF SAND AND POTTERY STONE ON PHYSICAL PROPERTIES OF TERRA COTTA BODY) อ. ที่ปรึกษา : ศ.ดร.ชิเกทากะ วาดะ, อ.ที่ปรึกษาร่วม : ผศ.ดร.ศิริธันว์ เจียมศิริเลิศ, 153 หน้า.

งานวิจัยนี้ได้ศึกษาผลของการเติมพอตเทอรีสโตนร่วมกับทรายและเศษดินเผาต่อสมบัติทางกายภาพของเนื้อดินเทอราคอตตา ปริมาณรวมของทราย พอตเทอรีสโตน และเศษดินเผาที่เติมลงในเนื้อดินสูตรต่างๆ คือ 20 30 และ 40 เปอร์เซ็นต์โดยน้ำหนัก จากนั้นทำการทดสอบสมบัติก่อนเผาและหลังเผา (900 – 1100 องศาเซลเซียส) ของเนื้อดินได้แก่ ความเหนียว ความไวต่อการแตกเนื่องจากการแห้งตัว การหดตัวก่อนเผา ความแข็งแรงก่อนเผา การหดตัวหลังเผา ความหนาแน่น การดูดซึมน้ำ ความแข็งแรงหลังเผา สัมประสิทธิ์การขยายตัวหลังเผา และองค์ประกอบของเฟส

จากการตรวจสอบและวิเคราะห์ตัวอย่าง พบว่าพอตเทอรีสโตนและทราย ช่วยปรับปรุงสมบัติทางกายภาพของเนื้อดินก่อนเผา โดยลดความเหนียวของเนื้อดิน ลดความไวต่อการแตกเนื่องจากการแห้งตัว ลดการหดตัวก่อนเผา ลดปริมาณน้ำที่ใช้ในการขึ้นรูป เนื้อดินที่เหมาะสมสำหรับใช้ในการผลิตประกอบด้วยอัตราส่วนโดยน้ำหนักของ ดิน:พอตเทอรีสโตน:ทราย:เศษดินเผา เท่ากับ 70:11:11:8 เนื่องจากสมบัติของชิ้นงานเมื่อเผาที่ 950 องศาเซลเซียส ให้สมบัติการดูดซึมน้ำ และมอดุลัสของการแตกร้าวใกล้เคียงกับผลิตภัณฑ์ที่ผลิตในโรงงาน แต่มีสมบัติของเนื้อดินก่อนเผาโดยเฉพาะอย่างยิ่งสมบัติด้านความเหนียว ความไวต่อการแตกเนื่องจากการแห้งตัว การหดตัวก่อนเผาดีกว่า ซึ่งมีผลทำให้ลดการสูญเสียในกระบวนการผลิต

ภาควิชา วัสดุศาสตร์ ลายมือชื่อนิสิต.....

สาขาวิชา วัสดุศาสตร์ ลายมือชื่ออาจารย์ที่ปรึกษา.....

ปีการศึกษา 2550 ลายมือชื่ออาจารย์ที่ปรึกษาร่วม.....

4873827623 : MAJOR MATERIALS SCIENCE

KEY WORD: TERRACOTTA / POTTERY STONE / SAND / PHYSICAL PROPERTIES

PRAPUN AUNGATICHART: EFFECTS OF SAND AND POTTERY STONE ON PHYSICAL PROPERTIES OF TERRA COTTA BODY. THESIS ADVISOR: PROF. SHIGETAKA WADA, Ph.D., THESIS COADVISOR : ASST. PROF. SIRITHAN JIEMSIRILERS, Ph.D., 153 pp.

The effects of adding pottery stone incorporating with sand and grog on physical properties of terracotta body were studied. The total amounts of sand, pottery stone and grog adding to the clay bodies were varied at 20, 30 and 40 wt%. The following green and fired (900 – 1100 °C) properties of the mixed clay bodies were investigated: plasticity, drying sensitivity, drying shrinkage, green strength, firing shrinkage, bulk density, water absorption, modulus of rupture (MOR), thermal expansion coefficient and phase composition.

Based on the experimental results, it was found that sand and pottery stone could improve the physical properties of the green body by reducing plasticity, drying sensitivity, drying shrinkage and working moisture. The clay body which consists of 70 wt% clay, 11 wt% pottery stone, 11 wt% sand, and 8 wt% grog, was the optimal formula suitable for applying to production because its physical properties such as water absorption and MOR of the body fired at 950 °C are similar to those of the current products of the factory. Moreover, the green properties especially plasticity, drying sensitivity and drying shrinkage of this clay body were significantly improved. As a result, the production yield would be improved as the reject caused by cracking in the drying process is reduced.

Department Materials Science Student's signature.....

Field of study Materials Science Advisor's signature.....

Academic year 2007 Co-advisor's signature.....

ACKNOWLEDGEMENTS

I am so grateful to my advisor, Professor Dr. Shigetaka Wada, for his constant guidance and invaluable suggestions, including a very frank and friendly attitude. I wish to thank Assistant Professor Dr. Sirithan Jiemsirilers, Associate Professor Dr. Supatra Jinawath, Associate Professor Saowaroj Chuayjuljit, Associate Professor Danai Arayaphong, Dr. Pavadee Aungkavattana and Dr. Thanakorn Wasanapiarnpong for their suggestions and comments. I also would like to thank Dr. Nirut Wangmooklang for his assistance and advice.

I also would like to express a special thank to my wife, Pimolmart Aungatichart, for her encouragement and support throughout my Ph.D. study. Finally, I would like to express appreciation to my children, Proud, Perm and Prim, for their understanding that I have to devote most of our holiday time to write this dissertation.

CONTENTS

Page

ABSTRACT (in Thai)..... iv

ABSTRACT (in English)..... v

ACKNOWLEDGEMENTS..... vi

CONTENTS..... vii

LIST OF TABLES..... x

LIST OF FIGURES..... xi

CHAPTER I INTRODUCTION..... 1

1.1 Introduction..... 1

1.2 Objectives..... 2

CHAPTER II LITERATURE REVIEW..... 3

2.1 Terracotta..... 3

2.2 Plasticity of Clay..... 4

2.2.1 Assessment of Plasticity..... 5

2.2.1.1 Atterberg limits..... 5

2.2.1.2 Pfefferkorn test..... 6

2.3 Drying of Ceramics..... 7

2.3.1 The Rate and Stages of Drying..... 7

2.3.2 Drying Sensitivity..... 11

2.4 The Effects of Non-Plastic Materials on the Properties of Ceramic Clay Bodies 12

CHAPTER III EXPERIMENTAL PROCEDURE..... 20

3.1 Raw Materials and Characterizations..... 20

3.1.1 Chemical Composition..... 20

3.1.2 Mineral Phase..... 20

3.1.3 Thermal Analysis..... 21

3.1.4 Morphology and Particle Size Distribution..... 21

3.2 Calibration of Clay Hardness Tester..... 22

3.2.1 Hardness Testers Used for the Experiment..... 22

Page

3.2.2 Sample Preparation..... 24
3.2.3 Experimental Method..... 24
3.3 Specimen Preparation..... 25
3.4 Property Measurement and Characterizations of Mixed Clay and Fired Specimens..... 29
3.4.1 Plasticity..... 29
3.4.2 Drying Sensitivity..... 30
3.4.2.1 Bigot curve method..... 30
3.4.2.2 Accelerated method proposed by Ratzenberger. 36
3.4.3 Drying Shrinkage..... 38
3.4.4 Firing Shrinkage..... 38
3.4.5 Bulk Density and Water Absorption..... 38
3.4.6 Modulus of Rupture of Green and Fired Specimens..... 39
3.4.7 Thermal Expansion Coefficient..... 39
3.4.8 Mineral Phase of Fired Specimens..... 39
CHAPTER IV RESULTS AND DISCUSSION..... 40
4.1 Properties of Raw Materials..... 40
4.1.1 Ratchaburi Red Clay..... 40
4.1.2 Pottery Stone..... 44
4.1.3 Sand and Grog..... 46
4.2 Calibration of Clay Hardness Tester..... 49
4.2.1 Hardness before Training and Calibration of the Testers... 49
4.2.2 Hardness after Training without Calibration of the Testers.. 50
4.2.3 Hardness after Training and Calibration of the Testers..... 51
4.3 Properties of Green Body..... 55
4.3.1 Plasticity..... 55
4.3.2 Drying Shrinkage and Green Strength..... 57

Page

4.3.3 Drying Sensitivity..... 60
4.3.3.1 Bigot curve..... 60
4.3.3.2 Accelerated method proposed by Ratzenberger..... 63
4.4 Properties of Fired Body..... 66
4.4.1 Firing Shrinkage..... 66
4.4.2 Water Absorption..... 69
4.4.3 Bulk Density..... 71
4.4.4 Strength of Fired Bodies..... 73
4.4.5 Thermal Expansion Coefficient..... 76
4.4.6 Mineral Phase of Fired Specimens..... 77
CHAPTER V CONCLUSIONS AND RECOMMENDATIONS..... 79
5.1 Conclusions..... 79
5.2 Recommendations..... 81
REFERENCES..... 83
APPENDICES..... 87
VITA..... 153

LIST OF TABLES

Table		Page
3.1	Raw materials used in this experiment ……	20
3.2	Diameters (ϕ), lengths (l) and angles of the hardness tester cones (θ)…….	24
3.3	Compositions of clay bodies for this experiment……	29
3.4	Pfefferkorn test result for formula A ……	34
3.5	Moisture content at Pfefferkorn coefficient of plasticity of clay bodies……	35
4.1	Chemical composition of red clay……..	40
4.2	Chemical composition of pottery stone…….	44
4.3	Chemical compositions of sand and grog…….	46
4.4	Plasticity of the clay bodies……..	55
4.5	Data obtained from Bigot curves for calculating the *DSI-B* values of the clay bodies……...	62
4.6	The first maximum moisture difference (*MD-I*), linear drying shrinkage (*LDS*) and *DSI-R* of various clay bodies …….	64

LIST OF FIGURES

Figure		Page
2.1	Terra cotta pottery…….	4
2.2	Atterberg limits and soil volume relationships……..	6
2.3	Change in moisture content in ceramics during drying……..	7
2.4	Drying rate plot. M = weight of water in the ceramic; A = surface area of the ceramic exposed to the drying environment…….	8
2.5	Idealized course of drying rate depending on moisture in ware……...	9
2.6	Principle of water evaporation on the surface of green product……	10
3.1	Appearances of the raw materials passed through 40 meshes screen……	21
3.2	Photograph of a hardness tester……..	23
3.3	Schematic structure of the hardness tester……	23
3.4	Photographs illustrating the measurement method of the hardness tester…	23
3.5	Flow chart of specimen preparation…….	26
3.6	Mixing process for preparing the clay dough…….	27
3.7	Picture of measuring method for controlling hardness of the clay dough…..	27
3.8	Extrusion of test specimens……	28
3.9	Drying of test specimens at room temperature……	28
3.10	Atterberg limits test equipment……	30
3.11	Pfefferkorn plasticity tester (a) and equipment for preparing the test specimen (b)……	31
3.12	Scale of Pfefferkorn plasticity tester……...	31
3.13	Test procedure to get Pfefferkorn coefficient of plasticity; (a) preparing the clay specimen, (b) setting the specimen to the Pfefferkorn tester, (c) the specimen is being compressed, and (d) compressed specimen…….	33
3.14	Relationship between the water content and the height of the specimen (*a*) for the specimen (A)……..	34
3.15	Bigot curve plotted between shrinkage and water content of the test specimen……..	36
3.16	Schematic structure of the test specimen for testing the drying	

Figure Page

sensitivity by Ratzenberger method..... 37
4.1 XRD patterns of the red clay; (a) as-received clay and (b) fine particle fraction (<2 μm)..... 41
4.2 TG-DTG-DTA curves of clay..... 42
4.3 Particle size distribution of clay..... 43
4.4 SEM micrograph of clay..... 43
4.5 XRD pattern of pottery stone..... 44
4.6 TG-DTG-DTA curves of pottery stone..... 45
4.7 SEM micrograph of pottery stone..... 45
4.8 XRD patterns of sand and grog..... 47
4.9 SEM micrographs of sand (a) and grog (b)..... 48
4.10 Hardness numbers obtained by 5 persons before training using non-calibrated tools..... 49
4.11 Hardness numbers obtained by 5 persons after training using non-calibrated tools..... 50
4.12 Hardness numbers obtained by 5 persons after training using calibrated tools..... 52
4.13 Schematic structures illustrating the measured results after calibration and training using the hardness testers with different designs..... 52
4.14 Hardness number obtained by 3 persons at different calibration (numbers in the parenthesis show the standard deviation for each person/tool measurement)..... 54
4.15 Comparison of plasticity index of the clay bodies..... 56
4.16 Effect of additive content on plasticity index of the clay bodies..... 56
4.17 Effect of sand/pottery stone ratio on plasticity index of the clay bodies..... 57
4.18 Effect of additive content on the drying shrinkage of the clay bodies..... 57
4.19 Working moisture of various clay bodies obtained from Pfeferkorn test at *a* = 3.3..... 58
4.20 Effect of sand/pottery stone ratio on the drying shrinkage of the clay bodies.. 58

Figure Page

4.21 Effect of additive content on green strength of the clay bodies…….. 59
4.22 Effect of sand/pottery stone ratio on the green strength of the clay bodies….. 59
4.23 Bigot curves (drying shrinkage vs. moisture content) of the clay bodies…….. 61
4.24 Effect of additive content on the Drying Sensitivity Index-Bigot (*DSI-B*) of all clay bodies…….. 62
4.25 Effect of sand/pottery stone ratio on the Drying Sensitivity Index-Bigot (*DSI-B*) of all clay bodies…… 63
4.26 Plots of moisture difference (*MD*) values vs. various drying times…….. 64
4.27 Effect of additive content on Drying Sensitivity Index-Ratzenberger (*DSI-R*) of all clay bodies…….. 65
4.28 Correlation between Drying Sensitivity Index-Ratzenberger (*DSI-R*) and Drying Sensitivity Index-Bigot (*DSI-B*)……... 66
4.29 Effect of additive contents on linear firing shrinkage of the clay bodies fired at 950 and 1100 °C……. 67
4.30 Effect of sand/pottery stone ratio on linear firing shrinkage of the clay bodies fired at 950 and 1100 °C……... 68
4.31 Water absorption of the original composition (formula A)…… 69
4.32 Water absorption of the fired bodies at 950 and 1100 °C…… 70
4.33 Bulk density of the original composition (formula A)…… 71
4.34 Bulk density of the fired bodies at 950 and 1100 °C…… 72
4.35 Moduli of rupture of the fired clay bodies at various temperatures…… 73
4.36 Effect of additive contents on fired strength of the clay bodies fired at 950 and 1100 °C……. 74
4.37 Effect of sand/pottery stone ratio on fired strength of the clay bodies fired at 950 and 1100 °C…… 75
4.38 Thermal expansion coefficient curves of fired clay bodies at 950 °C…….. 76
4.39 XRD patterns of specimens (formula A) fired at various temperatures…….. 77
4.40 XRD patterns of specimens (formula K) fired at various temperatures…….. 78

CHAPTER I

INTRODUCTION

1.1 Introduction

Ratchaburi red clay is an important clay resource for the production of earthenware ceramic called “Dragon jar” in Thailand. The first factory that produced earthenware jar was founded by Mr. Tia Song Hong and Mr. Er Jer Ming in 1933. Nowadays, there are approximately 50 factories using Ratchaburi red clay as main raw material to produce many kinds of earthenware products such as potteries and other garden decorative items. *(1)*

One of the most important physical properties of Ratchaburi red clay is its high plasticity which is suitable for producing Dragon jar or any other products having large size by hand. For the production of terracotta potteries by machine, however, high plasticity causes many problems as the clay mass sticks on machines during the mixing or forming processes. Moreover, the low drying rate and the high drying crack of green body always occur due to high plasticity. *(2)*

Generally, these problems can be solved by adding non-plastic materials such as silica sand and grog (fired clay) in the composition of the terracotta body. However, we can not add too much amount of silica sand into the composition as it decreases the fired strength *(3)* and the transformation of quartz during the firing process may cause cracking. Moreover, the improvement of the production process causes the shortage of grog as well.

Pottery stone is a non-plastic material which is cheap, and has similar chemical composition to clay. As mentioned, it is thought that pottery stone is an additional material to reduce the plasticity of clay, enhance the drying rate, and decrease the drying crack of terracotta body.

Before using pottery stone, sand and grog as the additives in the terracotta production, it is essential to know the effect of them on both green and fired properties of mixed terracotta body. In this dissertation, therefore, the effects of sand

and pottery stone on the physical properties of terracotta body should be studied before applying in the real production. The content of grog is kept constant because of its limited resource.

1.2 Objectives

1. To study the effects of sand and pottery stone on the green properties of terracotta body.
2. To study the effects of sand and pottery stone on the fired properties of terracotta body.
3. To find a proper ratio of the red clay, sand, and pottery stone in the terracotta production.

CHAPTER II

LITERATURE REVIEW

2.1 Terracotta

There are many definitions of the term “terracotta”. The various definitions of terracotta obtained from many sources are as follows:

- Italian word, means clay firing. It is an earthenware fired at low temperature about 900 – 1000 °C. *(4)*
- From the Latin for earth + burnt. Terracotta is the traditional material for flowerpots and tiles and also describes their characteristic color. *(5)*
- This term has been used interchangeably with earthenware. “Terracotta” is referred to as “baked clay” enter clay as a material and baked as a technique.*(6)*
- A hard, brown-orange earthenware clay of fine quality, often used for architectural decorations, figurines, etc. *(7)*
- Fired but unglazed clay, used mainly for floor and roof tiles. Can be fired in molds to produce a wide range of shapes. Usually red. *(8)*

The Ratchaburi terracotta potteries are made from very sticky red clay which is suitable to be formed by hand on the pottery’s wheel. Decoration and adornment on the surface of green body can be applied. The potteries can be fired both in wood-fired and gas-fired kilns at low temperature approximately 900 – 1000 °C. Some of the physical properties of Ratchaburi terracotta potteries are as follows: bulk density 1.90 – 2.00 g/cm^3, water absorption 12.0 – 15.0 % and modulus of rupture 18.0 – 20.0 MPa.*(3)* After firing, color becomes orange or reddish as the pictures shown in Fig. 2.1

Fig. 2.1 Terra cotta pottery

2.2 Plasticity of Clay

Plasticity of clay is defined as the ability of a clay-water mass at its maximum consistency to be shaped and to hold its shape after the forming forces are removed.*(9)* The word “ability” in this definition has two connotations, one with respect to shaping and the other to holding the shape. In the first case “ability” refers to the amount of plastic or viscous flow (strain) that can take place before rupture occurs. In the second “ability” refers to the internal strength of the plastic mass after the forming stresses are removed. This dual relation in the definition qualitatively means that clay will have high plasticity when a large force is required to deform it, and in this condition it will be deformed to a considerable degree before failure. As a matter of fact, a clay-water system of high plasticity requires large force to deform it and deforms to a greater extent without cracking than low plasticity one which deforms more easily and ruptures sooner.

There are many factors affecting the plasticity of clay bodies, and these factors should be well understood in order to manipulate this property. Some of the factors are primary and others are secondary. The primary factors are essential to achieve plasticity, while the secondary factors are used to control or regulate plasticity. The primary factors are:

(1) The anisodimensional shape of clay-mineral particle.

(2) The strong surface forces on clay-mineral particles due to the in completely coordinated small cations with large charge.

(3) The rigidity of the water structure surrounding the clay mineral particles.

The secondary factors affecting plasticity do not create or destroy plasticity of clay bodies but only increase or decrease its magnitude. These secondary factors are:

(1) The type of cations absorbed on the clay mineral particles and/or contained in their water hulls.

(2) The temperature of the clay-water system.

(3) The small particle size of the clay-mineral particles.

(4) The presence of nonclay particles in the clay-containing body.

2.2.1 Assessment of Plasticity

There are many methods to assess the plasticity of clay. However, two methods will be discussed here.

2.2.1.1 Atterberg limits *(10)*

A fine-grained soil can exist in any of several states, which state depends on the amount of water in the soil system. When water is added to a dry soil, each particle is covered with a film of adsorbed water. If water is added continually, the thickness of water film on a particle increases. Increasing the thickness of water films permits the particle to slide past one another more easily. The behavior of soil, therefore, is related to the amount of water in the system. At very low moisture content, the material acts like a solid. As the moisture content rises, the material moves from solid to semi-solid to plastic to liquid form finally. Atterberg defined the boundaries of four states in term of “limits” as the following.

The moisture content at the boundary between semi-solid and plastic state is known as the plastic limit (*PL*). The moisture content between the plastic and liquid states is known as the liquid limit (*LL*). The difference between the plastic and liquid limits is called the plasticity index (*Ip*), and indicates the size of the range over

which the material acts as a plastic-capable of being deformed under stress, but maintaining its form when unstressed.

Fine-grained soils also exhibit shrinking and swelling as the moisture content changes. As water content increases from dry to wet, no change in volume occurs below certain moisture content, known as the shrinkage limit (*SL*). Above the shrinkage limit, volume increases as moisture content increases. Atterberg limits and soil volume relationships are shown in Fig. 2.2.

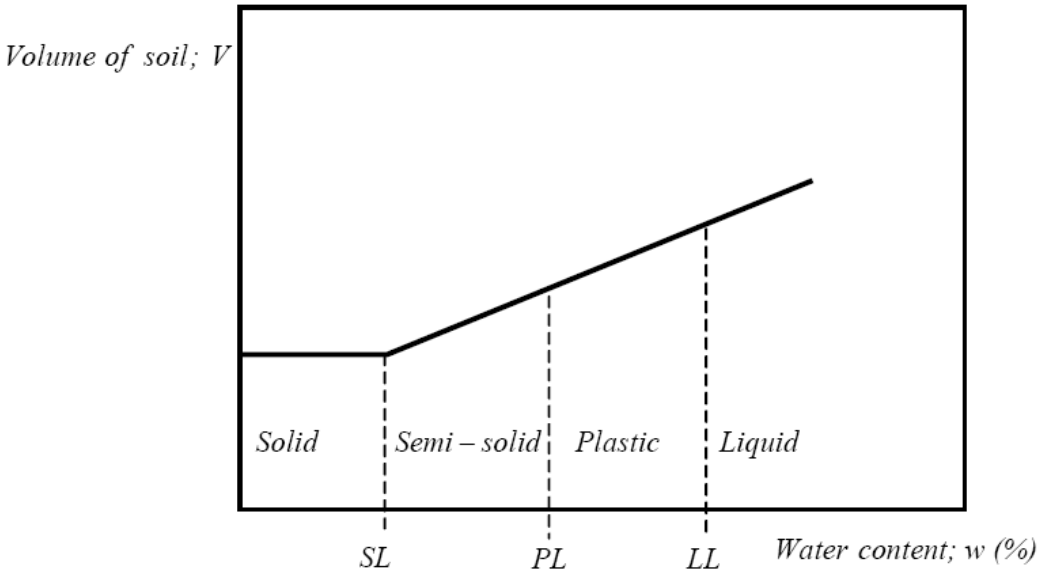

Fig. 2.2 Atterberg limits and soil volume relationships

2.2.1.2 Pfefferkorn test *(11)*

According to Pfefferkorn test, a standard weight is released from a fixed height and falls onto a cylindrical sample of the material under test. The cylindrical sample is deformed, the deformation ratio (a) indicated in the Pfefferkorn scale is defined as follows:

$$a = \frac{\text{the height of the uncompressed test specimen (40mm)}}{\text{the height of the specimen after deformed}}$$

The coefficient of plasticity is the percentage of the water content at which the test specimen is compressed to 30% of its initial height or the deformation ratio (*a*) is equal to 3.3.

2.3 Drying of Ceramics

Drying of ceramics is the process of removing water from an unfired ceramic object or raw material in the green or as-formed state or in the as-received state *(9)*. Drying of ceramics is much more complicated than drying many other objects because unfired ceramics typically exhibit shrinkage during drying. This shrinkage can lead to cracking and loss of acceptable quality in production.

2.3.1 The Rate and Stages of Drying

The rate of drying is the change in the weight of moisture in the ceramic per unit time. In a plot of the moisture weight in the ceramic versus time, the rate of drying is the slope of the line as shown in Fig. 2.3.

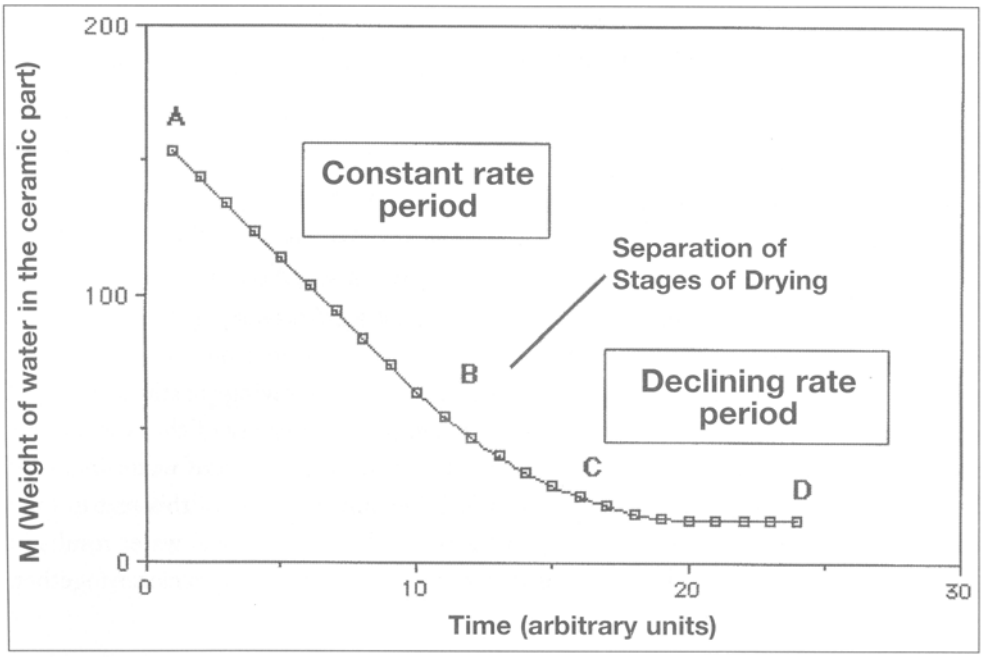

Fig. 2.3 Change in moisture content in ceramics during drying *(12)*

The information presented in Fig. 2.3 can be more conveniently presented in a plot of drying rate versus time. As shown in Fig. 2.4, it is clear that the

drying rate is constant during the initial drying of ceramic (from point A to point B). For this reason, the initial period is called the constant rate period of drying.

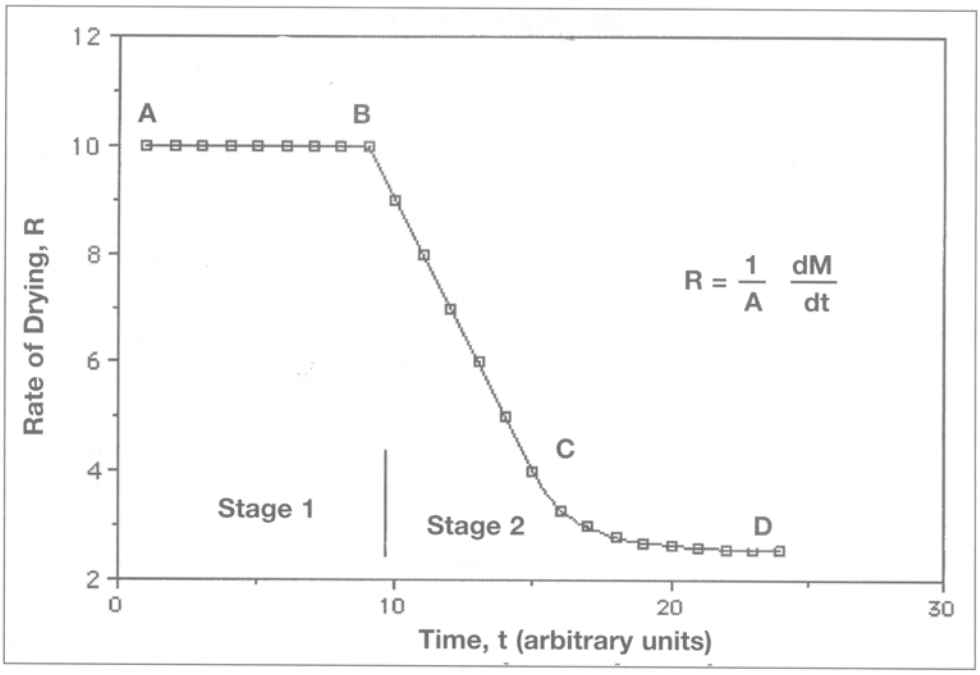

Fig. 2.4 Drying rate plot. M = weight of water in the ceramic; A = surface area of the ceramic exposed to the drying environment *(12)*

As drying beyond point B, the drying rate declines with the rate of decline constant. The period of drying is progressing from point B to point C is called the first declining rate period. In the next period of drying (progression from point C to point D), the rate of drying is progressively slow until drying is completed, this period is called the second declining rate period.

It is important to divide the drying process into two stages. Stage I is the constant rate period, and stage II contain both the first and second declining rate periods. The moisture content of point B in Fig. 2.3 and 2.4 is called the critical moisture content (M_c) because shrinkage takes place as drying continue down to M_c, but shrinkage is negligible below M_c. When clay ceramics reach M_c, they are called leather-hard. In traditional ceramics, this is the point at which the product can be moved without fear of warpage. In conclusion, drying of ceramics can be divided into two stages. Stage I: the constant rate period during which shrinkage is occurring. When M_c is reached, shrinkage stops. Stage II: the first and second declining rate periods.

Since shrinkage is occurring in stage I, the rate of drying in stage I must be limited to prevent cracking. Once stage I ends (i.e. M_c is achieved), the drying strategy changes since shrinkage is no longer a critical consideration. It is commonplace to supply additional temperature to product in stage II to accelerate drying. In the second declining rate period, high temperatures are required to complete the drying process in a reasonable time frame.

The relation between the drying rate and the moisture in ware can also be plotted as shown in Fig. 2.5.

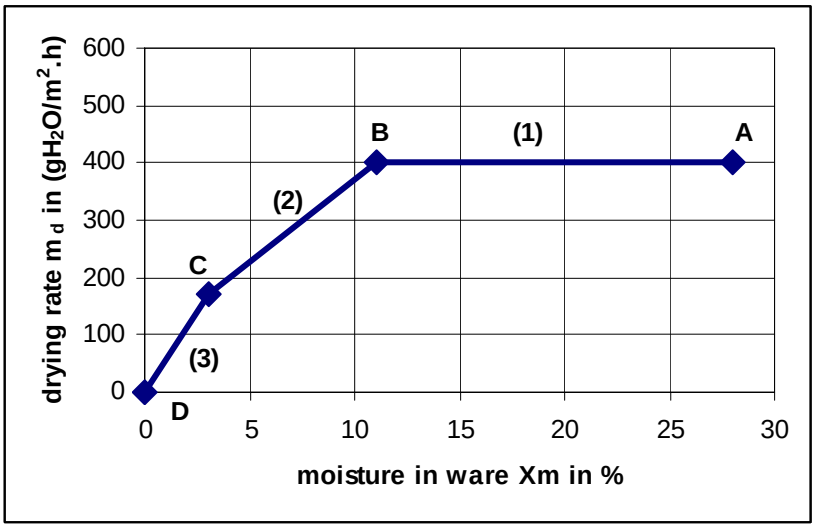

(1) Stage I (point A to B): the constant rate period

(2) Stage II (point B to C): the first declining rate period

(3) Stage II (point C to D): the second declining rate period

Fig. 2.5 Idealized course of drying rate depending on moisture in ware *(13)*

At the constant rate period, water on the surface of the green product evaporates first of all. During the Stage I (point A to B), the conditions are similar to those when vaporization takes place on the surface of water (see Fig. 2.6). The loss of mixing water evaporated on the surface is supplied by the lightly bound gap water from the interior of the ware via its network of pores to the surface in order to even out the moisture deficit in that area. As long as sufficient water from the interior reaches the surface of the green product due to its capillarity, the drying rate and temperature of the ware remain constant.

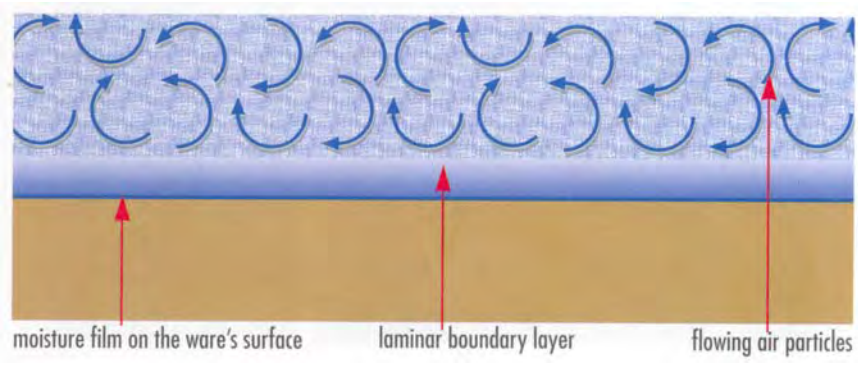

Fig. 2.6 Principle of water evaporation on the surface of green product *(13)*

The moisture content of a green product decreases more and more due to the loss of pore water. The moisture distribution within the ware to be dried is no longer homogeneous at this point, i.e. the edge areas are already significantly drier than the interior of the ware. Accordingly the individual clay particles in the area of the surface of the ware are already recognizably nearer to each other than in the core area. When the individual mass particles move closer together a reduction in the volume of the green product is caused. This volume reduction is described as drying shrinkage.

As drying progresses, the capillary system of a green product can no longer take moisture from the interior of the ware at the same rate as it evaporates from the surface. Consequently the moisture content at the surface constantly decreases.

The evaporation process of the mixing water finally moves to the interior of the green product and the drying rate begins to fall. The leather-hard state has now been reached.

At the first declining rate periods, the process in the ware to be dried differs physically in a significant way from the constant rate period since the evaporation level moves from the surface of the ware slowly into the interior of the ware.

In order that the mixing water from the interior of the ware to reach the surface, considerable obstructions, so-called diffusion resistance have to be overcome. In practice, it is from time to time very important to know that not only the evaporation of the more strongly bound surface water, but also the overcoming of diffusion resistances, means that additional energy is required. At this period, the drying rate constantly falls as the moisture content reduces (see Fig. 2.5, point B to C).

In practice, the green products are taken out of the drying plant during this drying period, or at the end of it at the latest. Between 2 and 4 % residual moisture then remains in the green ware. The transition from the constant rate period to the first declining rate period is called the critical moisture content (M_c) (see Fig. 2.5, point B).

At the second declining rate period (Stage II (point C to D)), the final more strongly bound water particles (cladding and layer water, chemically bound combined water) are expelled. During this phase the ware to be dried is normally no longer in the dryer, but already in the heating-up zone of the tunnel kiln. The processes expelling the water are identical to those in the second drying phase, i.e. moisture is evaporated in the interior of the ware and moves through the green product's capillary network to the surface. However, the drying rate continues to decrease due to increasing diffusion resistance and high retention forces (polar bonds and sorption forces) to the water molecules. Consequently a second transition point (see Fig. 2.5, point C) results between the first declining rate period and the second declining rate period.

2.3.2 Drying Sensitivity

Drying sensitivity is a phenomenon resulting from the basic constituents of clay-type raw materials. It mainly occurs in highly plastic raw materials with a considerable content of clay minerals liable to swelling (bulking materials) *(14)*.

The term "drying sensitivity" should be understood as the type of drying crack susceptibility which gives verbal or numerical expression to the tendency of a green clay product to crack while it is drying under defined conditions. Drying crack susceptibility is mainly caused by increased content of three-sheet silicates, particularly those liable to swelling. The drying sensitivity covers cases of susceptibility to cracking caused either by severe drying shrinkage and high moisture differentials in the green products or to inadequate bonding power (cohesive force), due to an insufficient clay mineral content *(15)*.

Ch. Schmidt-Reinholz *(16)* reported that the total quantity of layer silicates with swelling ability is directly connected to the drying sensitivity of clay ceramic articles. Drying sensitivity increases progressively with a higher quantity of layer

silicates with swelling ability. Silica sand, flue ash, lime, turf, decanter material, sawdust and newspaper are the suitable additives to lessen the drying sensitivity.

H. Ratzenberger *(17)* published the paper entitled “An accelerated method for the determination of drying sensitivity”. The principle is the moisture drop occurs in the first and second drying stages, between the interior and evaporation surface of the clay products. The first maximum moisture difference ascertained (*MD-I*) came to be used as the sole criterion for evaluation. The tendency to cracking increases in proportion to the magnitude of this moisture difference (*MD*) and the consequent mechanical stress arising due to differential shrinkage.

2.4 The Effects of Non-Plastic Materials on the Properties of Ceramic Clay Bodies

F. Saboya Jr. et al. *(18)* discussed on the usage of powder marble to enhance the properties of brick ceramic. The results showed that a raw-material composition 15 wt% of waste content fired at 850 °C might be used without impairment of their mechanical properties. If the firing temperature is above 950 °C, a higher content of waste material can be used without loss of quality.

E. A. El-Alfi et al. *(19)* revealed that the substitution of sand for clay allows controlled drying with shorter times required for complete dryness, and also improves dry and firing shrinkage, bulk density, apparent porosity, and crushing strength. The batch containing 10 wt% of sand exhibited the best results and was therefore selected as the optimum batch for making clay sand bricks.

J. C. Knight *(20)* reported that addition of ash (0 - 30 wt%) to the high plasticity clay appears detrimental. In particular, compared with the properties of the clay without ash, increasing amounts of ash progressively and significantly decrease both the green and fired strength and slightly increase the fired porosity. Furthermore, increased critical flaw size with increased ash content seems to account for the deleterious effects of the ash on the fired properties of the high plasticity clay.

W. Russ et al. *(21)* used spent grains, which are a form of waste, as additive in clay bricks to increase porosity of the bricks. The results showed that the bricks produced with spent grains possessed a comparable or higher strength, a higher porosity and a reduced density after firing than those from standard production clay.

Because the sintering of bricks including spent grains begins at somewhat lower temperature and more homogenous distribution of pores, the fired clay product is more strongly sintered, exhibiting both greater strength and higher porosity.

E. A. Dominguez and R. Ullmann *(22)* made ecological bricks using clay incorporating steel dust. The result showed that the brick incorporating 20 wt% steel dusts meets standard commercial regulations being inert to the extraction procedure toxicity test (EP-TOXIC) and full toxic characteristic leaching procedure protocols (TCLP) tests. The addition of steel dust reduces the firing temperature of the ceramic process.

W. Acchar et al. *(23)* investigated the changes in the behavior of the clay material used in a red-clay industry due to additions of granite and marble sludge, which is the by product of an ornamental stone industry in Rio Grande do Norte-Brazil. Mixtures of clay and waste material (10–50 wt%) were uniaxially pressed and sintered at temperatures ranging from 950 to 1150 °C. The results from chemical and mineralogical analysis (XRF and XRD), thermal analysis (DTA, TG and dilatometry), apparent density, water absorption and flexural strength show that the granite and marble sludge can be added to the clay material with no detrimental effect on the properties of the sintered red-clay products. The granite and marble sludge acts as a fluxing agent, reducing the sintering temperature of the clay material.

I. Demir *(24)* investigated the utilization of sawdust and tobacco residues for the production of clay bricks. Organic residues (0, 2.5, 5 and 10 wt%) were mixed with raw brick-clay. All samples were fired at 900 °C. Adding organic residues to the clay body increases the required water content for extrusion (apparent plasticity). The fibrous nature of residues did not create problems during shaping when used up to 10 wt%. No extrusion failures were observed. Drying shrinkage of the clay body increased very much in addition to the expected stabilization effect of cellulose fibers, mostly due to the very high water content. A residue addition of 10 wt% is found to be unsuitable because of the excessive drying shrinkage. The compressive strength of the fired samples is decreased by the addition of residues. Nevertheless, the values are still higher than required by Turkish standards. The residues increased the open porosity and decreased the bulk density; this effect may improve the thermal insulation properties and lower dead load in buildings.

M. M. Elwan et al. *(25)* used solid waste sludge as an additive material for brick manufacture. The effect of addition of solid waste sludge as the substitute for clay up to 25 wt% on the ceramic properties of the products fired up to 750 and 850 °C were investigated. It is concluded that the solid sludge should be heat-treated for 2 hrs at 260 °C to make environmentally safe material. Also, the addition of 10-15% preheated solid sludge to the brick clays of El-Tabbin leads to produce building bricks with reasonable physicomechanical properties after firing up to 750-850 °C. An increasing sludge addition or firing temperature leads to a significant decrease in shrinkage, bulk density and crushing strength of the fired bodies with simultaneous increase of weight loss and apparent porosity.

T. Basegio et al. *(26)* tested tannery sludge in the manufacture of a ceramic mainly composed of clay. The raw materials, tannery sludge and clay, were mixed together in different proportions (0 – 30 wt% of tannery sludge). The ceramic specimens were characterized with respect to water absorption, porosity, linear shrinkage and transverse rupture strength. Leaching tests, in accord with the Brazilian and German regulations, were done on ceramic bodies made with different additions of sludge. All the leaching tests have shown that the main sludge contaminant i.e. chromium, could be immobilized within a finished ceramic product. The studies of air emissions have shown that zinc and chlorine are mainly collected from emitted gas and hence are not immobilized by the ceramic system. The study shows that the properties of the ceramic materials produced are acceptable for applications such as bricks for the building industry.

M. Dondi et al. *(27)* reported the technological feasibility of the Orimulsion fly ash recycling in clay bricks. A laboratory simulation of the brickmaking process was carried out with various clay/ash mixtures up to 6 wt% ash. Two different clays were selected and the mixtures were characterized by XRF, XRPD, TGA–DTA, TDA and PSD analyses. Orimulsion ash caused some detrimental changes of technological properties for both unfired and fired products, concerning particularly plasticity, drying rate and drying sensitivity, porosity and color. These effects were slightly different on the two raw materials; the carbonate-rich clay was less sensitive to

the presence of ash with the carbonate-free clay. In all events, drawbacks appeared to be tolerable, in technological terms, for low waste additions, approximately 1–2 wt% ash.

I. Demir and M. Orhan *(28)* investigated the addition of waste-brick material in brick production. After pulverizing, the waste-brick were divided into two categories: A passing through a 4.75 mm sieve (coarse) and B passing through a 600 μm sieve (fine). In order to obtain comparable test results, ratios of the waste (0, 10, 20 and 30 wt%) were added to the raw-brick clay. The results show that use of both the coarse and fine crushed waste brick additives decreased plasticity of the mixture. An increase in the content of waste additives leads to a decrease in the drying shrinkage. The coarse particle was more effective in this regard, compared with the fine particle. This is regarded as a positive effect that minimizes damage in the drying procedure. Increases of the additive and firing temperature lead to a decrease and increase in the total shrinkage, respectively. Compressive strength values increase with increasing sintering temperature. An increase in the waste brick content leading to a decrease in frost durability and compressive strength meets the required specification in all mixtures. The water absorption value increases as the waste addition amount increases, but an increase in the firing temperature causes a decrease in the water absorption. At a mass of 30% fine-waste material additive, fired at 900 °C, the test sample has an adequate strength. The reuse of this material in the industry would contribute to the protection of farmland and the environment.

X. Lingling et al. *(29)* studied the effect of fly ash with high replacing ratio of clay on firing parameters and properties of bricks. The results indicate that the plasticity index of the mixture with fly ash decrease dramatically with increasing of replacing ratio of fly ash. The additive can be chosen to improve the plasticity index of mixture to meet the extrusion process used in most brick making factories. The sintering temperature of bricks with high replacing ratio of clay by fly ash was about 1050 °C, which is 50 – 100 °C higher than that of fired clay bricks. The properties of fired bricks were improved by using pulverized fly ash. The fired bricks with high volume ratio of fly ash had high compressive strength, low water absorption, no cracking due to lime, no frost and high resistance to frost-melting.

S. N. Monteiro et al. *(30)* used crushed fired brick in mixtures with clayey body to make typical red ceramics for bricks. The effect of the grog addition up to 20 wt% on the extrusion stage as well as on properties and microstructure of bricks fired at 700 °C was evaluated. The results indicate that grog additions up to 20 wt% did not impair the plasticity of the industrial clayey body and thus may be considered adequate for extrusion process. According to all evaluated properties, the additions of grog up to 5 wt% did not impair both the processing and the quality of the final ceramic. Addition of grog in higher amount increases the porosity of the fired pieces, which is detrimental to the technological properties of the red ceramic bricks.

I. B. Garcia et al. *(31)* utilized gravel pits by-product originated from the sand and gravel washing process in the middle-course Jarama river Quaternary sediments, located in Madrid region, central Spain to produce the ceramic products. Thirty silty–clay by-products, collected from seven gravel pits, have been tested at a laboratory scale. The mineralogical composition of these materials is mainly represented by phyllosilicates (muscovite-illite, smectite, kaolinite and chlorite), quartz and feldspars. For the technological characterization, six representative mixtures were designed combining suitable mineralogy and grain-size distribution of the 30 raw samples. Drying sensitivity (Bigot curves and Ratzenberger test) was tested for the extruded body. Smectitic content influences directly the parameters measured on dried bodies. Three maximum firing temperatures were studied: 850, 950 and 1050 °C. On mixtures fired at 950 °C, firing shrinkage is less than 4 wt%, bending strength may reach 69 MPa and water absorption range from 23 wt% to 0.5 wt%. Efflorescence susceptibility is faint, color is red for all the samples and getting darker for increasing temperature.

S. Kurama et al. *(32)* employed a boron waste from borax production in different amounts in order to develop an experimental terracotta floor tile in combination with a feldspathic waste provided from a local sanitary ware plant and a ball clay. Several formulations were prepared and shaped by dry pressing under laboratory conditions. The obtained samples were fired at 1050, 1100 and 1150 °C to establish their optimum firing temperatures. According to the results, increased presence of waste compared to the standard mixture of clay and the sanitary ware waste, as a co-fluxing material, in the experimental terracotta body considerably accelerated the vitrification.

The overall results indicated a prospect for using the waste as a raw material in mixtures with both clay and sanitary ware waste for the production of a terracotta floor tile body.

E. Kalkan and S. Akbulut *(33)* studied the effects of silica fume on the water permeability, swelling pressure and compressive strength of natural clay liners. The test results showed that silica fume decreased the liquid limits and plasticity index and increased the plastic limits in all the clay samples. For this reason, the soil with high silica fume contents changed from high-plastic clays to low-plastic clays. Silica fume slightly increased the optimum water content. As the permeability and swelling pressure decreased by adding silica fume, the compressive strength of clay samples proportionally increased with silica fume contents for all the samples. Observations of scanning electron microscope showed that the structure of raw clay samples could be changed through silica fume contents in the sample. The structure of a material had a significant influence on its engineering properties such as permeability, strength and stiffness. Thus, silica fume appears to be promising for construction material of liners subjected to leachate in solid waste containment systems.

M. Aineto et al. *(34)* studied the fly ash exhausted from integrated gasification in combined cycle (IGCC) power plant as additive to clays for building ceramic. The addition of this new kind of fly ash to clay of medium plasticity to elaborate pressed specimens, which were baked at 900 °C, improves the sintering of the specimens. Consequently, water absorption and mechanical properties of the fired bodies were improved with no negative effects on shrinkage, color alteration and efflorescence. In contrast, this fly ash does not mend the excessive firing shrinkage when added to clay with a high plasticity index.

Y. Pontikes et al. *(35)* utilized bauxite residue in the production of heavy-clay ceramics. In the mixtures with bauxite residue, sintering initiated at a lower temperature and the firing shrinkage was increased. Moreover, a second shrinkage zone was observed for high bauxite residue content and firing temperature above 950 °C, which suggested the development of a low viscosity liquid phase. The main mineralogical phases after firing in the mixtures with bauxite residue were quartz, hematite, clinopyroxenes, gehlenite and plagioclase.

S. A. El Sherbiny et al. *(36)* added waste by-pass cement dust in different percentages ranging from 2 wt% to 10 wt% to a standard mixture for sewer pipes manufacture, as a substitute for expensive feldspar. It was found that cement dust made lesser the drying shrinkage than that of feldspar. The plasticity of mixtures and modulus of rupture of green samples decrease with the addition of either feldspar or cement dusts. The firing shrinkage increases in the presence of cement dust and stabilized after about five hours firing. On the other hand, the water absorption decreased in the presence of cement dust and reaches a very low level when fired at 1300 or 1350 °C. A mixture consisting of 45% kaolin, 36% ball clay, 9% grog and 10% by-pass dust fired at 1300 °C for 4 h yielded the sample that meets the standards.

R. R. Menezes et al. *(37)* characterized and evaluated the possibilities of using the granite sawing wastes as alternative raw material in the production of ceramic bricks and tiles. The results showed that the granite wastes have physical and mineralogical characteristics that were similar to those of conventional ceramic raw materials. The wastes were essentially composed of quartz, feldspar, calcite and mica. One of them basically composed of quartz and kaolinite. The addition of wastes in ceramic compositions for production of bricks, up to 35 wt% caused a slight increase in the water absorption, but an increase in the modulus of rupture was observed. The ceramic compositions with additions of wastes can be used to produce wall and floor tiles with water absorption lower than 3% when fired at 1200 °C.

A. Acosta et al. *(38)* reported the application of slag from the integrated gasification in combined cycle (IGCC) power plant to the construction of soft mud bricks. The contents of the slag in the bricks were varied at 0 – 50 wt%. The industrial level tests have also been performed. The results of experiment suggest that the slag improves water absorption and resistance to the frost conditions. Furthermore, the ceramics with slag present the most vitreous sound. Not only can IGCC slag be applied to a ceramic process, but also its use gives several advantages, such as water and energy savings, as well as improvements on the final properties of products.

E. Kalkan *(39)* investigated the uses of red mud waste generated by the Bayer Process for the preparation of clay liners. The amounts of red mud used in the mixtures were 5 – 50 wt%. This study examines the effects of red mud on the

unconfined compressive strength, hydraulic conductivity, and swelling percentage of compacted clay liners as a hydraulic barrier. The test results show that compacted clay samples containing red mud and cement–red mud additives have a high compressive strength and decreased the hydraulic conductivity and swelling percentage as compared to natural clay samples. Consequently, it is concluded that red mud and cement–red mud materials can be successfully used for the stabilization of clay liners in geotechnical applications.

CHAPTER III

EXPERIMENTAL PROCEDURE

3.1 Raw Materials and Characterizations

All of the materials used in this research are shown in Table 3.1. The appearances of the materials are shown in Fig. 3.1.

Table 3.1 Raw materials used in this experiment

Materials	Sources
Red clay	Ratchaburi
Sand	Maeklong River, Ratchaburi
Grog	Siamese Merchandise Co.,Ltd.
Pottery stone	Lopburi

* The particle sizes of all materials are smaller than 40 meshes

3.1.1 Chemical Composition

The chemical composition of the raw materials was analyzed by X-ray fluorescence (XRF, SRS3000, Siemens, Germany) at Sibelco Asia – Glass & Ceramic Technical Centre.

3.1.2 Mineral Phase

Phase composition of the raw materials was identified by X–ray diffraction using Bruker difractometer model D8 advance (Ni-filtered Cu Kα radiation; λ = 1.5406 Å). The materials were crushed and ground to powder under 100 meshes. The qualitative analyses were determined at the following conditions: voltage 40kV, current 40mA, divergence slit 0.5° deg., antigence slit 0.5° deg., 2θ 5-60° and step time 0.5s/0.02°.

(a) Red clay (b) Sand

(c) Grog (d) Pottery stone

Fig. 3.1 Appearances of the raw materials passed through 40 meshes screen

3.1.3 Thermal Analysis

Thermal analysis of red clay and pottery stone was carried out at a heating rate of 10 °C/min using thermal analyzer, which is a combined TG-DTG-DTA unit (Simultaneous thermal analysis, STA 409C/3/E, Netzch, Germany) at the Scientific and Technological Research Equipment Center, Chulalongkorn University.

3.1.4 Morphology and Particle Size Distribution

Morphology of the raw materials was observed by a scanning electron microscope, SEM (JSM-6480LV, JEOL, USA) at the Instrument and Equipment Center of Faculty of Science, Chulalongkorn University. Particle size distribution of clay was measured by a particle size analyzer in Japan.

3.2 Calibration of Clay Hardness Tester

In this experiment, we have to control hardness of the wet mixed bodies (dough) into the same hardness value. Therefore, the NGK type clay hardness tester was used to measure the hardness of dough. When we use NGK type tester as one of the standard evaluation methods for the hardness of clay, required standard and reliability of it are very important. Although there is some information on the usage of it *(1-3)*, the NGK type tester comes in many designs according to producers and we can not find any basic data on the relation between the design and its performance. Therefore, it is important to perform an experiment to study the design and reliability of the hardness tester and to find out the standard method to measure the hardness of the clay dough since the basic data obtained will benefit the reproducibility of the products. The experiment was conducted as follows:

3.2.1 Hardness Testers Used for the Experiment

The appearance of NGK type hardness tester is shown in Fig. 3.2. It is composed of a cone, a spring, a hardness scale, a reading scale indicator, an adjustment screw, a spring stopper, a head cover and a case as schematically illustrated in Fig. 3.3. As demonstrated in Fig. 3.4, when the cone is pressed into the clay dough till reaching the supporting base, the reading scale indicator gradually moves from zero to larger number on the hardness scale and stops at some value depending on the hardness of the material. That is, the force resisting to the penetration of the cone into the dough balances against the force of spring. The hardness of the material is indicated by the hardness number engraved in the surface of the case. If the number is small, the dough is soft. On the contrary, if the number is large, the dough is stiff.

Five NGK type hardness testers having a little difference in the design were used for the experiment. All of the tools were two brand news (PN-01 and PN-02) and three of used ones (JOD-01, POD-01 and POD-02). The differences between the two groups of the tools were diameter, length and cone angle. The data of the diameter (ϕ) at the supporting base, the length (l) and the angle (θ) of the cones are shown in Table 3.2. The hardness numbers engraved on the case were 0 - 25 for PN-01 and PN-02, and 0 - 20 for JOD-01, POD-01 and POD-02.

Fig. 3.2 Photograph of a hardness tester

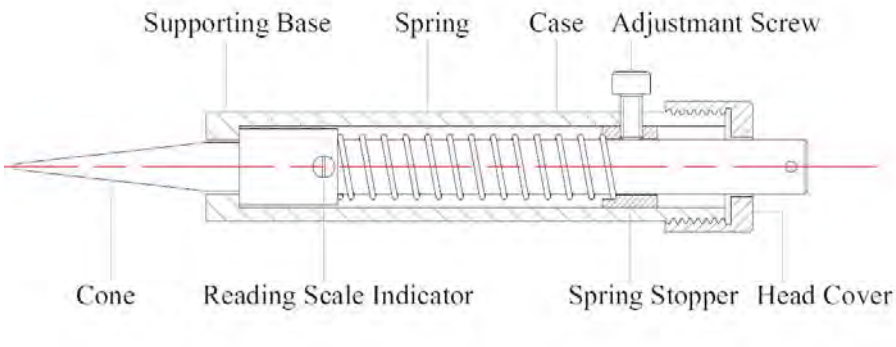

Fig. 3.3 Schematic structure of the hardness tester

Fig. 3.4 Photographs illustrating the measurement method of the hardness tester

The diameter and the length of the cone were measured by a vernier calliper. These values were difficult to measure accurately due to the cone figure. The angle of the cone tip (θ) was calculated from the diameter (ϕ) and the length (l). From the values in Table 3.2, it was noticed that PN-01 and PN-02 had longer and sharper cone figure than those of the rest.

Table 3.2 Diameters (ϕ), lengths (l) and angles of the hardness tester cones (θ)

Hardness tester	ϕ (mm)	l (mm)	θ = (degree)
JOD-01	9.25	34.3	15
PN-01	9.75	44.7	12
PN-02	9.90	45.1	12
POD-01	9.55	33.7	16
POD-02	9.50	34.5	16

3.2.2 Sample Preparation

The clay dough from the production process of Siamese Merchandise Co., Ltd. was used for this experiment. The test pieces were extruded cylindrical shape with dimension approximately 20 cm in both diameter and length. Afterwards, these specimens were wrapped with plastic film and kept for one night to homogenize the moisture.

3.2.3 Experimental Method

To study the effect of human error on the measurement, five persons joined the experiment. Each person was denoted as person A, B, C, D and E. The conditions of the measurement were as follows:

(a) Before training and calibration of the testers

Five hardness testers were used at the condition as received. Each person used 5 hardness testers alternately without any instruction. Ten measurements were done for each person/tool pair.

(b) After training without calibration of the testers

The same testers were used. The training instructions were as follows: (i) the hardness tester should be pressed perpendicular to the surface of the test piece

and (ii) it should be pressed slowly and then held until the drift of the reading scale stops. The hardness number should be read after the drift stops.

(c) After training and calibration of the testers

The persons who used the hardness testers were trained and the hardness testers were calibrated as follows:

i) At a fixed load

All hardness testers were calibrated by adjusting the force of the spring through the adjustment screw. The spring was so calibrated that the hardness number showed 10 when 7.8 N of the load was applied to it.

ii) At various loads

To know the effect of the spring strength on the deviation of the hardness number, the spring of the tester (JOD-01) was set at soft, medium and hard conditions by adjusting the adjustment screw. At these three conditions, the hardness number of 5 corresponded to the loads of 3.7, 6.8 and 8.8 N, respectively. Three persons measured the hardness at these conditions.

3.3 Specimen Preparation

The process flow chart of specimen preparation is shown in Fig. 3.5. Firstly, all of the prepared materials which were clay, grog, sand and pottery stone were mixed together in dry mixer to get the homogeneous composition (see Fig. 3.6a). All compositions of clay bodies are shown in Table 3.3. Then, the wet mixing was performed by adding water approximately 20 wt% (dry basis). After that the wet mixture was kneaded by hand to get a clay dough (Fig 3.6b and c). Then, the dough was wrapped with plastic film and kept for 2 days to homogenize the moisture in the dough. After 2 days, the dough was extruded to 40 mm in diameter and approximately 70 mm in length for measuring its hardness. The hardness of the dough was measured by hardness tester (JOD-01), which was calibrated by adjusting the force of spring through the adjustment screw. The spring was so calibrated that the hardness number 10 when 7.8 N of the load was applied to it. The measurement method is shown in 3.2.3(b) (see Fig 3.7). The hardness of all compositions was controlled closing to 10 of hardness scale number. If the hardness of the dough was over 10, a small amount of water was

added and the dough was kneaded by hand again. On the contrary, if the hardness was less than 10, the dough was dewatered on plaster of Paris plate and mixed again until the hardness became 10.

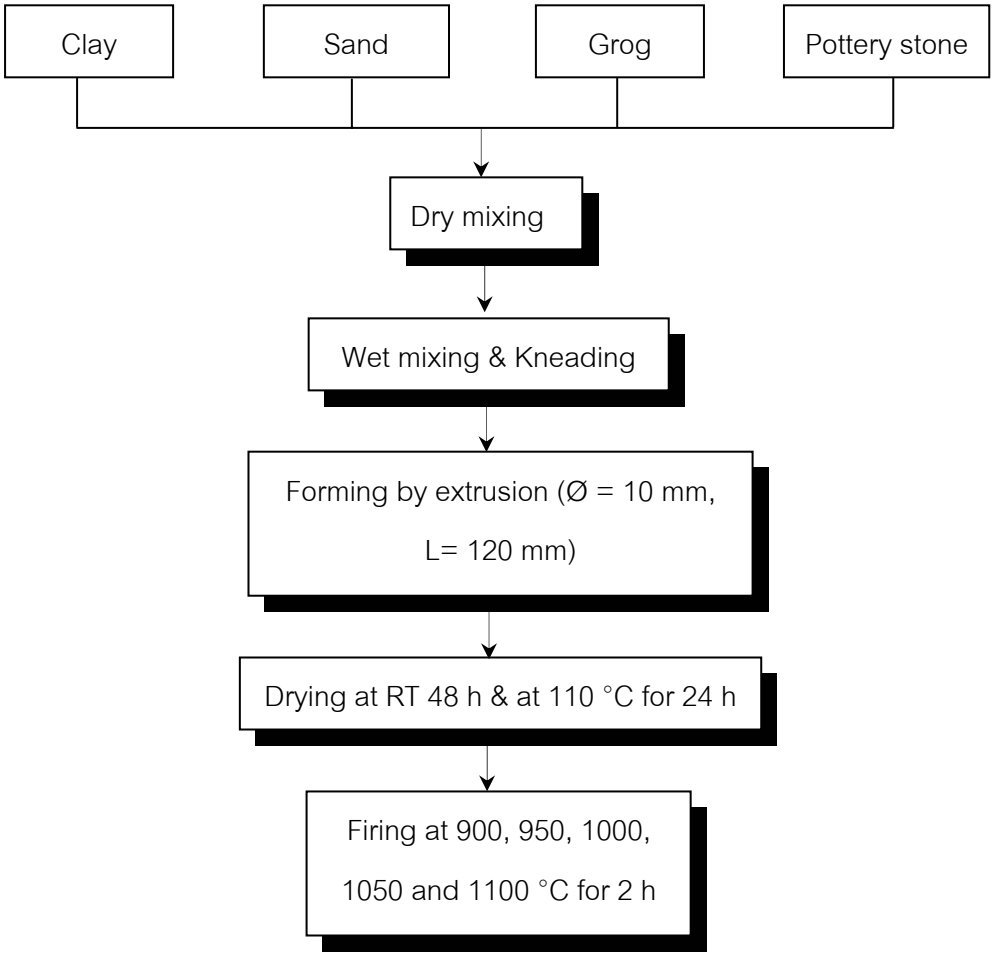

Fig. 3.5 Flow chart of specimen preparation

The specimens were extruded into round rods approximately 10 mm in diameter and 120 mm in length (see Fig. 3.8). Then, specimens were dried at room temperature for 48 h (see Fig. 3.9). After that, they were dried in an oven at 110 °C for 24 h. In this drying process, the drying shrinkage was measured. Dried specimens were fired at 900, 950, 1000, 1050 and 1100 °C for 2 h, at a heating rate of 3 °C/min. Then, the firing shrinkages were also measured.

a) Dry mixing

b) Kneading

c) Dough

Fig. 3.6 Mixing process for preparing the clay dough

Fig. 3.7 Picture of measuring method for controlling hardness of the clay dough

Fig. 3.8 Extrusion of test specimens

Fig. 3.9 Drying of test specimens at room temperature

Table 3.3 Compositions of clay bodies for this experiment

Formula	Clay (wt%)	Grog (wt%)	Sand (wt%)	Pottery stone (wt%)
A	80	8	12	-
B	80	8	3	9
C	80	8	6	6
D	80	8	9	3
E	70	8	11	11
G	70	8	16.5	5.5
H	70	8	5.5	16.5
I	60	8	24	8
K	60	8	8	24
L	60	8	16	16
M	100	-	-	-

3.4 Property Measurement and Characterizations of Mixed Clay and Fired Specimens

3.4.1 Plasticity

Liquid limit (*LL*), plastic limit (*PL*) and plasticity index (*Ip*) of clay and mixed clay were measured by Atterberg limits in conformity with ASTM D4318-00 *(10)*. The equipment set of Atterberg limits is shown in Fig. 3.10. The plasticity index of clay was calculated as follows:

$$Ip = LL - PL$$

Where:

Ip = plasticity index, %

LL = liquid limit, %

PL = plastic limit, %

Fig. 3.10 Atterberg limits test equipment

3.4.2 Drying Sensitivity

Two methods used for measuring drying sensitivity of the clay bodies were Bigot curve and accelerated method proposed by Ratzenberger *(17)*. The details of the methods are as follows:

3.4.2.1 Bigot curve method

Before drawing Bigot curve, we have to find out the moisture content in the clay dough at the start point of drying, which corresponds to the Pfefferkorn coefficient of plasticity (*a* = 3.3) by using Pfefferkorn plasticity tester (see Fig. 3.11).

Upon completion of the test, the extent of the compression is shown on the two scales of the Pfefferkorn apparatus (see Fig. 3.12). The right-hand scale is provided with a metric division (mm). The left-hand scale indicates the relation of the height ratio (*a*) of the specimen before and after the test.

$$a = h_0/h_1$$

h_0 = the height of the uncompressed test specimen (40 mm)

h_1 = the height of the specimen after hitting by the rammer

The deformability of clays is classified into three groups by the proportionality factor *a* .

When *a* is less than 2.5, the clays is difficult to use because it is too dry.

When *a* lies between 2.5 and 4.0, the particular clay belongs to the group of satisfactory deformability.

When *a* is greater than 4.0, the clay begins to grow sticky.

(a) (b)

Fig. 3.11 Pfefferkorn plasticity tester (a) and equipment for preparing the test specimen (b)

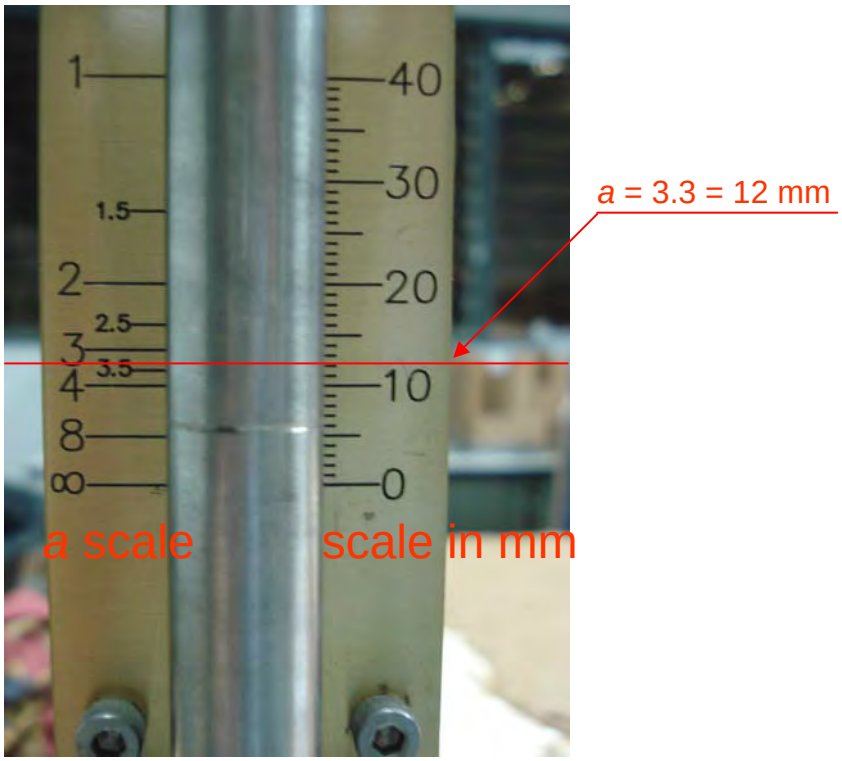

Fig. 3.12 Scale of Pfefferkorn plasticity tester

The details of finding the moisture content at a = 3.3 using Pfefferkorn plasticity tester are as follows:

(i) Preparing the test specimens

Raw materials of each formula were mixed with water into a semifluid pulp. Then, the pulp was poured on the plaster slab and allowed it to solidify to a plastic mass. In order to vary the water content, allow the pulp to dry up more or less on the plaster slab. Then, the specimen was formed in a cylindrical mould (∅ 33 × h 40 mm). Before starting the compression test, the specimen was weighed (G_1). This is necessary in order to ascertain the water content after the test.

(ii) Performing the test

Lift the rammer of Pfefferkorn tester and maintain it in the lifted position by inserting the circular eyelet pin into, and across, the shaft of the rammer. Cover the surfaces of the two brass plates of the Pfefferkorn tester with a thin oil film. Then, the test specimen prepared from *(i)* was placed centrically on the lower brass plate. Then, allowed the rammer to drop onto the test specimen. Make a note of the values (a) indicated by the round mark of the rammer on the graduated scales of the Pfefferkorn tester. The test procedure is also illustrated in Fig. 3.13.

(iii) Utilizing the results of the test

Upon the completion of the test, the compressed specimen was dried at the temperature of 110 °C until the weight of the specimen remains constant (G_2). Then, calculate the water content of the specimen as follows:

$$W = \frac{G_1 - G_2}{G_1} \times 100$$

where: W = water content of the test specimen

G_1 = the weight of the uncompressed, damp test specimen

G_2 = the weight of the specimen dried at 110 °C

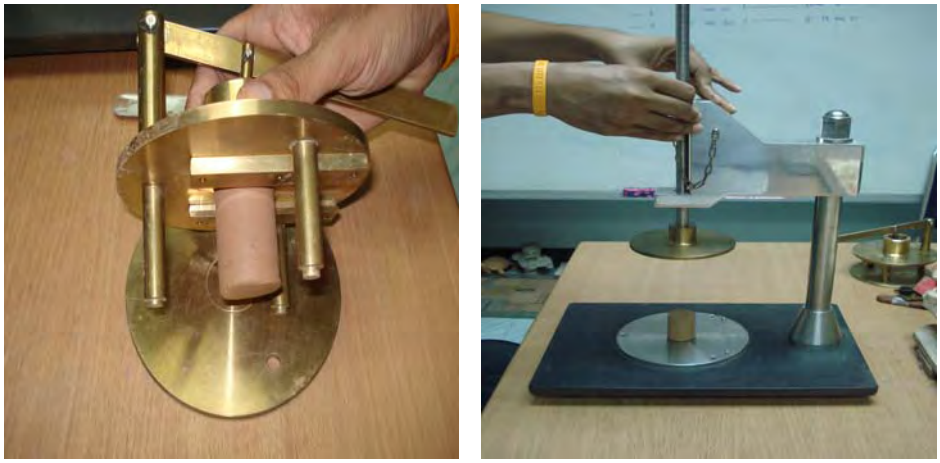

(a) (b)

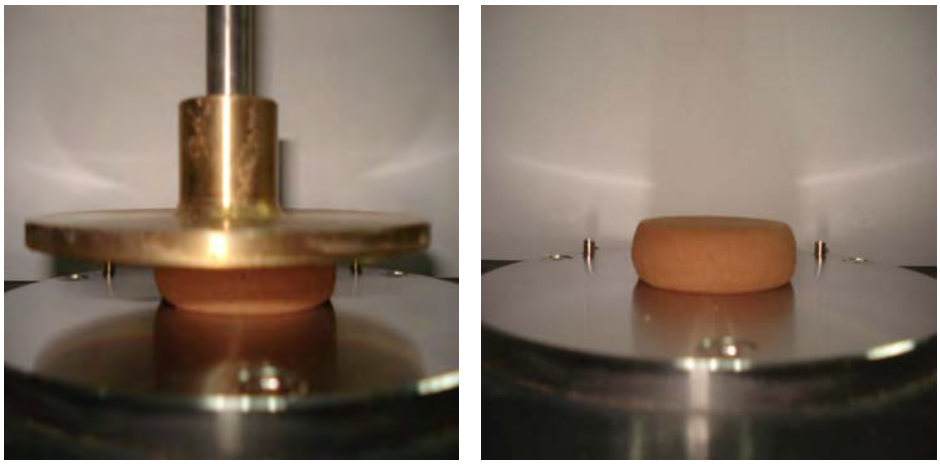

(c) (d)

Fig. 3.13 Test procedure to get Pfefferkorn coefficient of plasticity; (a) preparing the clay specimen, (b) setting the specimen to the Pfefferkorn tester, (c) the specimen is being compressed, and (d) compressed specimen

The process to determine the coefficient of plasticity is shown in the following example:

The mixed dough with different water content was prepared and the Pfefferkorn test was performed. The data of water content and height of specimen after the test are shown in Table 3.4.

Table 3.4 Pfefferkorn test result for formula A

a (mm)	*W* (%)
8.2	20.16
11.0	19.45
13.5	19.00
15.0	18.12

The heights of the specimens (*a*) were plotted against the water content of the specimens as shown in Fig. 3.14.

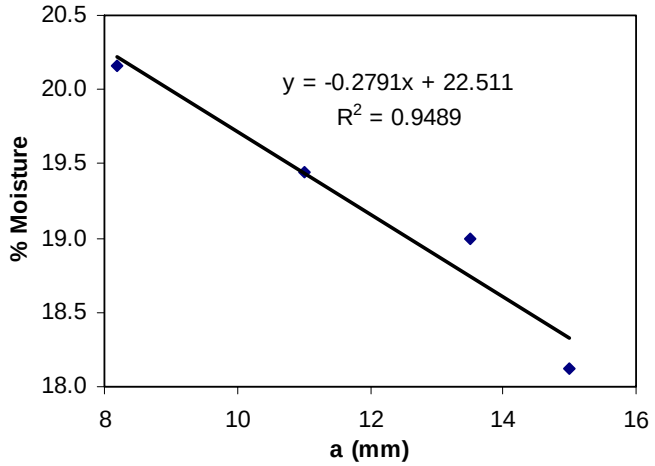

Fig. 3.14 Relationship between the water content and the height of the specimen (*a*) for the specimen (A)

From the intersection point of the value *a* = 12 mm or 3.3 in the curve, moisture content (W) is 19.16 %. The value 19.16 is the Pfefferkorn coefficient of plasticity for the mixed clay of formula A. This percentage of water content (19.16%) is the amount of water that will be used for mixing the clay bodies (formula A) on the drying sensitivity test. Pfefferkorn coefficients for other formulae are shown in Table 3.5.

Table 3.5 Moisture content at Pfefferkorn coefficient of plasticity of clay bodies

Formula	% moisture (wet basis) at *a* = 12 mm (3.3)
A	19.16
B	19.24
C	19.42
D	18.87
E	18.04
G	18.19
H	18.11
I	16.31
K	17.16
L	16.91
M	21.30

After obtaining the water content in all mixed clay formulae (Table 3.5) by Pfefferkorn test, the drying sensitivity of the bodies was tested by Bigot curve method as the following steps.

(i) Making the dough of each formula by adding the amount of water shown in Table 3.5. Then, wrapped the dough with plastic film and kept them at room temperature for 48 h. After 48 h of aging, the dough was formed into the plate of 120 × 20 × 5 mm.

(ii) The specimen was put on a glass plate inserting with a thin paper. The paper will shrink with the specimen during drying.

(iii) On the top surface of the specimen, 100 mm distance was marked.

(iv) The specimen was put in the room under the condition of no air flow.

(v) Measure the weight of the specimen together with the glass and the paper, and the length of the mark on the specimen was also measured at 0, 1, 2, 3,… until 48 h.

(vi) The specimen was dried at 110 °C until the weight became constant.

(vii) Plot the graph of the relationship between shrinkage and water content. An example of the graph is shown in Fig. 3.15.

(viii) Calculate the Drying Sensitivity Index-Bigot (*DSI-B*) using the following equation.

$$DSI - B = \frac{(M_i - M_c)}{100} \times DS$$

where: *DSI-B* = Drying Sensitivity Index-Bigot

M_i = the initial moisture of the dough (%)

M_c = the critical moisture at which the linear drying shrinkage finishes (%)

DS = drying shrinkage from Bigot curve after dried at 110 °C for 24 h (%)

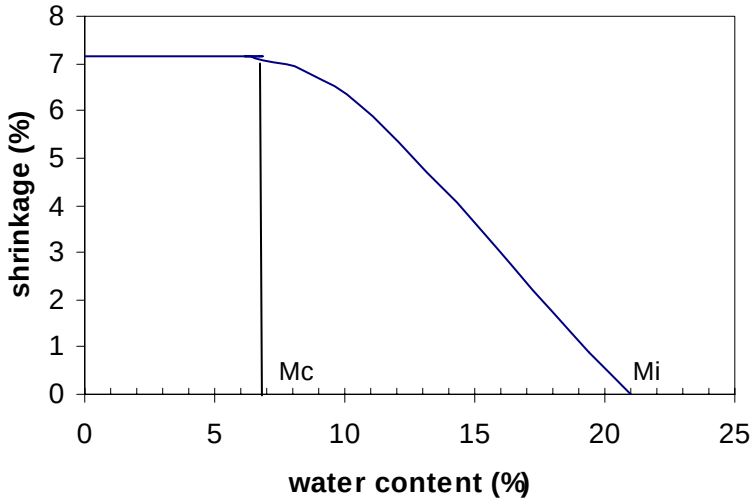

Fig. 3.15 Bigot curve plotted between shrinkage and water content of the test specimen

3.4.2.2 Accelerated method proposed by Ratzenberger

The principle of this method is calculated based on the first maximum of moisture difference (*MD-I*) between the edges and the center of the test piece. Generally, *MD-I* of the clay body occurs at the initial drying phase (the constant rate period of drying), i.e. in the range of the linear increase in drying shrinkage. This is the period in which cracks are liable to occur during drying of the green ware *(17)*. After the drying shrinkage has been completed, the risk of cracking disappears, owing to the fact that the mechanical stresses arising have largely been offset. Therefore, we have to

observe the *MD-I* of each clay body and used this value for calculating the Drying Sensitivity Index-Ratzenberger (*DSI-R*) of the test specimen. To find out the *MD-I* of each clay body, the experiment was carried out by determining the moisture difference (*MD*) of the test specimen with variation of drying times. The experimental procedures are as follows:

The mixed clay dough was made by the same method as Bigot curve method using the water contents in Table 3.5. After 48 h of aging, the dough was extruded into a cylindrical bar (150 mm length × 25 mm diameter). The cylinder surface of specimen was coated with polyurethane resin (Peony 52-60) to protect against moisture evaporation; only the two circular ends served as evaporation surfaces. The specimen was dried in an oven at 65 °C with different drying times of 2.5, 5, 7.5, 10, 15, 20 and 50 h. After drying at each drying time, the two cylinder ends (20 mm each) of the specimen were cut and dried at 110 °C for 24 h to find out the moisture content. The moisture contents of the two cylinder ends were averaged and denoted as External Water (*EW*). The Internal Water (*IW*) is the moisture content in the central twenty millimeters of the specimen. The test specimen is depicted in Fig. 3.16. The Moisture Difference (*MD*) is the variation of internal and external water: *IW* – *EW*. Drying Sensitivity Index (*DSI-R*) is calculated as follows:

$$DSI - R = LDS \times MD - I$$

Where *LDS* is the linear drying shrinkage of extruded specimen dried at 110 °C for 24 h

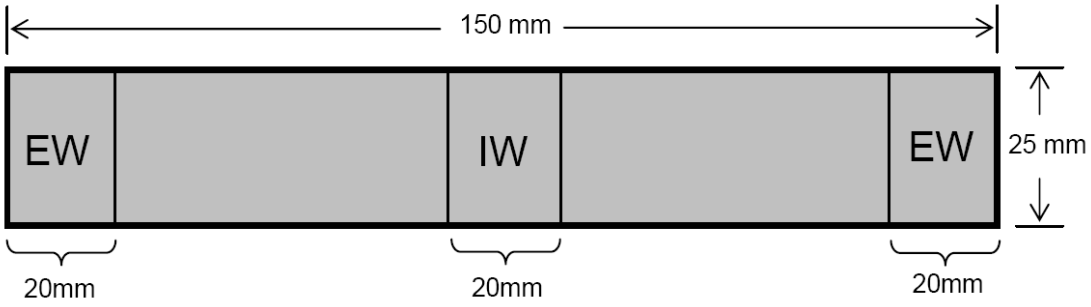

Fig. 3.16 Schematic structure of the test specimen for testing the drying sensitivity by Ratzenberger method

3.4.3 Drying Shrinkage

Linear drying shrinkage (S_d) of specimens was measured by measuring the length of specimens before drying (L_p) compared with the length of specimens after dried at 110 °C (L_d) according to ASTM C326-82 *(40)*. The percentage of linear drying shrinkage was calculated as follows.

$$S_d = (L_p - L_d)/L_p \times 100$$

where: S_d = linear drying shrinkage, %

L_p = length of specimen before drying, and

L_d = length of dried specimen

3.4.4 Firing Shrinkage

The percentage of linear firing shrinkage was calculated as follows:

$$S_f = (L_d - L_f)/L_d \times 100$$

where: S_f = linear drying shrinkage (%)

L_d = length of dried specimen, and

L_f = length of fired specimen

3.4.5 Bulk Density and Water Absorption

Bulk density and water absorption of fired specimens were measured by Archimedes' method according to ASTM C373-88 *(41)*.The calculations are as follows:

$$B = D/(D - S)$$

where: B = bulk density (g/cm^3)

D = dry weight (g)

S = suspended weight in water (g)

$$A = [(M - D)/D] \times 100$$

where: A = water absorption (%)

M = saturated weight (g)

3.4.6 Modulus of Rupture of Green and Fired Specimens

Moduli of rupture of green and fired specimens were measured by 3-point bending test in conformity with ASTM C 674-88 *(42)*. All tests were performed by universal testing machine (Instron 5844, USA). The crosshead speed was constant at 0.5 mm/min. The modulus of rupture of each specimen was calculated as follows:

$$M = \frac{8PL}{\pi d^3}$$

Where: M = modulus of rupture (MPa)

P = load at rupture (N)

L = distance between supports (mm)

d = diameter of specimen (mm)

3.4.7 Thermal Expansion Coefficient

Thermal expansion curve of fired bodies was measured using dilatometor (DIL 402C, Netzsch, Germany) with heating rate of 10 °C/min up to 700 °C. The test piece for the analysis was prepared by making a rod specimen with 8 mm long and 5 mm in diameter. Thermal expansion coefficient was calculated from the curve.

3.4.8 Mineral Phase of Fired Specimens

The qualitative analyses of fired specimens were performed by the same X-ray diffractometor and at the same conditions designated as in section 3.1.2.

CHAPTER IV

RESULTS AND DISCUSSION

4.1 Properties of Raw Materials

4.1.1 Ratchaburi Red Clay

Chemical analysis (Table 4.1) of original clay (Ratchaburi red clay) shows a relative abundance of silica (~63%) and alumina (~18%) with Fe content about 4%. It includes approximately 1% of K_2O and TiO_2 and a little amount of CaO, MgO and Na_2O, which act as fluxing agent for the clay body. Loss on ignition (L.O.I.) value of clay is very high (10.54%), because organic matters and combined water in clay are burnt out.

Table 4.1 Chemical composition of red clay

Compositions (wt%)										
SiO_2	Al_2O_3	Fe_2O_3	CaO	MgO	Na_2O	K_2O	TiO_2	MnO	P_2O_5	L.O.I.
62.98	17.94	4.14	0.52	0.56	0.16	1.10	1.04	0.01	0.05	10.54

The X-ray diffraction (XRD) pattern of clay is shown in Fig. 4.1. For the as-received clay (Fig. 4.1(a)), the main mineral is quartz and there are some amounts of kaolinite, and illite minerals shown in the XRD pattern. These minerals can be found in general clay. The peak intensities of kaolinite and illite are strongly disturbed by the peak of quartz. To characterize only clay fraction, fine particle of clay (<2 μm) was separated by sedimentation method and identified by XRD. It was observed that the fine grained kaolinite and illite are the constituent of this clay. It shows that this clay is a mixed layer structure, so called illitic-kaolinitic clay.

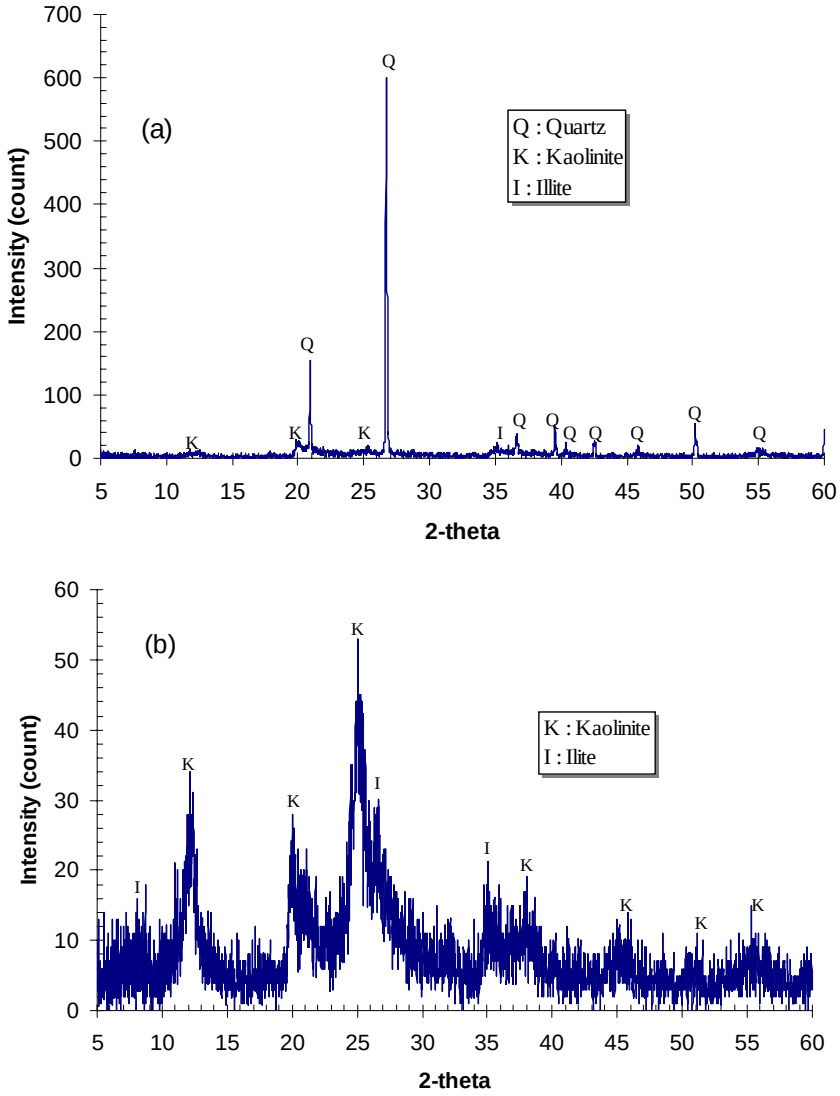

Fig. 4.1 XRD patterns of the red clay; (a) as-received clay and (b) fine particle fraction (<2 μm)

Thermal behaviors of the clay were analyzed by TG-DTG-DTA unit. TG-DTG-DTA curves of clay are shown in Fig. 4.2. The DTA curve shows two endothermic peaks at 120 °C corresponding to the loss of adsorbed water and at 549 °C corresponding to the decomposition of kaolinite, loss of its hydroxyl groups as water (reaction 1). A further peak, which is exothermic, occurs at about 923.8 °C. It is associated with the recrystallization process. The mineral decomposed is metakaolin and the new mineral phase from the recrystallization process might be silicon spinel (reaction 2). The decomposition and recrystallization reactions of kaolinite are shown in reaction (1), (2) and (3).*(44)*

$$Al_2Si_2O_5(OH)_4 \xrightarrow{450^\circ C} Al_2Si_2O_7 + 2H_2O \quad \text{----------(1)}$$

Kaolinite Metakaolin

$$2(Al_2O_3.2SiO_2) \xrightarrow{925^\circ C} 2Al_2O_3.3SiO_2 + SiO_2 \quad \text{----------(2)}$$

Metakaolin Silicon spinel

$$2Al_2O_3.3SiO_2 \xrightarrow{1100^\circ C} 2(Al_2O_3.SiO_2) + SiO_2 \quad \text{----------(3)}$$

Silicon spinel pseudo-mullite

Total mass loss of clay from TG curve is about 11.05 wt%. This amount is a little larger than the value of L.O.I. (10.54 %) by chemical analysis.

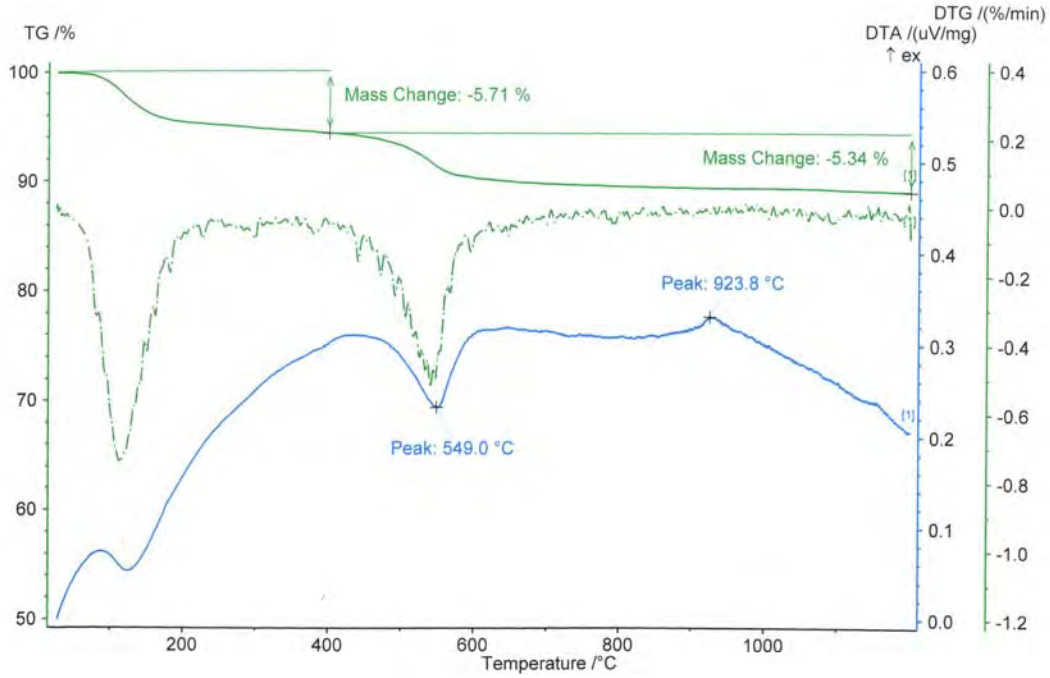

Fig. 4.2 TG-DTG-DTA curves of clay

The particle size distribution and particle morphology of clay are shown in Fig. 4.3 and 4.4, respectively. The particle size of clay is very small. The range of particle is between 0.2 to 10 μm and the average particle size is only 4 μm. Larger particles over 2-3 μm might be quartz and smaller ones might be clay. The particles observed in Fig. 4.4 are quartz because the particle size of clay should be smaller than 2 μm.

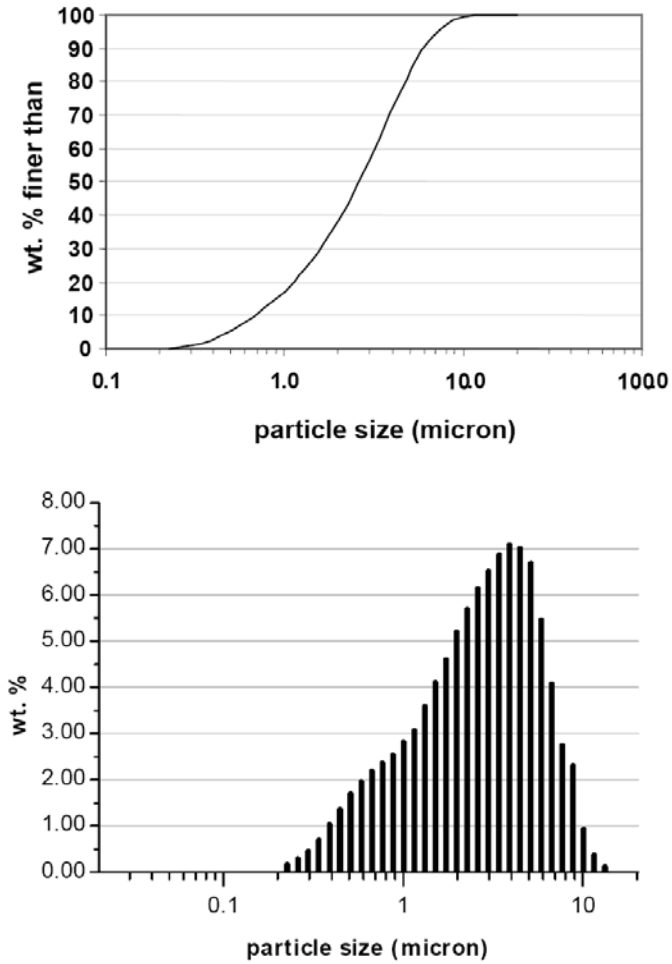

Fig. 4.3 Particle size distribution of clay

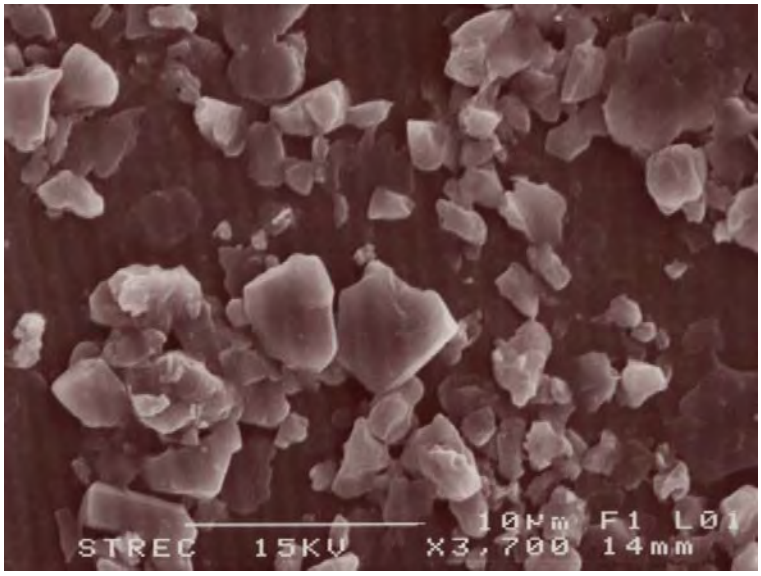

Fig. 4.4 SEM micrograph of clay

4.1.2 Pottery Stone

Chemical composition of pottery stone analyzed by X-ray fluorescence (XRF) is shown in Table 4.2.

Table 4.2 Chemical composition of pottery stone

Compositions (wt%)									
SiO_2	Al_2O_3	Fe_2O_3	CaO	MgO	Na_2O	K_2O	TiO_2	P_2O_5	L.O.I.
77.59	12.39	0.75	0.21	0.10	2.94	4.37	0.17	0.03	0.95

XRD pattern of pottery stone is shown in Fig. 4.5. The major phases appeared in the XRD pattern are tridymite (SiO_2) and feldspar ($Na(AlSi_3O_8)$). There are also small peaks of quartz and kaolinite phases present.

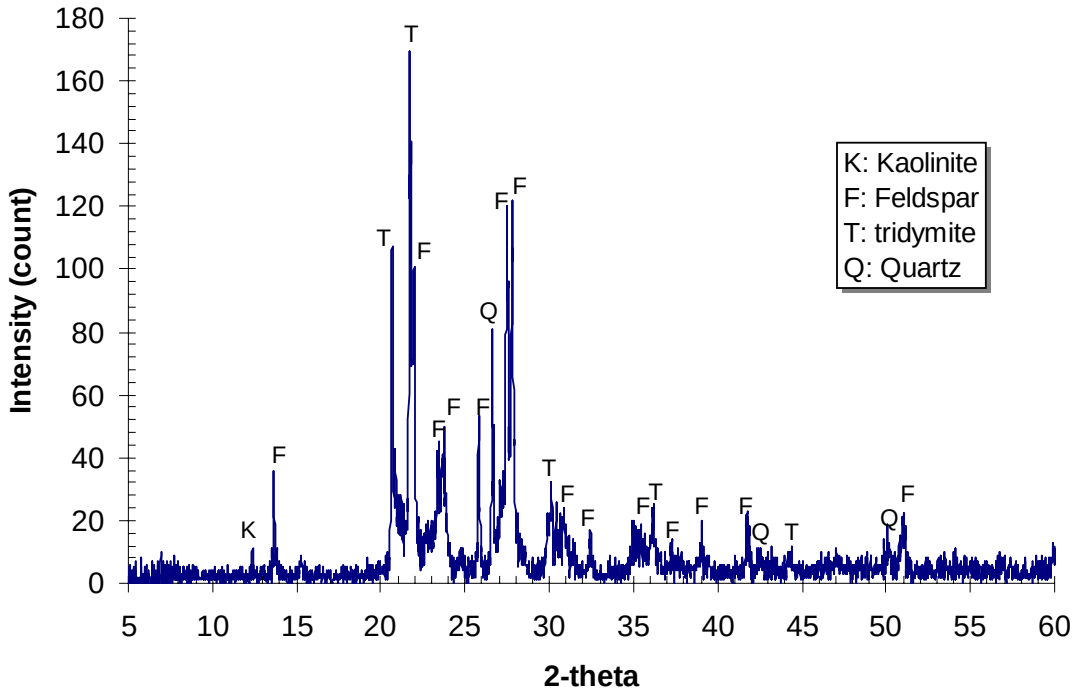

Fig. 4.5 XRD pattern of pottery stone

TG-DTG-DTA curves of pottery stone are shown in Fig. 4.6. TGA curve shows two small slopes of mass loss at around 100 °C corresponding to the loss of adsorbed moisture and at 500 °C corresponding to the loss of organic materials in pottery stone and/or structural water of clay in pottery stone. They are clearly observed

by DTG curve. The total mass loss at the temperature ranging from room temperature to 1200 °C is 0.83% which corresponds to 0.95% of L.O.I. from chemical analysis data. In addition, there is almost no any change in DTA curve. There are only two very small endothermic peaks observed at around 200 °C and 500 °C corresponding to the loss of adsorbed and structural water, respectively.

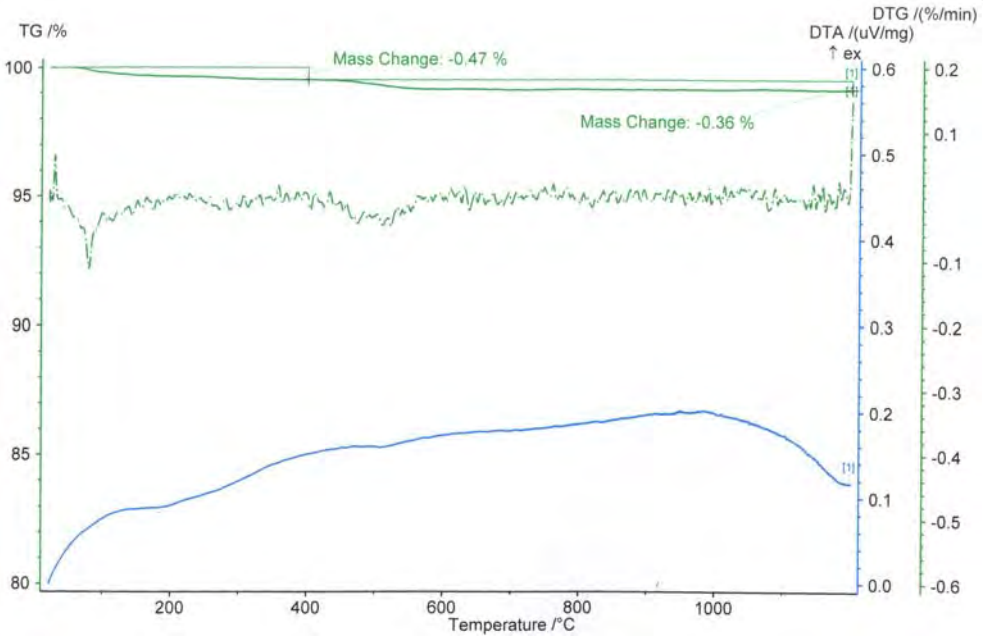

Fig. 4.6 TG-DTG-DTA curves of pottery stone

The particle morphology of pottery stone passed 40 mesh sieve is shown in Fig. 4.7.

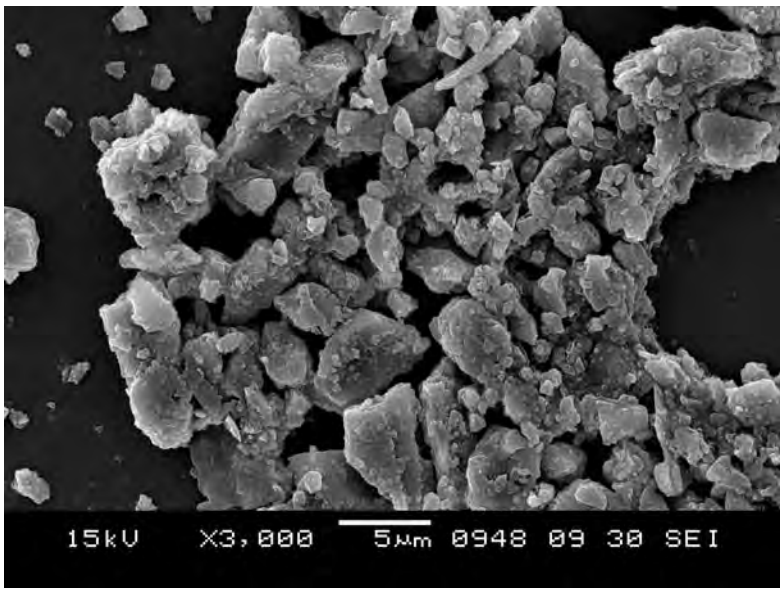

Fig. 4.7 SEM micrograph of pottery stone

4.1.3 Sand and Grog

Chemical compositions of sand and grog analyzed by X-ray fluorescence (XRF) are shown in Table 4.3. Sand includes mainly silica (~87%) with 6 and 3.4% of alumina and potassium oxide, respectively. It also includes a little amount of impurities like Fe_2O_3, CaO, MgO, Na_2O and TiO_2. As seen in Fig. 4.8, XRD pattern of sand shows the peaks of quartz (SiO_2) and microcline ($K_2O.Al_2O_3.6SiO_2$). The amount of K_2O in sand is 3.41%. Then, the amounts of Al_2O_3 and SiO_2 belonged to microcline are calculated to be 3.69% and 13.08%, respectively. Therefore, the remaining Al_2O_3 (2.39%) corresponding to SiO_2 2.82% might belong to clay mineral (kaolinite, $Al_2O_3.2\ SiO_2.2H_2O$). As a result, there is approximately 71.49% of SiO_2 as quartz. It is concluded that the sand consists of 71.49% quartz, 20.18% microcline, 6.05% clay mineral, 1.19% impurities, and 1.09% of mass loss due to burning out of organic materials.

Table 4.3 Chemical compositions of sand and grog

Wt%	SiO_2	Al_2O_3	Fe_2O_3	CaO	MgO	Na_2O	K_2O	TiO_2	P_2O_5	SO_3	L.O.I.
Sand	87.39	6.08	1.19	0.41	0.16	0.13	3.41	0.14	-	-	1.09
Grog	66.47	19.87	4.80	1.00	0.55	0.98	1.88	1.13	0.12	0.87	2.14

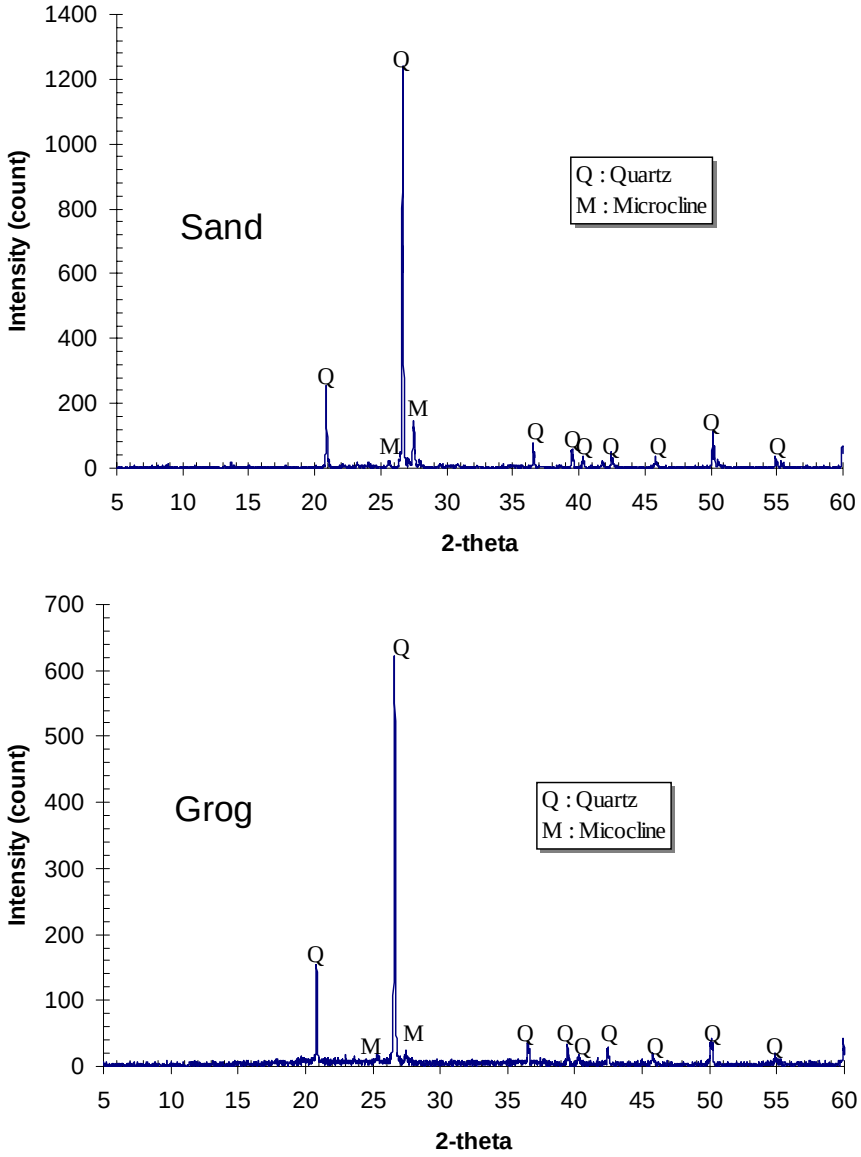

Fig. 4.8 XRD patterns of sand and grog

Grog is the material obtained from broken pottery made of mainly red clay and sand. Therefore, its chemical composition is similar to the original red clay. It includes a large amount of silica, alumina and small amount of impurities (Fe, Ca, Mg, Na and Ti). In addition, the silica content in grog is a little higher than that of the original clay because the pottery is produced from red clay and sand. The XRD pattern of grog (Fig. 4.8) shows mainly peak of quartz with very small peak of microcline.

Particle morphology of sand and grog by SEM is shown in Fig. 4.9. Both of sand and grog used in this experiment were screened through a sieve number 40 meshes (~375 μm). Thus, the particle size of sand and grog are surely smaller than 375 μm, but the size distribution of particle is not similar. By looking at the SEM images in Fig. 4.9, sand look like round particle with similar size, but grog shows sharp edged particle with various sizes.

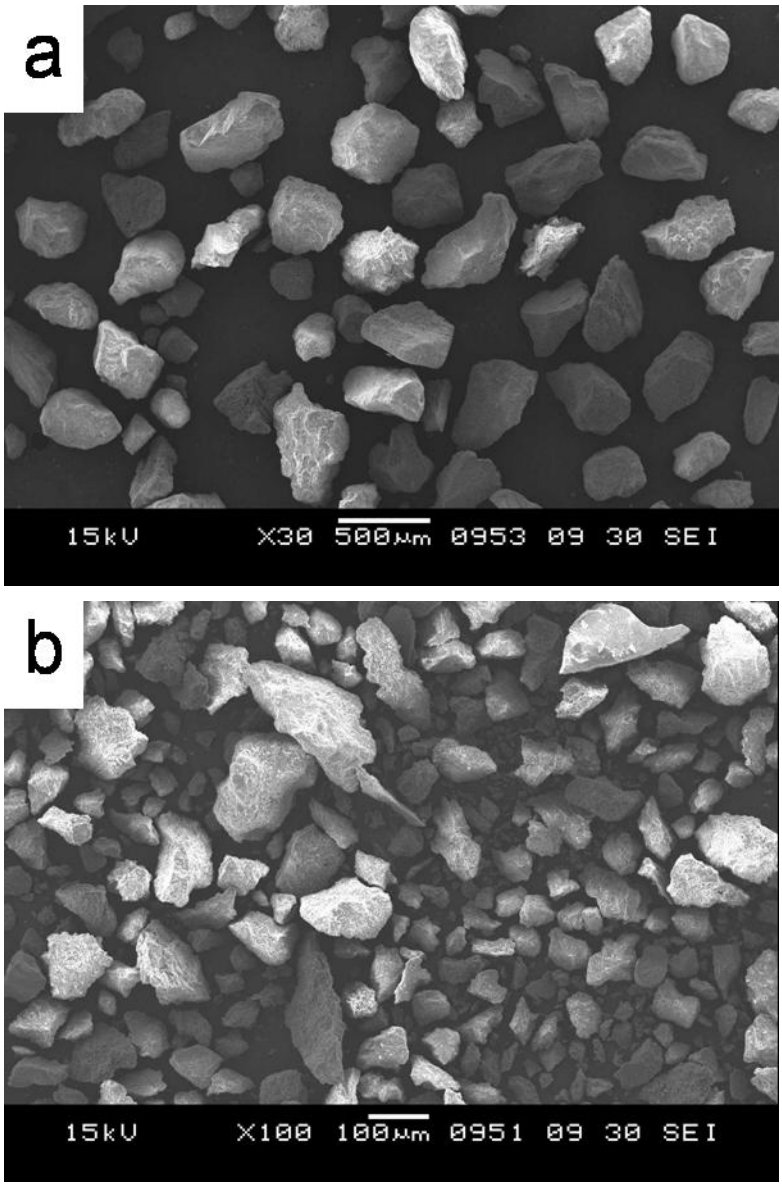

Fig. 4.9 SEM micrographs of sand (a) and grog (b)

4.2 Calibration of Clay Hardness Tester

4.2.1 Hardness before Training and Calibration of the Testers

The hardness numbers obtained by 5 persons before training and calibration are shown in Fig. 4.10. The average hardness numbers with standard deviations due to personnel obtained for each tool are 8.5 ± 0.6 for POD-01, 9.8 ± 0.4 for JOD-01, 10.5 ± 0.3 for POD-02, 11.7 ± 0.6 for PN-01 and 12.1 ± 0.6 for PN-02. In comparison, these standard deviations are less reliable due to calculation from such a few numbers of data (only 5). The error bars shown in the figure are the standard deviation for each person/tool pair which is calculated using ten numbers of data. Hence, they are more reliable. Considering all the data from 5 persons for each tool, the hardness number values wildly fluctuated. The causes of those fluctuations are thought to be the sum of the human error, difference among non calibrated tools, intrinsic accuracy limit coming from the tool, and the hardness inhomogeneity of the dough.

During the experiment, it was found that the speed of pressing was different from person to person. When the cone was pressed quickly, reading scale showed large number, and after pressing the hardness number tended to drift down with time. When the cone was pressed slowly, there was no overrun in the hardness number. When the cone was pressed slantingly to the surface of the dough, the hardness number was a little smaller than the value when it was pressed vertically.

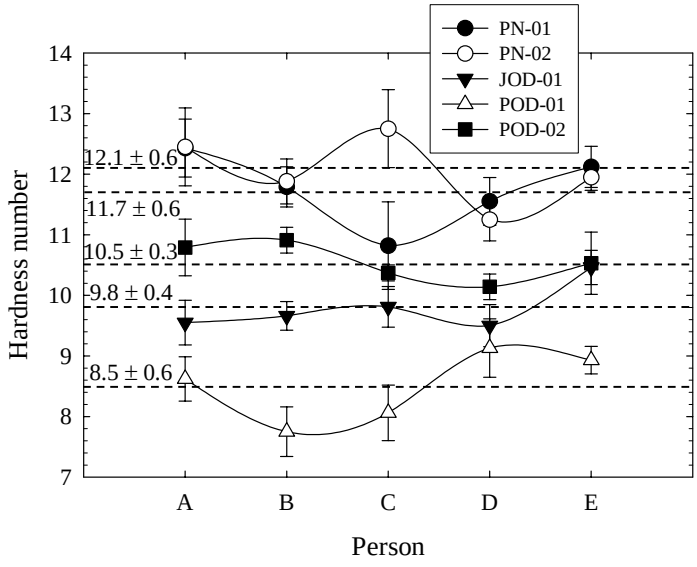

Fig. 4.10 Hardness numbers obtained by 5 persons before training using non-calibrated tools

Considering the observations mentioned above, it is supposed that the human errors are largely caused by lacking of standard testing procedure, i.e. the different speed of pressing the cone, reading time of the hardness number after pressing and pressing angle of the cone to the dough surface.

4.2.2 Hardness after Training without Calibration of the Testers

Considering the results of 4.2.1 presented in Fig. 4.10, the same five persons were trained that the tool should be pressed perpendicular to the surface of the dough, the pressing speed should not be too quick, and the hardness number should be read after the drift of the reading scale almost stopped. Before the formal experiment, they trained themselves following the instructions.

The hardness numbers obtained by 5 persons after training without calibration of tools are shown in Fig. 4.11. The average hardness numbers with standard deviations obtained from the 5 tools are 9.8 ± 0.2 for POD-01, 10.8 ± 0.2 for JOD-01, 11.5 ± 0.2 for POD-02, 13.6 ± 0.2 for PN-01 and 14.0 ± 0.1 for PN-02. After training, the results clearly indicate that the fluctuations of the data of each hardness tester are less than those of before training. This means that the testing procedure is one of the major causes of the fluctuation of the data. However, the hardness number of each hardness tester still varies because the hardness testers have not been calibrated.

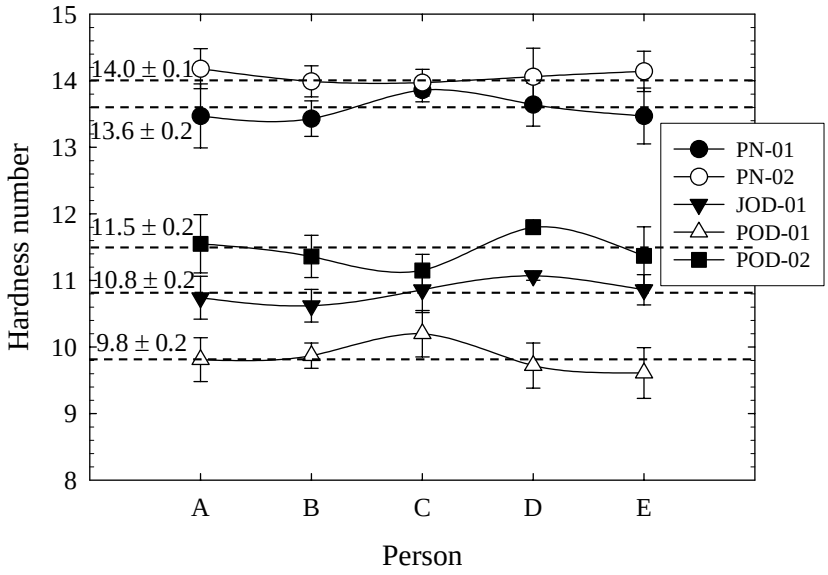

Fig. 4.11 Hardness numbers obtained by 5 persons after training using non-calibrated tools

Incidentally, the average hardness numbers shown in Fig. 4.10 and 4.11 are not significantly different. Comparing the hardness value of each tool, the differences are 1.3 for POD-01, 1.0 for POD-02, 1.0 for JOD-01, and 1.9 for PN-01 and PN-02. The difference may also come from the variation of the dough. However, it can be concluded that the absolute value was different for the tools of different design. We could not make clear the cause of the difference in this experiment.

4.2.3 Hardness after Training and Calibration of the Testers

(1) At a fixed load

The relationship between hardness number and the person after training using the calibrated tools is shown in Fig. 4.12. The graph shows that the data are obviously separated into two groups. Group 1 consisting of POD-01, POD-02 and JOD-01 shows lower hardness values on the graph. The average hardness numbers are 9.4 ± 0.2 for POD-01, 9.7 ± 0.3 for POD-02 and 9.7 ± 0.1 for JOD-01. It is noted that the hardness values are insignificantly different when the tools were calibrated. The difference of the decimal numbers (about 0.3) is regarded as the error from reading. PN-01 and PN-02, which indicated higher hardness values, belong to group 2. Their hardness values are the same value of 11.5. This is due to the distinction between the designs of the two tool groups, especially the length of their cones as mentioned in 3.2.1. It implies that even though the hardness testers were calibrated so that the hardness number shows 10 at the same load of 7.8 N, still the hardness number values corresponding to the cone area resisting to the force of spring is dependent on the design. This phenomenon can be schematically illustrated as Fig. 4.14.

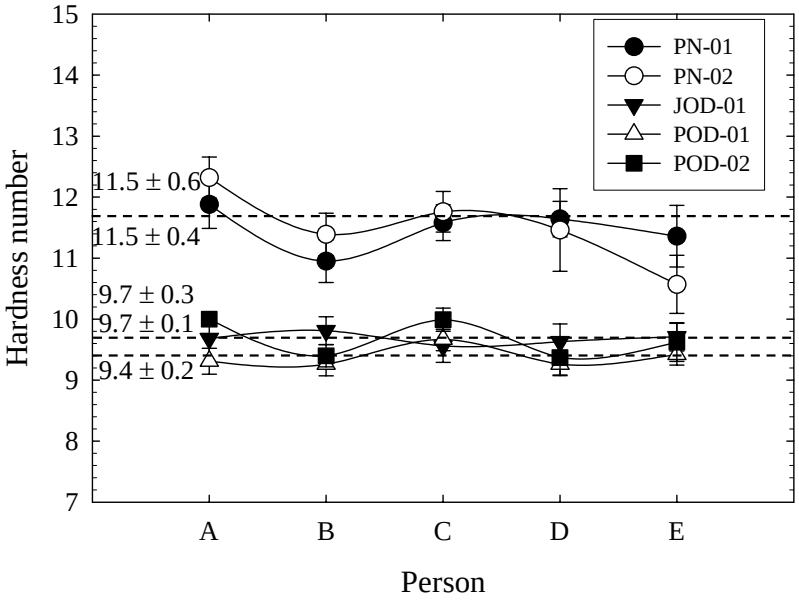

Fig. 4.12 Hardness numbers obtained by 5 persons after training using calibrated tools

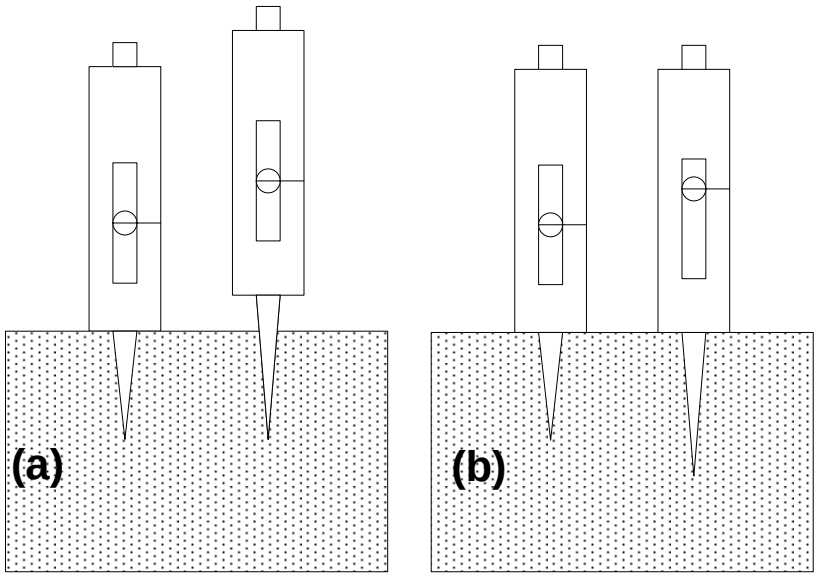

Fig. 4.13 Schematic structures illustrating the measured results after calibration and training using the hardness testers with different designs

Figure 4.13(a) depicts that the supporting base of PN-01 and PN-02 can not reach the clay surface while the hardness number on the scale become 10. In the case of JOD-01, POD-01 and POD-02, which have the shorter cones, their supporting bases reach the clay surface. This condition is instructed as the corrective condition for measuring the hardness of the clay. If PN-01 and PN-02 are used in the corrective way,

the additional force has to be applied to them to push their supporting bases to reach the surface of the samples as shown in Fig. 4.13(b). As a result, the hardness number becomes 12 instead of 10 (see Fig. 4.13(b)). Hence, this is the reason why the hardness number from PN-01 and PN-02 are always higher than those of JOD-01, POD-01 and POD-02. It is concluded that the hardness values obtained from the testers of the same type but of different designs as described above can not be compared. It means that the hardness number values can be compared only when the design, especially the figure of the cone is exactly the same.

The large deviations of the average hardness numbers of PN-01 and PN-02 come from the larger value obtained by person A and the small value obtained by person E. It is possible that they might not follow the measurement instructions.

(2) At various loads

When spring is calibrated “Hard” the cone sticks into the clay specimen deeply and when spring is calibrated “Soft”, it is in reverse. When the cone does not stick in deeply, a small area of cone resists the force of the spring. In such a condition, we think that the deviation of the measured hardness value may increase due to a small cone area.

To know the effect of the spring strength on the hardness values and deviations of the hardness testers, the springs was set at soft, medium and hard conditions as described in 3.2.3(c(ii)). The measured values of three persons are plotted in Fig. 4.14. The average hardness values from three persons are about 10 at soft, 9 at medium and 8 at hard. The deviation of the hardness number is not significantly different as shown in the error bar and number in parenthesis in Fig. 4.14. As a result, it is suggested that the calibration load of the spring be not restricted to some values. One of the calibration requirements is that the reading scale indicator of the tool should be set to the center of the hardness number in the case.

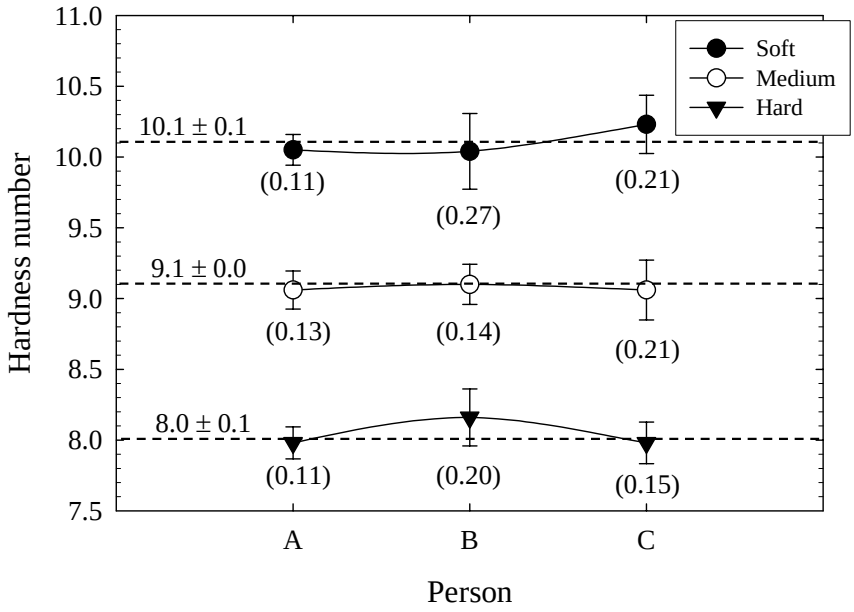

Fig. 4.14 Hardness number obtained by 3 persons at different calibration (numbers in the parenthesis show the standard deviation for each person/tool measurement)

From the results of the experiment, it was concluded that the factors affecting the hardness values of the clay sample measured with the different design hardness testers can be drawn as follows:

(1) The human error is one of the big factors affecting the deviation of the hardness number value and when a person is guided properly, the human error can be decreased easily.

(2) The design of the hardness tester, especially the figure of the cone, strongly affects the hardness number. When the figure of the cone is different, the testers can not be calibrated to give the similar hardness value even the spring is set at the same load. The hardness number values can be compared only when the testers have the same design.

(3) The hardness number values obtained are changed by the calibration. The hardness number values of each tester give a narrow distribution after the calibration.

4.3 Properties of Green Body

4.3.1 Plasticity

The plasticity parameters of the compositions for the clay bodies, in terms of the Atterberg limits, are shown in Table 4.4. It can be observed that the values of the plasticity index of all formulae except M (pure clay) range from 36.0 to 46.7 %. As seen in Fig. 4.15 and 4.16, plasticity index decreases with increasing the additive content. From this data, it can be concluded that adding sand and pottery stone can reduce the plasticity of the clay body.

Table 4.4 Plasticity of the clay bodies

Formula	Liquid limit (*LL*) (%)	Plastic limit (*PL*) (%)	Plasticity index (*Ip*) (%)
A	58.3	12.7	45.6
B	60.9	14.3	46.6
C	58.8	13.9	44.9
D	57.7	14.2	43.5
E	54.1	12.8	41.3
G	51.7	12.1	39.6
H	55.0	13.4	41.6
I	46.1	10.0	36.1
K	50.0	13.1	36.9
L	48.5	12.2	36.3
M	69.0	15.2	53.8

It is clearly observed from Fig. 4.16 that additive content in the bodies strongly affects the plasticity index (*Ip*) of the clay bodies. It can be concluded that the lower clay content, the lower plasticity index is. In addition, sand/pottery stone ratio has less effect on plasticity index than the total content of additive content in the body. This might be due to the similarity between the compositions of sand and pottery stone since

they both contain mainly SiO_2. Effect of sand/pottery stone ratio on the plasticity index of the clay bodies is shown in Fig. 4.17.

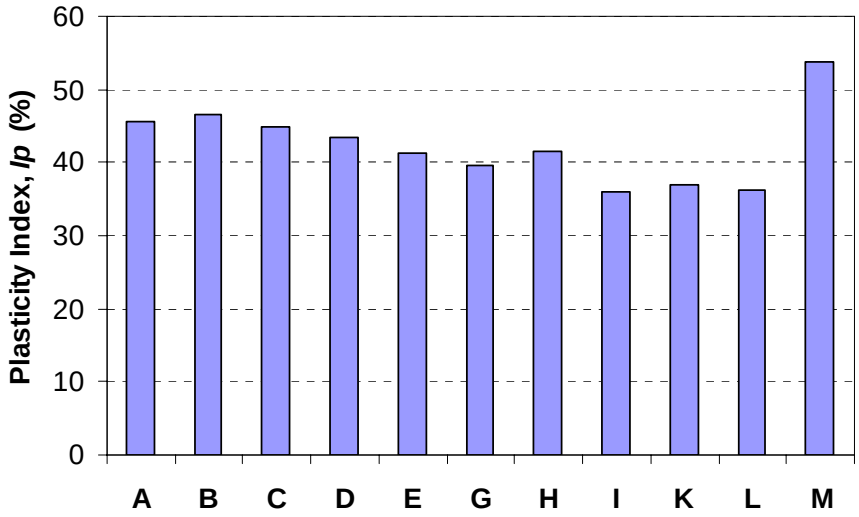

Fig. 4.15 Comparison of plasticity index of the clay bodies

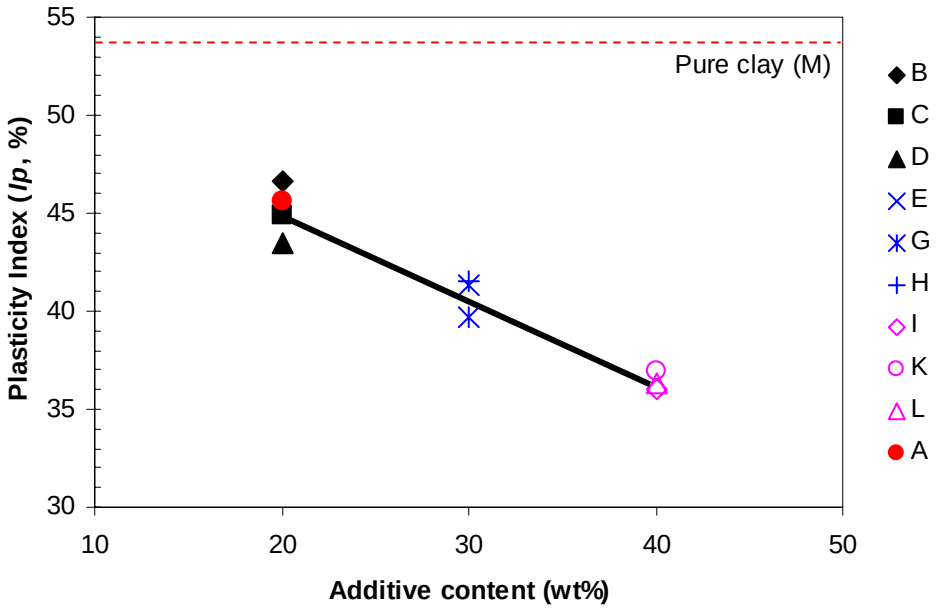

Fig. 4.16 Effect of additive content on plasticity index of the clay bodies

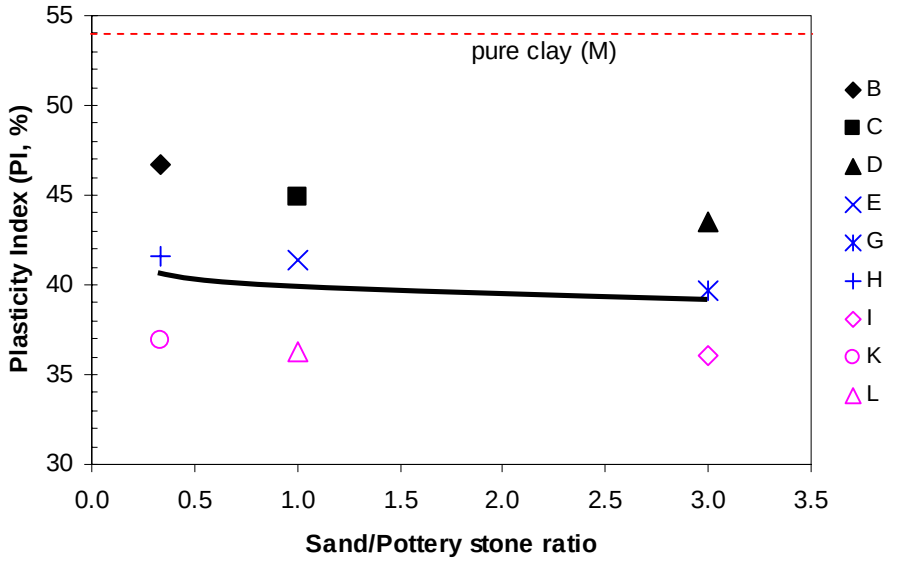

Fig. 4.17 Effect of sand/pottery stone ratio on plasticity index of the clay bodies

4.3.2 Drying Shrinkage and Green Strength

As expected, drying shrinkage decreased with increasing additive content in the clay bodies as shown in Fig. 4.18. During the drying process, the clay bodies shrank about 6% (L) up to 7.6% (C). This behavior is also related to the different amount of working water used in the processing presented in Fig. 4.19, since the more working moisture is required, the higher the drying shrinkage.

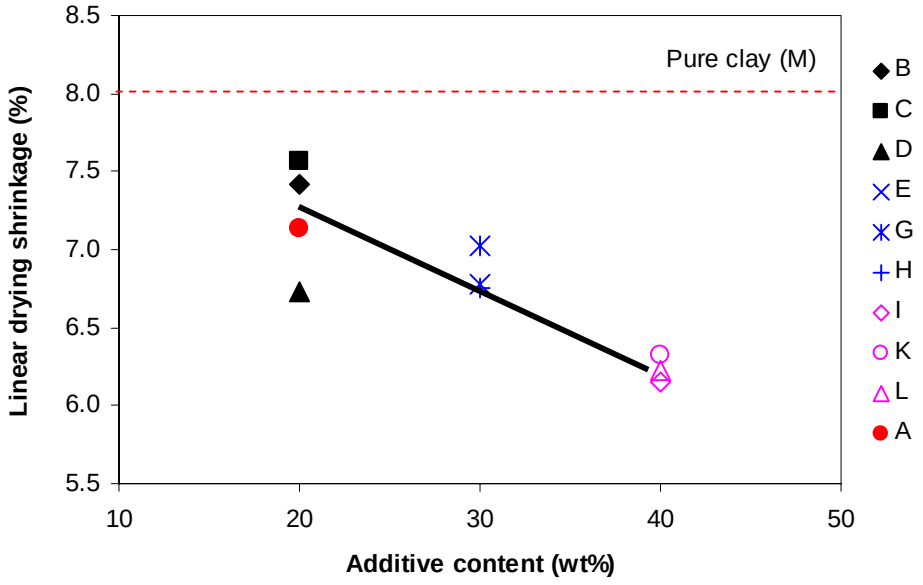

Fig. 4.18 Effect of additive content on the drying shrinkage of the clay bodies

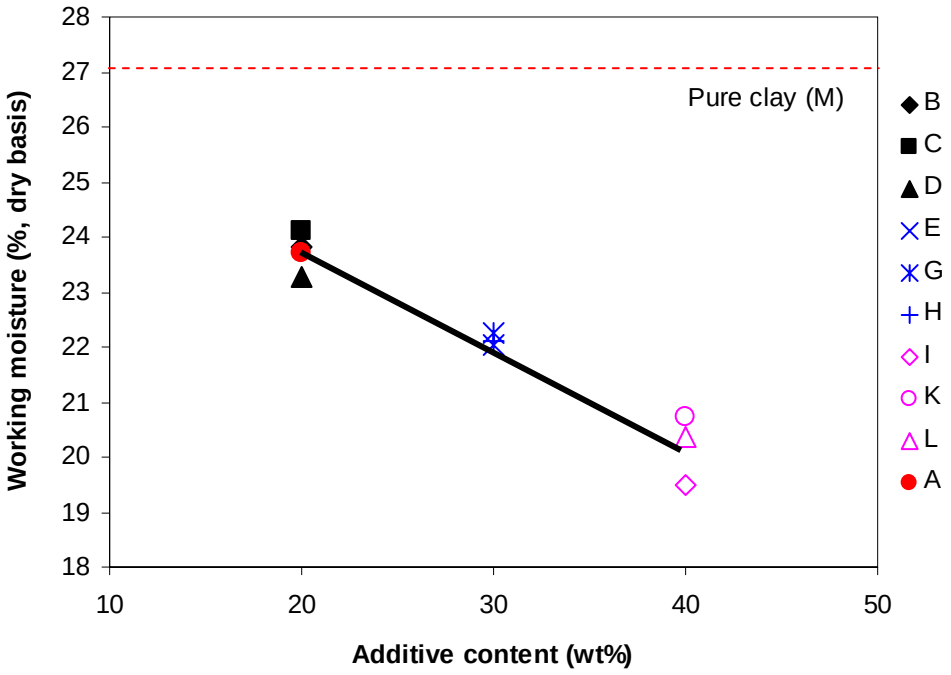

Fig. 4.19 Working moisture of various clay bodies obtained from Pfeferkorn test at *a* = 3.3

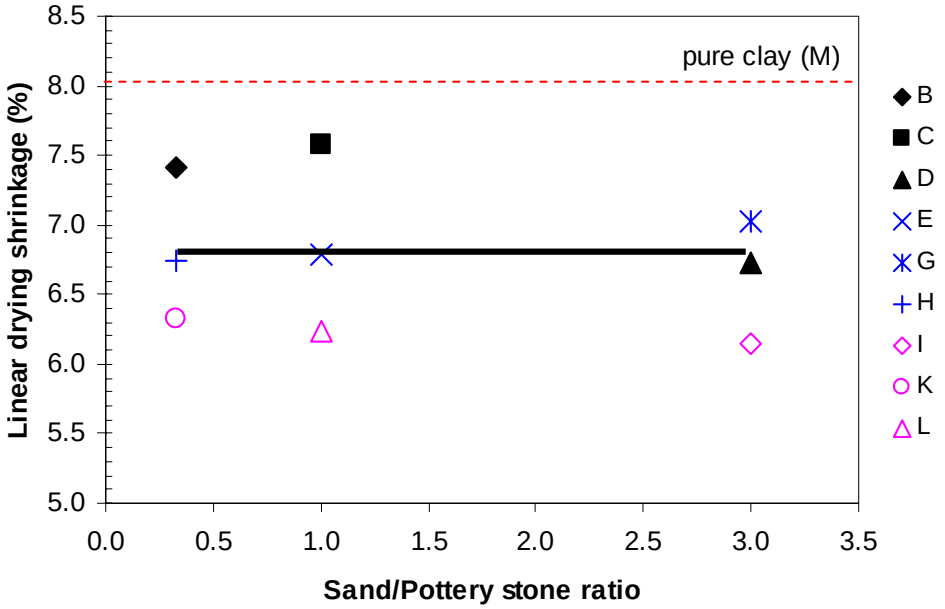

Fig. 4.20 Effect of sand/pottery stone ratio on the drying shrinkage of the clay bodies

Considering the effect of sand/pottery stone ratio for the drying shrinkage, there is no effect as shown is Fig. 4.20.

The effect of additive content on the green strength is shown in Fig. 4.21. Green strength of all clay bodies is strongly influenced by clay fraction in the bodies.

This phenomenon can easily be understood when comparing the green strength of the clay bodies with pure clay (M). Again there are no any effects of sand/pottery stone ratio on the green strength of clay bodies as shown in Fig. 4.22.

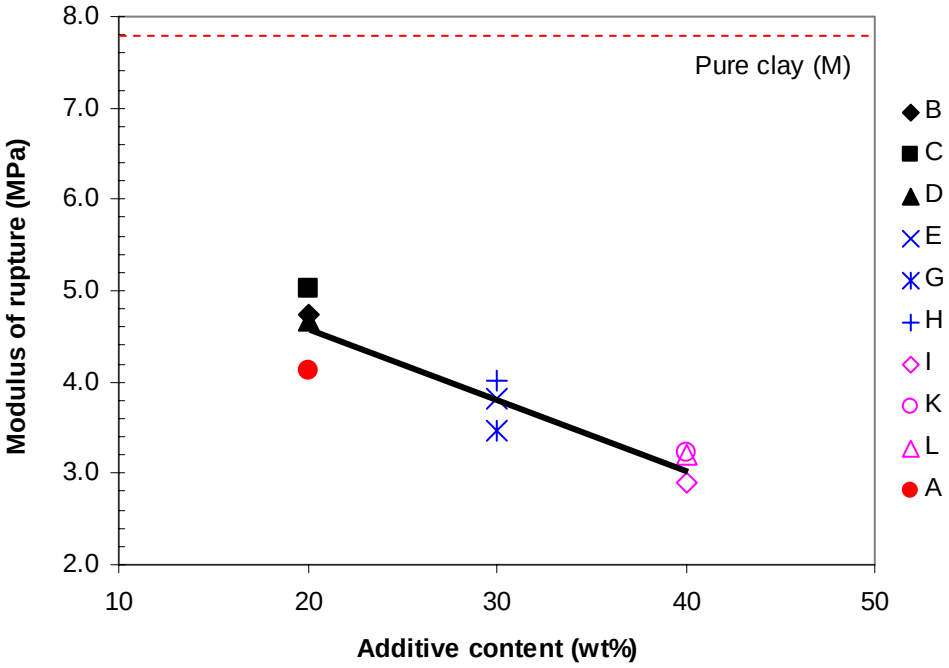

Fig. 4.21 Effect of additive content on green strength of the clay bodies

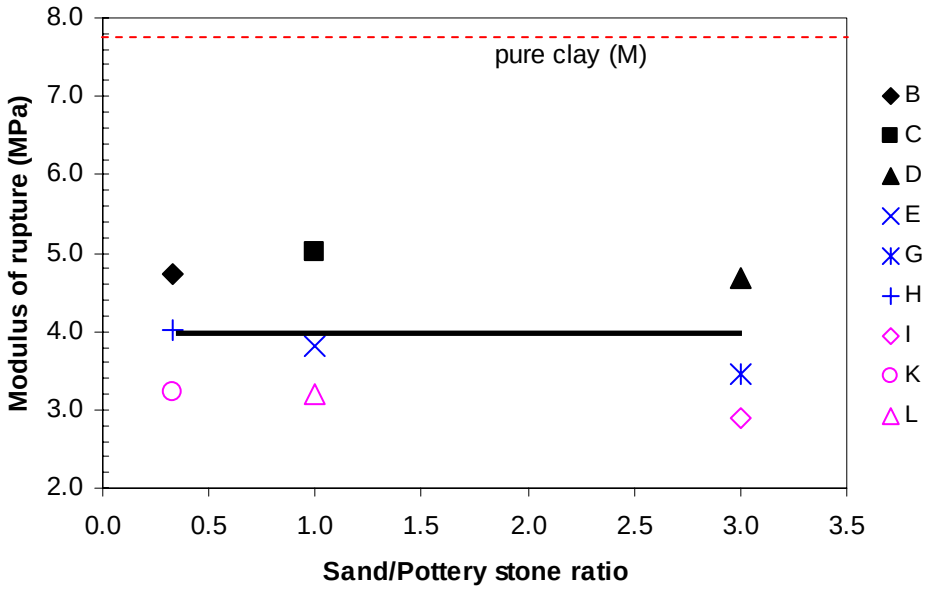

Fig. 4.22 Effect of sand/pottery stone ratio on the green strength of the clay bodies

4.3.3 Drying Sensitivity

4.3.3.1 Bigot curve

Plots of drying shrinkage vs. moisture content (Bigot curve) of various clay bodies are shown in Fig. 4.23. The Bigot curves exhibit the two characteristic stages of the drying process: (i) initial weight loss with shrinkage (constant rate period) and (ii) successive weight loss with minor shrinkage (declining rate period). The elimination of the working moisture during drying is not a linear process, producing volume reduction of specimens up to the leatherhard limit, during the constant rate period. The second stage of drying (at non-linear period of Bigot curve or non-constant rate of drying) develops with both minor shrinkage and the formation of a pore volume *(45-46)*. The most important difference concerns the critical point at which the clay reaches the leatherhard consistency and there is no further shrinkage. When the variations in shrinkage reached their minimum values, the drying process could be accelerated.

The initial moisture (M_i) and the critical moisture at which the drying shrinkage finishes (M_C) of each clay formula obtained from the Bigot curves (Fig. 4.23) are shown in Table 4.5. These data are used for calculating the Drying Sensitivity Index-Bigot (*DSI-B*) shown in Fig. 4.24. Remarkably, the initial moisture contents of each formula in the Table 4.5 are 1 - 2 wt% higher than the moisture contents at the Pefferkorn coefficient (a = 3.3) shown in Table 3.3. These excess values are due to the original moisture content in the raw materials used.

The effects of additive content and sand/pottery stone ratio on the *DSI-B* of all clay bodies are shown in Fig. 4.24 and 4.25, respectively. By comparing Fig. 4.24 and 4.25, they indicate that the amount of additive content has more influence on *DSI-B* of the clay bodies than the ratio of sand to pottery stone in the bodies. The more additive content, the less *DSI-B* is. It means that the sample having higher *DSI-B* value has higher risk to be cracked during drying process. It is also said that the sample having higher clay content is more sensitive to drying than that of lower clay content.

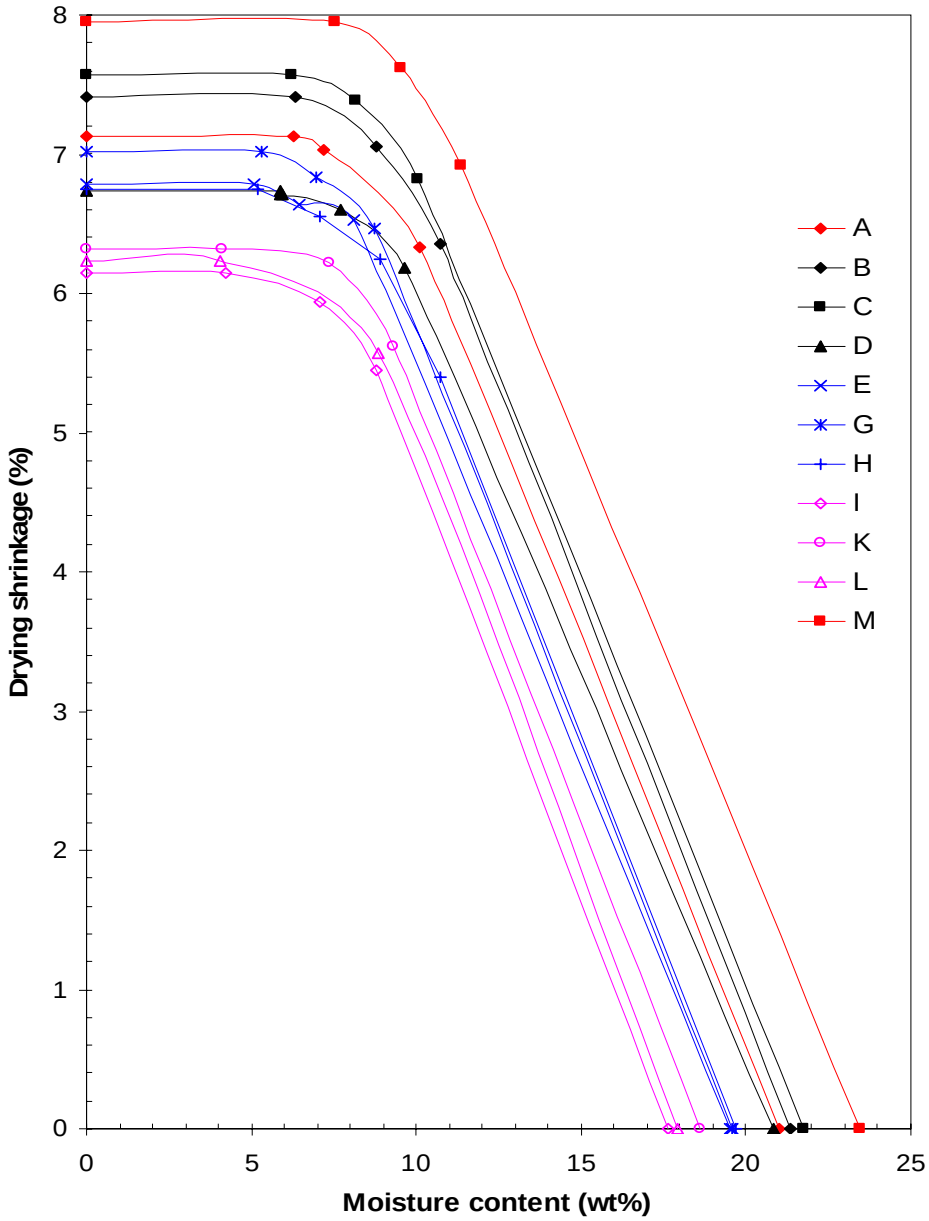

Fig. 4.23 Bigot curves (drying shrinkage vs. moisture content) of the clay bodies

Table 4.5 Data obtained from Bigot curves for calculating the *DSI-B* values of the clay bodies

Formula	M_i	M_c	M_i - M_c	*DS*	*DSI-B*
A	21.0	9.00	12.0	7.13	0.85
B	21.3	9.37	11.9	7.42	0.89
C	21.7	9.27	12.4	7.57	0.94
D	20.8	8.90	11.9	6.73	0.80
E	19.5	8.80	10.7	6.78	0.73
G	19.6	8.73	10.9	7.02	0.76
H	19.7	8.67	11.0	6.75	0.74
I	17.7	8.07	9.6	6.15	0.59
K	18.6	8.53	10.1	6.32	0.63
L	17.9	8.20	9.7	6.23	0.61
M	23.5	9.40	14.1	8.03	1.13

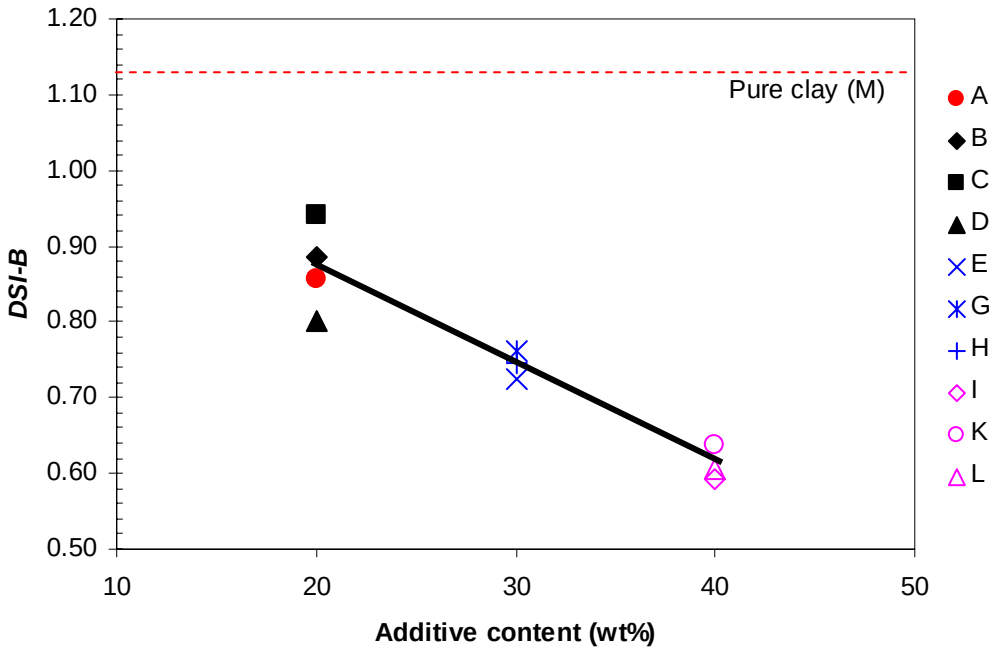

Fig. 4.24 Effect of additive content on the Drying Sensitivity Index-Bigot (*DSI-B*) of all clay bodies

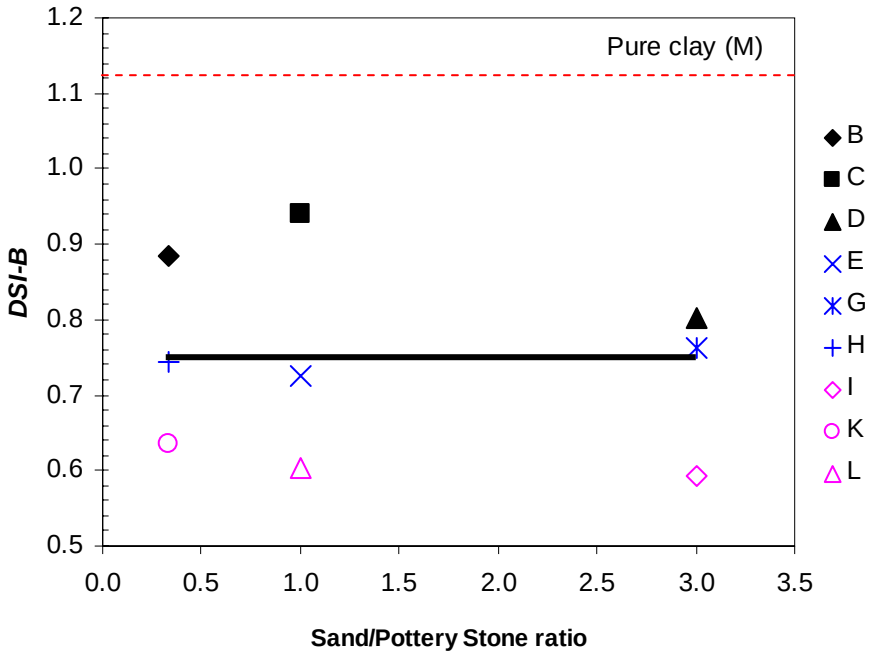

Fig. 4.25 Effect of sand/pottery stone ratio on the Drying Sensitivity Index-Bigot (*DSI-B*) of all clay bodies

4.3.3.2 Accelerated method proposed by Ratzenberger

The drying sensitivity of all clay bodies in this study was also determined by the accelerated method proposed by Ratzenberger *(17)* in order to confirm the results observed in the Bigot curves. The graph plotted between moisture differences (*MD*) and drying times of each formula are shown in Fig. 4.26. Figure 4.26 presents that the first maximum of moisture difference (*MD-I*) of test specimens is shown at 5 h of drying time for all compositions except 2.5 h for formula K. The first maximum of moisture difference (*MD-I*), linear drying shrinkage (*LDS*) and *DSI-R* values of all clay bodies are presented in Table 4.6. The tendency of *DSI-R* of all clay bodies is also illustrated in Fig. 4.27.

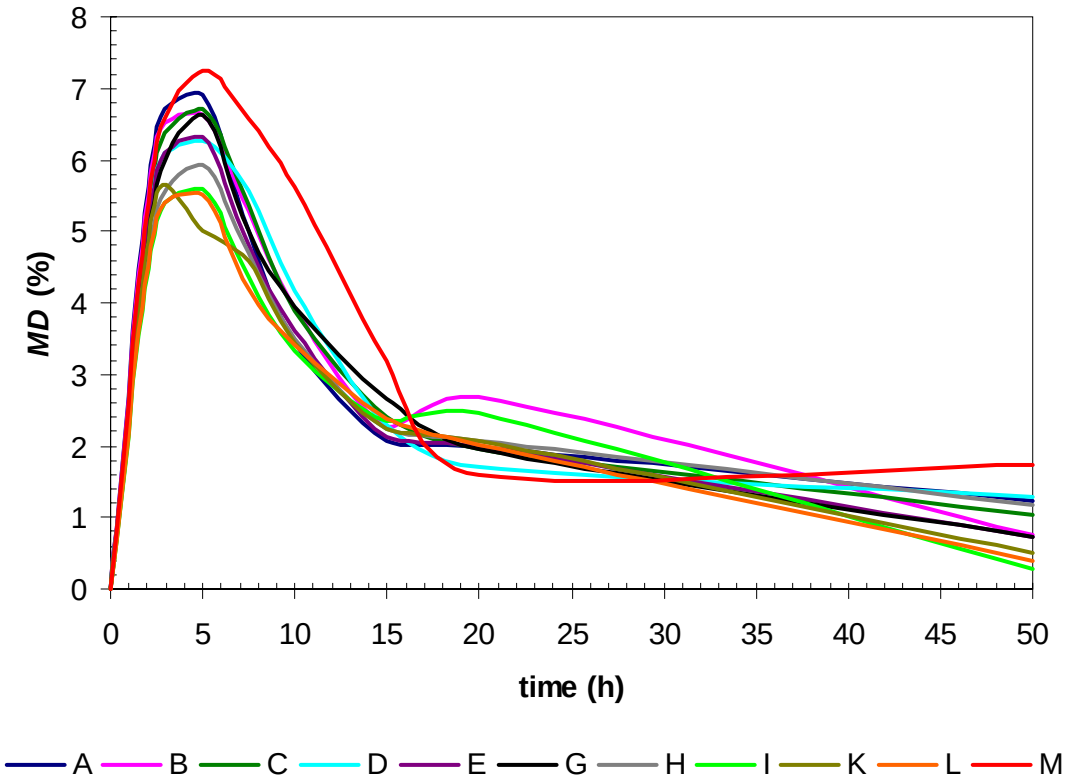

Fig. 4.26 Plots of moisture difference (*MD*) values vs. various drying times

Table 4.6 The first maximum moisture difference (*MD-I*), linear drying shrinkage (*LDS*) and *DSI-R* of various clay bodies

Formula	*MD-I*	*LDS* (%)	*DSI-R*
A	6.91	7.38	51.0
B	6.62	7.45	49.3
C	6.72	7.36	49.5
D	6.27	7.25	45.5
E	6.32	7.26	45.9
G	6.63	7.24	48.0
H	5.94	7.23	42.9
I	5.60	6.95	38.9
K	5.00	7.04	38.9
L	5.52	7.19	39.6
M	7.24	8.38	60.7

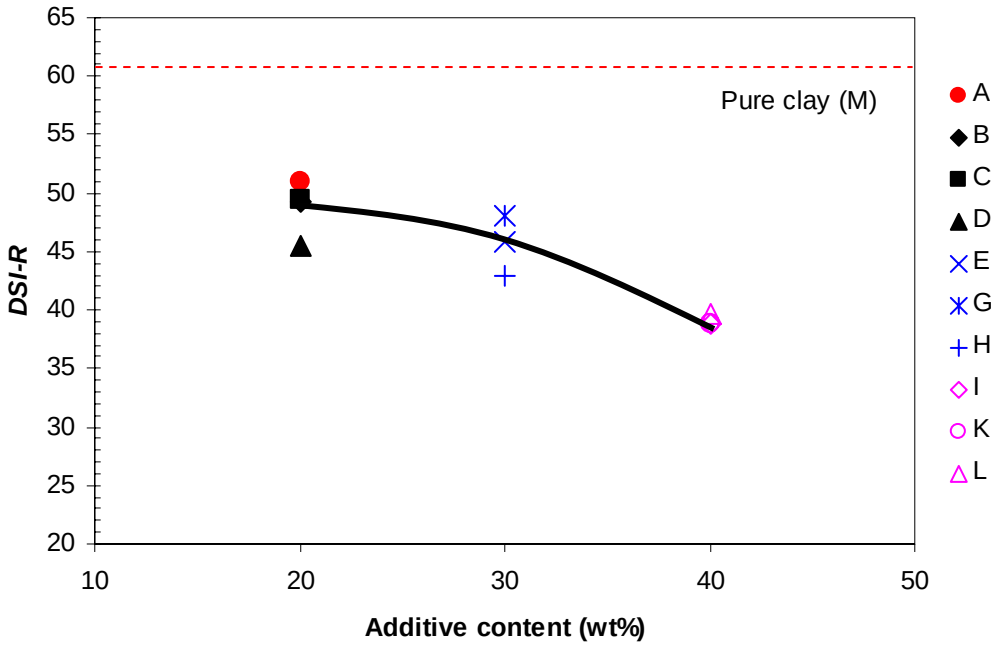

Fig. 4.27 Effect of additive content on Drying Sensitivity Index-Ratzenberger (*DSI-R*) of all clay bodies

The data of Drying Sensitivity Index-Ratzenberger (*DSI-R*) (Table 4.6 and Fig. 4.27) reveal that the more additive content is employed, the smaller *DSI-R* is. It also confirms the result of the drying sensitivity obtained from Bigot curves that the drying sensitivity of the clay bodies depends on the total amount of additive added to the bodies (sand + pottery stone).

From the results of both Drying Sensitivity Index-Bigot (*DSI-B*) and Drying Sensitivity Index-Ratzenberger (*DSI-R*), it is concluded that the samples having higher clay content is more sensitive to drying than those of lower one. It means that the samples having high drying sensitivity index value is prone to crack during drying process.

Figure 4.28 shows the correlation between *DSI-B* and *DSI-R* of the clay mixtures. There is a good linear relation between the two, though there are some percent of errors in the both experiments. The correlation line in Fig. 4.28 is equated as follows and the correlation coefficient was calculated as 0.92.

$$DSI\text{-}R = 38.6(DSI\text{-}B) + 15.9$$

Therefore, we can estimate the *DSI-R* value from the linear equation when the *DSI-B* value is known and the converse is also true.

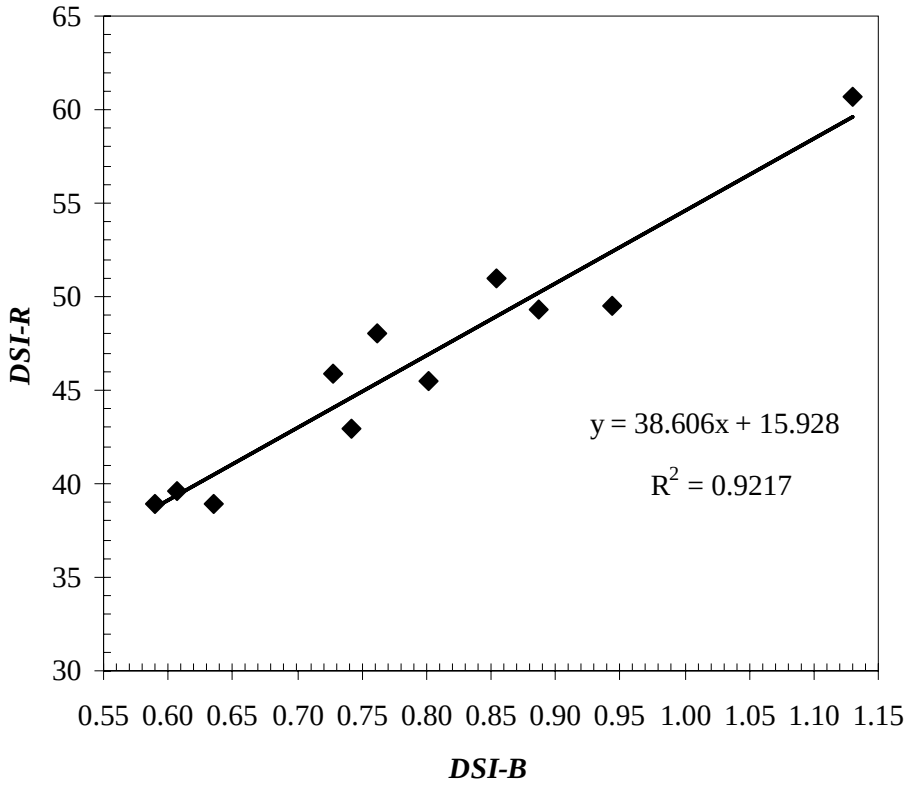

Fig. 4.28 Correlation between Drying Sensitivity Index-Ratzenberger (*DSI-R*) and Drying Sensitivity Index-Bigot (*DSI-B*)

4.4 Properties of Fired Body

4.4.1 Firing Shrinkage

The linear firing shrinkage of all clay formulae at the firing temperatures of 900, 950, 1000, 1050 and 1100 °C are shown in Appendix E. The graph shows that the linear firing shrinkage decreases with increasing quantity of additives.

Figure 4.29 and 4.30 show the effect of additive contents and the effects of sand/pottery stone ratio on linear firing shrinkage of the clay bodies at 950 °C in comparison with that of 1100 °C, respectively. At the lower firing temperature (950 °C), firing shrinkage values clearly depends on the quantity of additive content as seen in Fig.4.29. And sand/pottery ratio does not affect the shrinkage as seen in Fig.4.30. When

firing at 1100 °C, however, both additive content and sand/pottery ratio affected the shrinkage. Each formula of the same quantity of additive shows the differences in firing shrinkage values obviously as seen in Fig.4.30. It means that pottery stone give the larger firing shrinkage at high firing temperature. Since terracotta is usually fired at 900 - 1000 °C, the sand/pottery ratio is not so important. However, the ratio will become important in the product such as tableware and refractory which are fired at higher temperature as over 1100 °C.

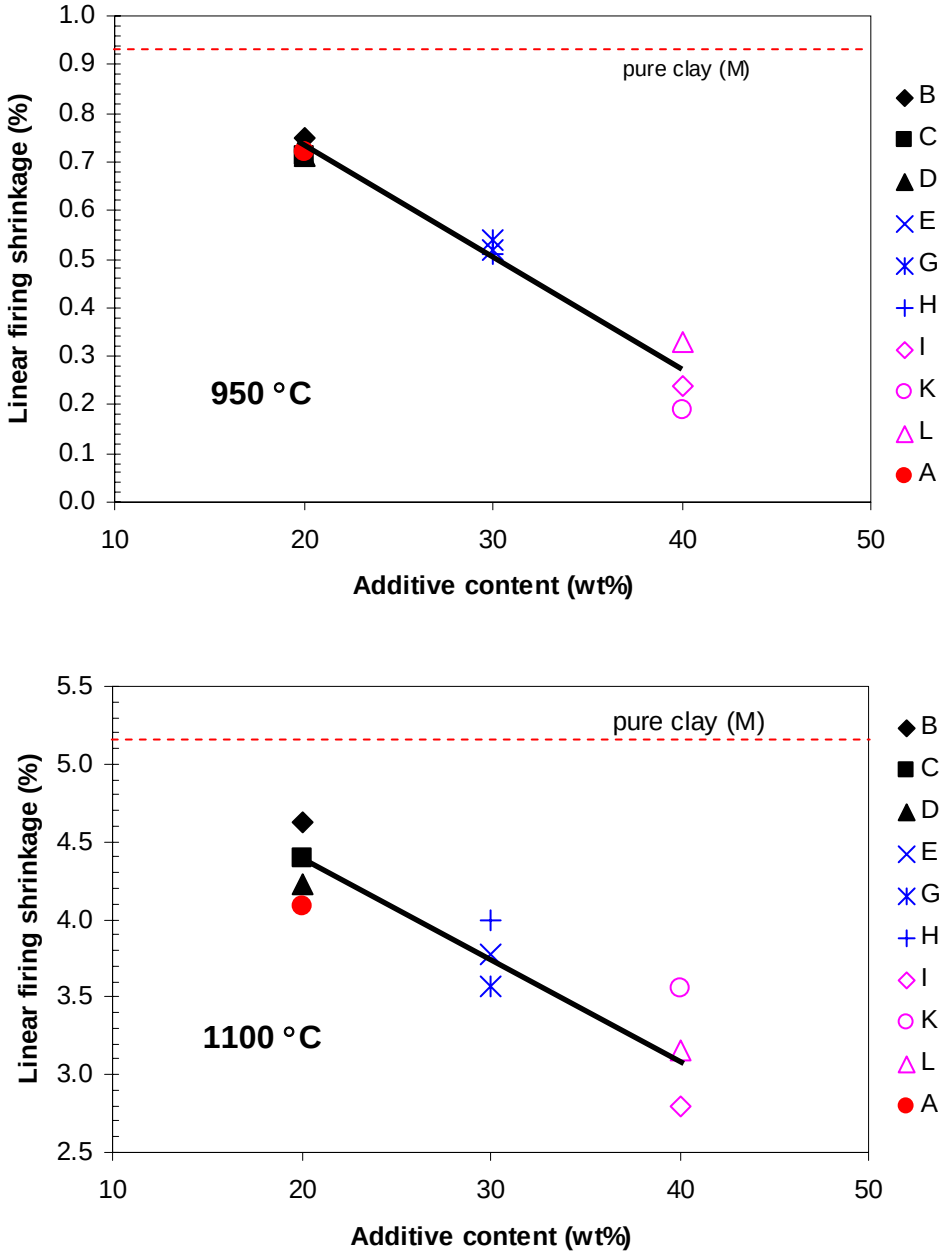

Fig 4.29 Effect of additive contents on linear firing shrinkage of the clay bodies fired at 950 and 1100 °C

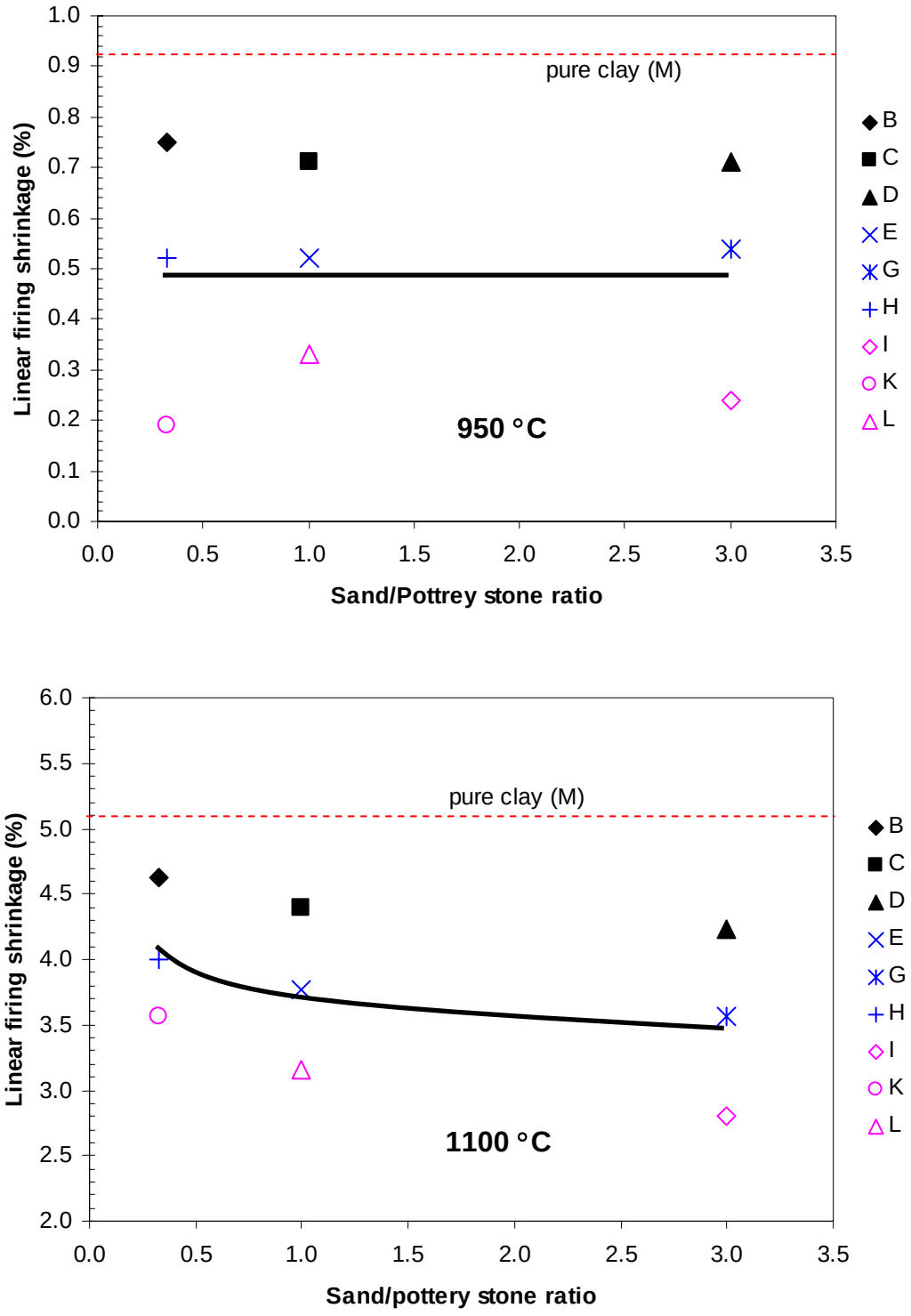

Fig 4.30 Effect of sand/pottery stone ratio on linear firing shrinkage of the clay bodies fired at 950 and 1100 °C

4.4.2 Water Absorption

Water absorption of all clay formulae fired at 900, 950, 1000, 1050 and 1100 °C is shown in Appendix F.

The water absorption starts to decrease when firing temperature is over 1000 °C. Water absorption is almost the same for all compositions when fired at temperature lower than 1000 °C. This phenomenon is obviously observed in Fig. 4.31.

Figure 4.32 shows the effect of additive content on the water absorption of fired bodies at 950 °C and 1100 °C. At the lower firing temperature (950 °C), there is a slightly increase in water absorption when the content of additive is increased. At higher firing temperature (1100 °C), however, the water absorption obviously increases when the content of additive is increased. In addition, the specimens having higher ratio of pottery stone show lower water absorption. This can be explained by the effect of high alkali content, especially $K_2O + Na_2O$ in the pottery stone. The soaking time of firing at 950 °C has no effect on the water absorption as presented in Appendix F because the vitrification has not been attained.

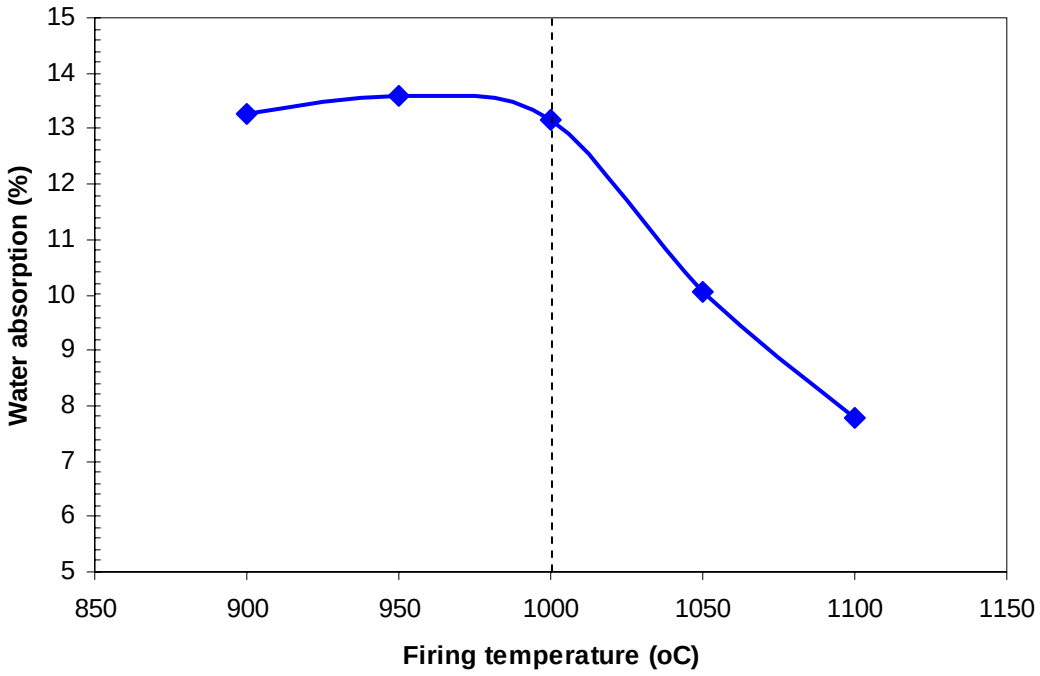

Fig. 4.31 Water absorption of the original composition (formula A)

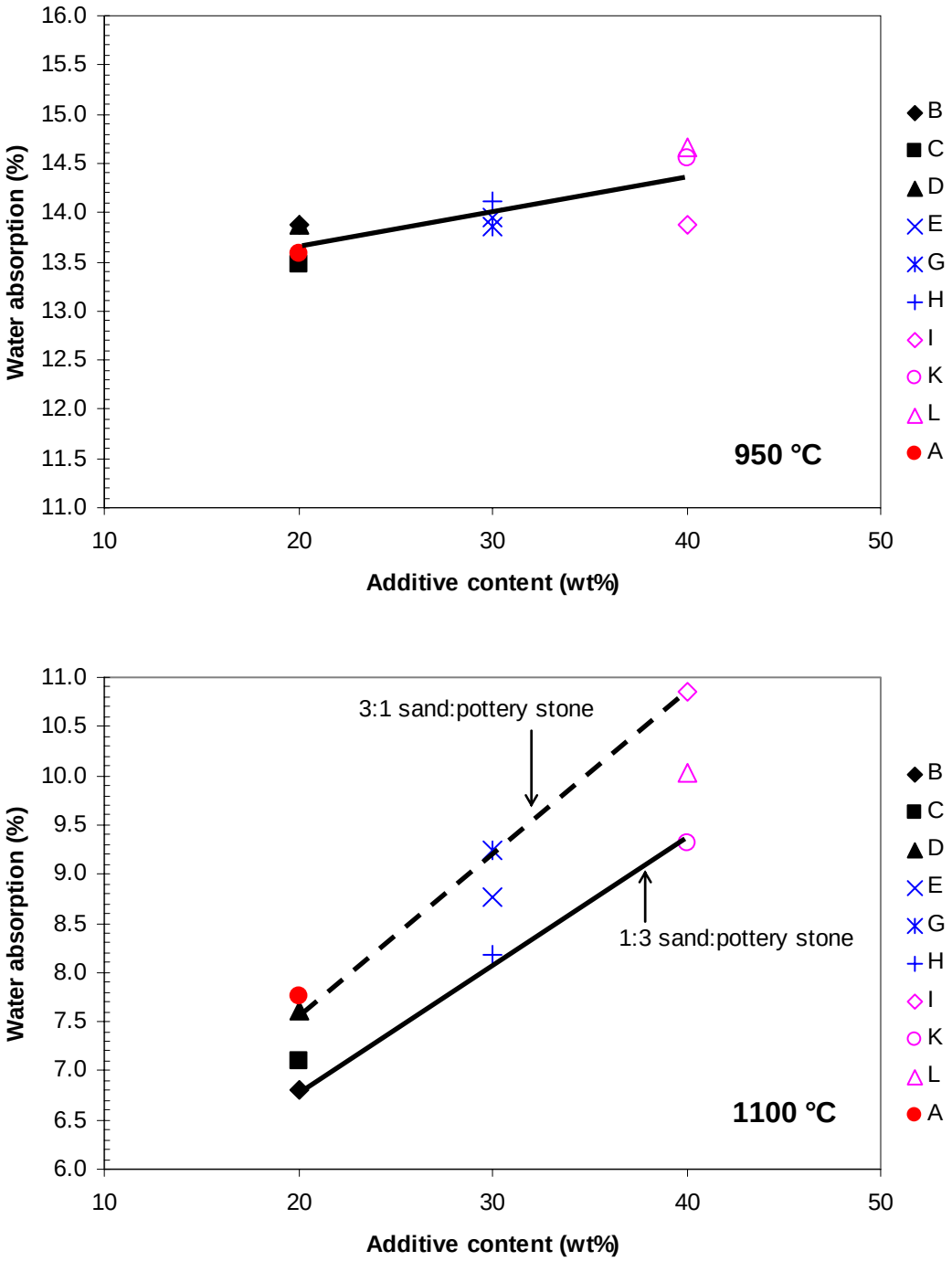

Fig. 4.32 Water absorption of the fired bodies at 950 and 1100 °C

4.4.3 Bulk Density

Bulk density of all clay formulae fired at 900, 950, 1000, 1050 and 1100 °C is shown in Appendix F.

Bulk density starts to increase when firing temperature is over 1000 °C. Bulk densities are almost the same for all compositions when fired at temperature lower than 1000 °C. This phenomenon is obviously observed in Fig. 4.33.

The increase in the content of additive results in the decrease in bulk density at all firing temperatures. Sand/pottery stone ratio also affects the bulk density. It is presented in Fig. 4.34 that the specimens having lower ratio of sand/pottery stone and sintered at 950 °C show lower bulk density. In contrast, the specimens having higher ratio of sand/pottery stone show lower bulk density when firing at 1100 °C. Again the soaking time of firing at 950 °C has almost no effect on the bulk density as presented in Appendix F.

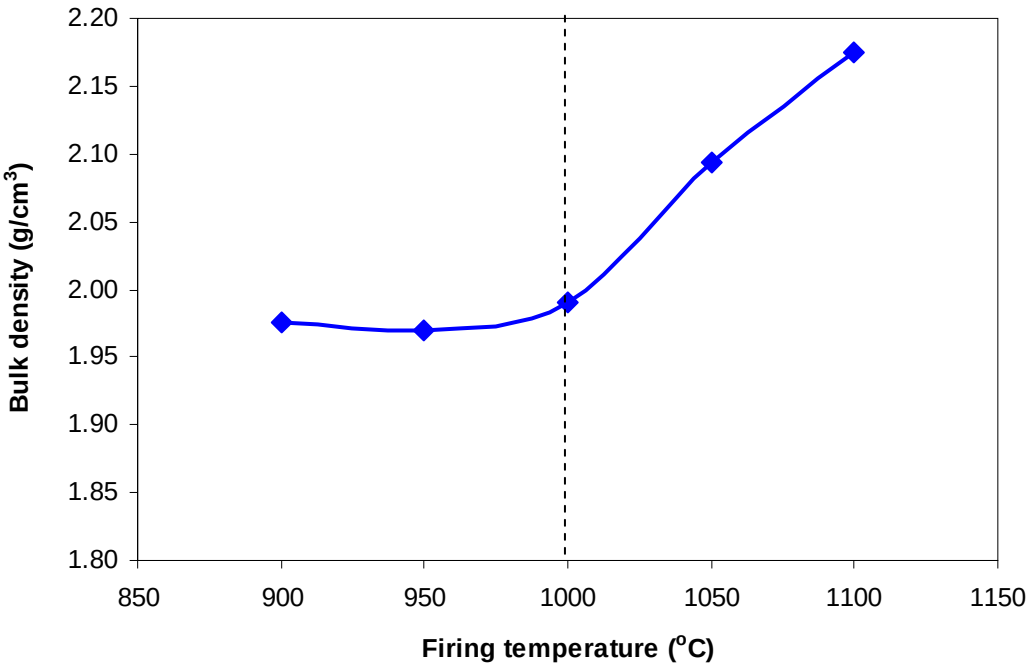

Fig. 4.33 Bulk density of the original composition (formula A)

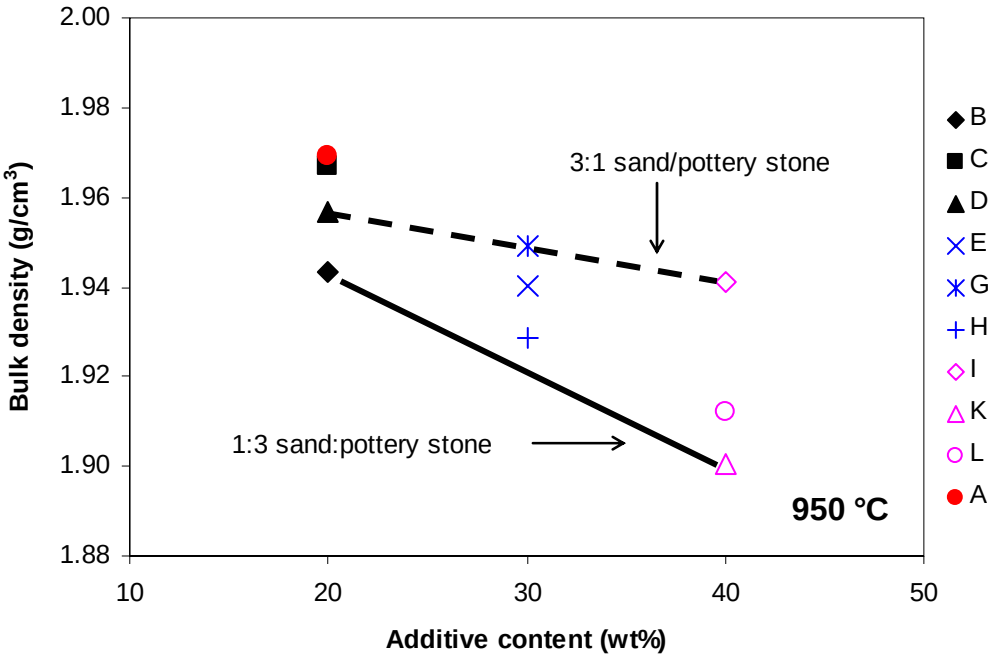

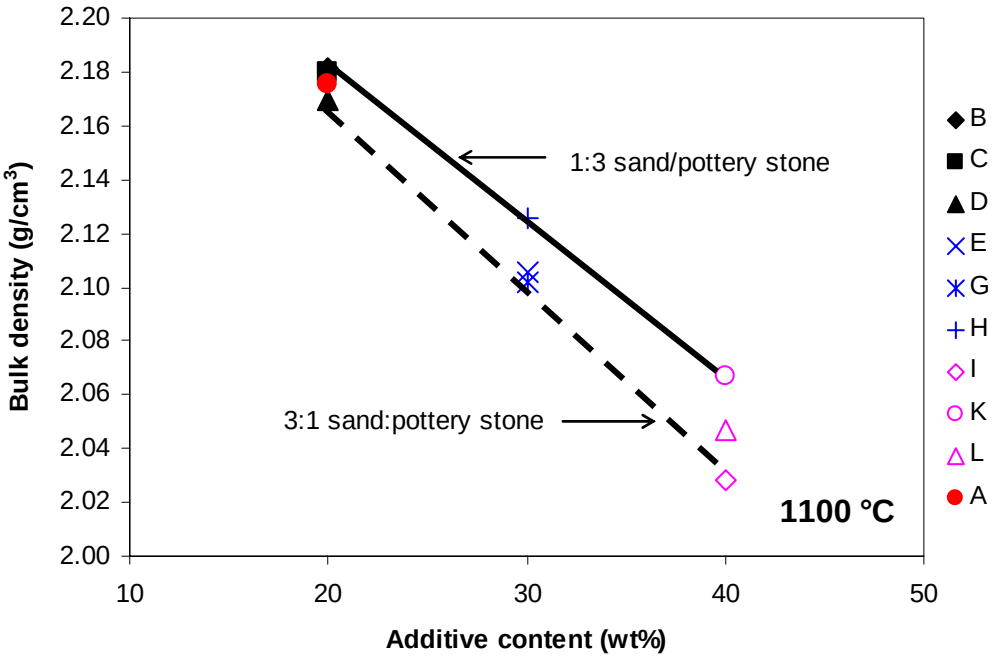

Fig. 4.34 Bulk density of the fired bodies at 950 and 1100 °C

4.4.4 Strength of Fired Bodies

The moduli of rupture of all clay formulae fired at 900, 950, 1000, 1050 and 1100 °C are shown in Fig.4.35. The absolute value of strength changed so much by the chemical composition and firing temperature. As expected, the flexural strength values of the fired clay bodies increase with increasing firing temperature. The values vary from 9.5 to 30.7 MPa, where the highest values are shown for the samples fired at 1100 °C with 20% of additive (3% sand + 9% pottery stone + 8% grog).

Figure 4.36 shows the effect of additive contents on the strength of the clay bodies fired at 950 and 1100 °C. SMC is the company's current formula used as reference which includes 80% clay + 8% grog (coarse particle) + 12% sand (coarse particle). The MOR value of SMC fired at 950 °C is 17.6 MPa. On the other hand, the MOR value of the same composition, formula A, but with grog and sand of passing through 40 meshes is 20.9 MPa. This shows that the smaller the particle size of sand and grog is, the higher the MOR value. At the firing temperature of 950°C, the strength is affected only by the amount of additives. At the firing temperature of 1100 °C, the MOR decreases with the increase in the additive content. However, each formula of the same quantity of additive shows the difference in MOR value obviously. It means that pottery stone gives higher MOR at high firing temperature.

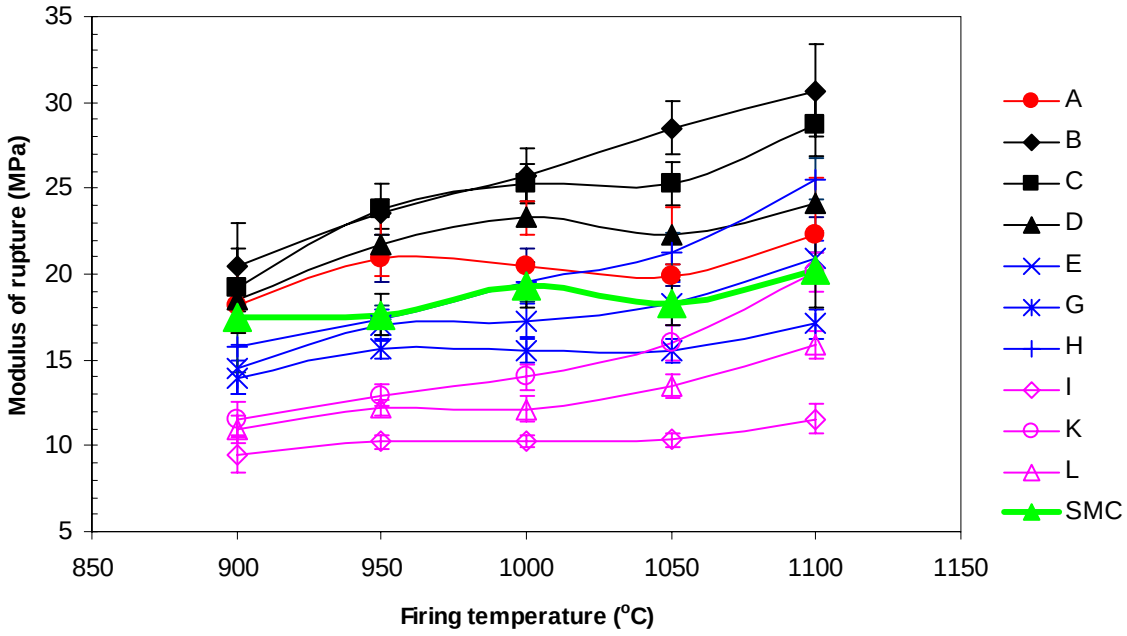

Fig 4.35 Moduli of rupture of the fired clay bodies at various temperatures

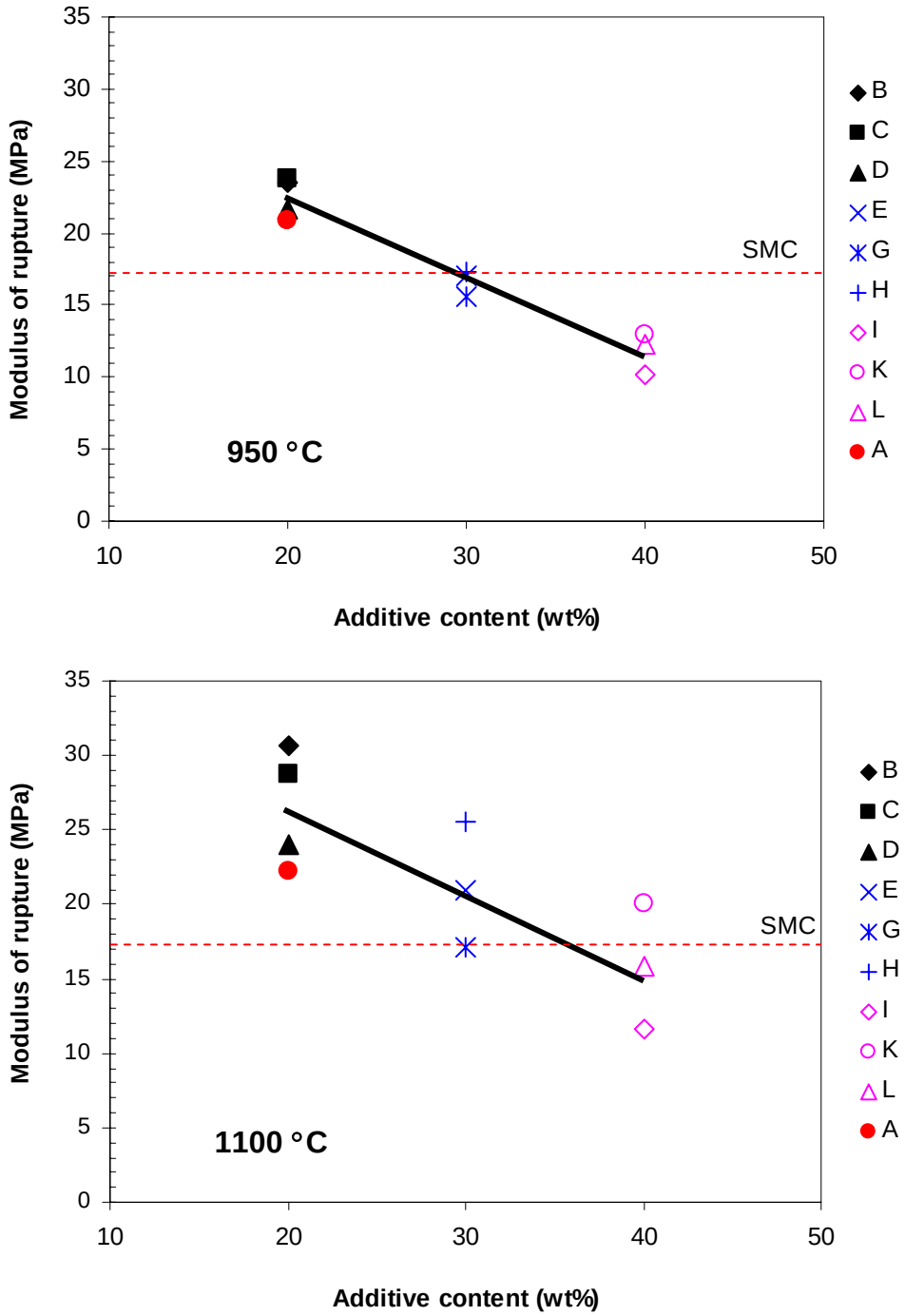

Fig 4.36 Effect of additive contents on fired strength of the clay bodies fired at 950 and 1100 °C

Figure 4.37 shows the relationship between the sand/pottery stone ratio and the modulus of rupture. At low firing temperature (950°C), the effect of sand/pottery stone ratio on the strength is not so much. However, the ratio affected strongly on the mechanical strength of fired clay body when firing at high temperature (1100 °C). The

lower ratio of sand/pottery stone, in other words, higher pottery/sand ratio increases the modulus of rupture at all firing temperatures. This means that pottery stone can increase the firing strength of the clay bodies better than sand. However, the effect of sand/pottery ratio on the firing strength is not so much comparing with the additive contents.

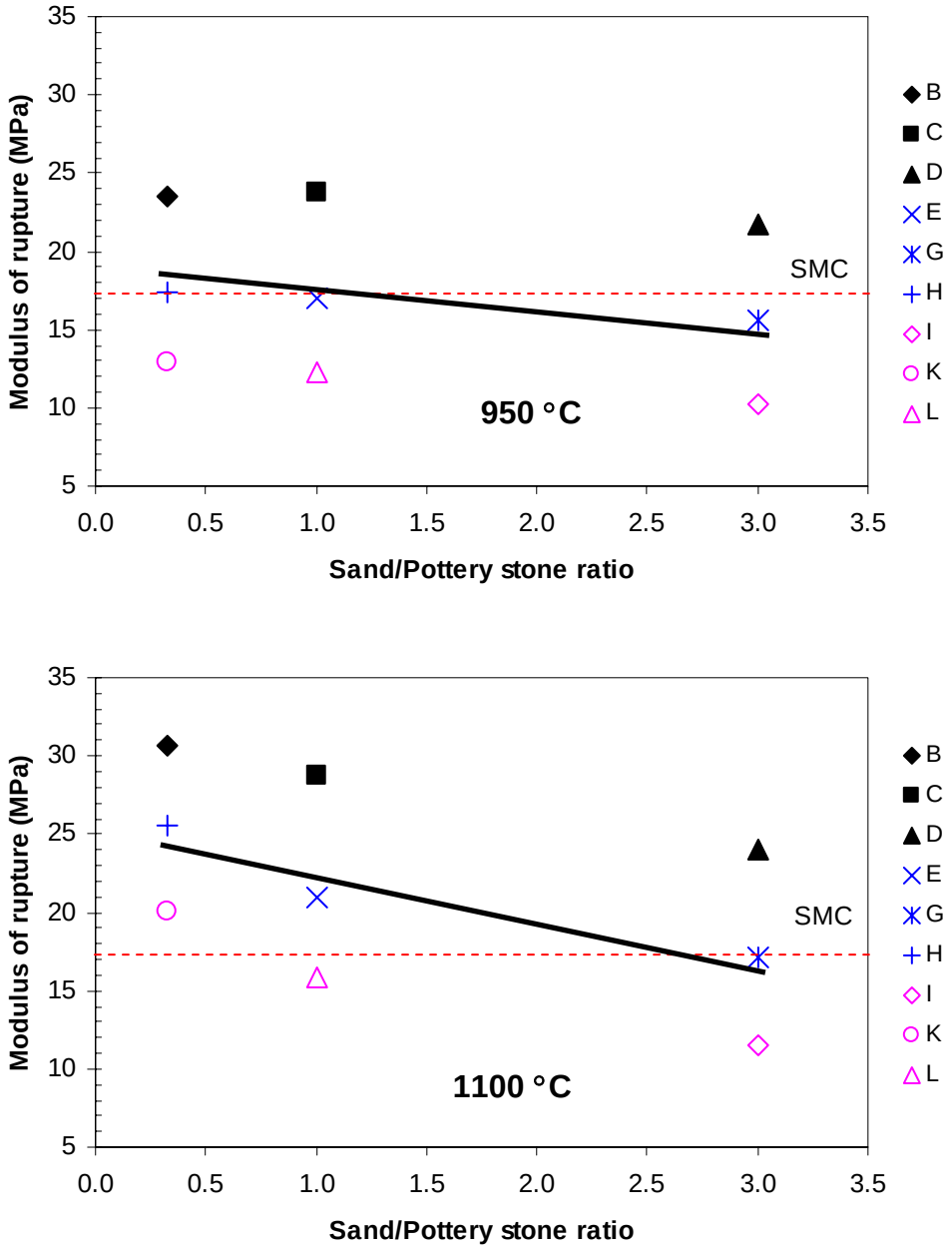

Fig 4.37 Effect of sand/pottery stone ratio on fired strength of the clay bodies fired at 950 and 1100 °C

4.4.5 Thermal Expansion Coefficient

Thermal expansion curves of the selected bodies (formula A, M, I and K) fired at 950 °C for 2 h are shown in Fig. 4.38. The sharp change in the curves at 540 - 560 °C corresponds to the low to high phase transformation of quartz. Cristobalite peak is observed in the XRD of formula K as shown in Fig.4.40, however, there is no abrupt change at about 220 °C in the thermal expansion curve because of a very few quantity. The values of thermal expansion coefficient at 50 – 500 °C are 9.68, 8.95, 9.61 and 9.90 × 10^{-6} /°C for formula A, M, I and K, respectively. The thermal expansion coefficient values of formula A, I and K are similar, but formula M (pure clay) shows a little lower value. The thermal expansion values for several materials are 14.0, 9.0, 6.0, 5.5 and 5.3 × 10^{-6} /°C for quartz (normal to c-axis), quartz (parallel to c-axis), porcelain, fire-clay body and mullite, respectively. Therefore, the higher values of formula A, I and K might be caused by the higher amount of quartz content as a result of much amount of additive content (quartz and pottery stone) in the body. Formula M (lower quartz content) shows lower value in thermal expansion coefficient.

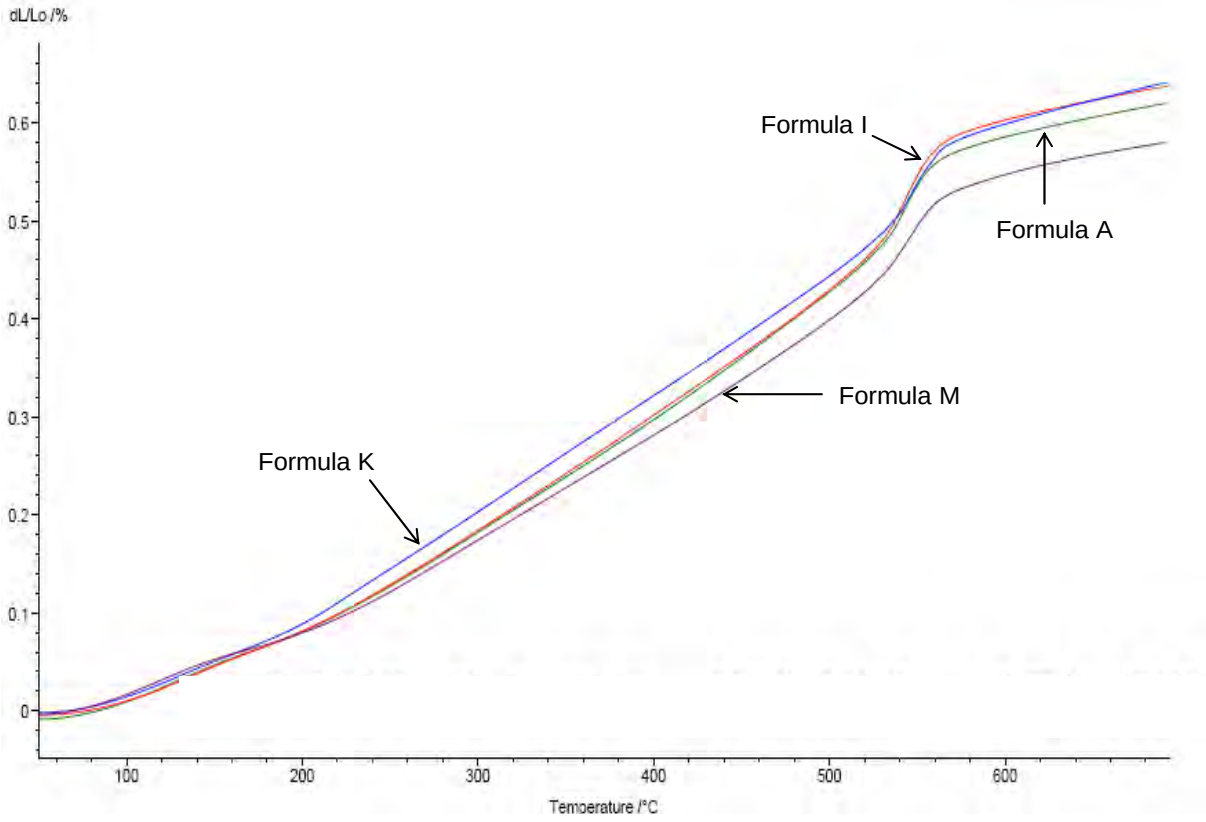

Fig. 4.38 Thermal expansion curves of fired clay bodies at 950 °C

4.4.6 Mineral Phases of Fired Specimens

The X-ray diffraction patterns of the clay specimens (formula A and K) after firing at various temperatures are shown in Fig. 4.39 and 4.40, respectively. In the case of formula A (8% grog + 12% sand addition), the major phase is quartz (SiO_2) and there are small peaks of mullite ($3Al_2O_3.2SiO_2$) and microcline ($K_2O.Al_2O_3.6SiO_2$) as minor phases. In the case of formula K (8% grog + 8% sand + 24% pottery stone), the major phase is also quartz and there are also small peaks of mullite ($3Al_2O_3.2SiO_2$) and microcline ($K_2O.Al_2O_3.6SiO_2$). However, the peak of cristobalite (SiO_2) phase is observed in formula K. Cristobalite may come from the transformation of silica in pottery stone which is activated by alkali matters like potassium and sodium.

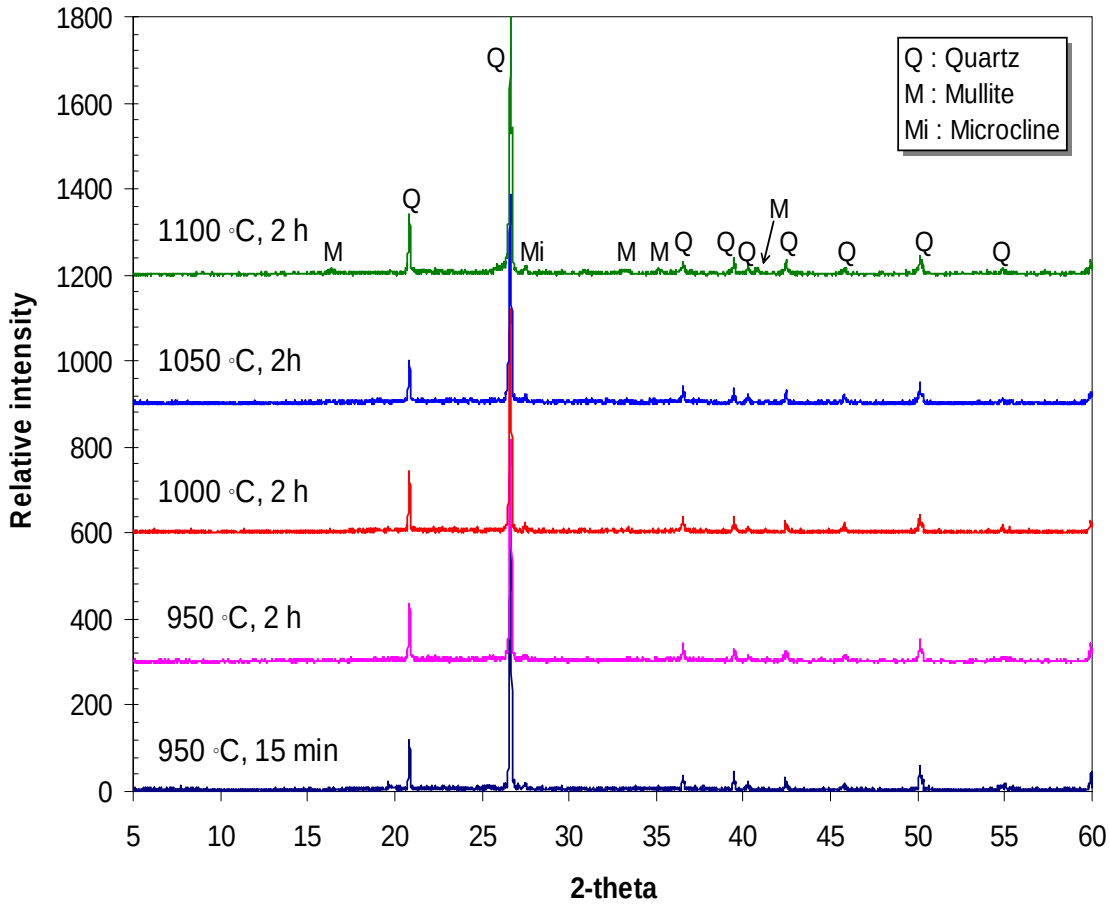

Fig 4.39 XRD patterns of specimens (formula A) fired at various temperatures

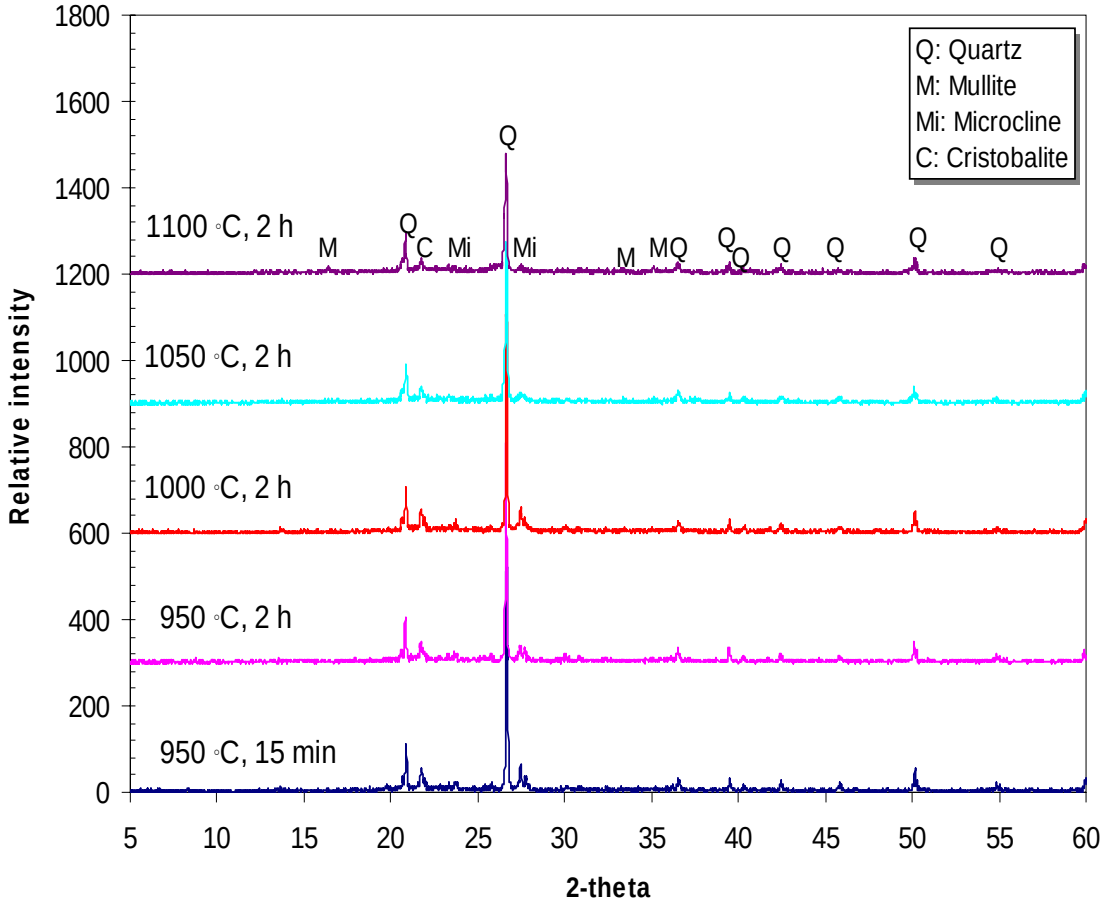

Fig 4.40 XRD patterns of specimens (formula K) fired at various temperatures

CHAPTER V

CONCLUSIONS AND RECOMMENDATIONS

5.1 Conclusions

This research was performed with the general aim of investigating the effects of sand and pottery stone on physical properties of terra cotta body. In relation to the objectives of this research, the following conclusions have been made.

5.1.1 Clay Hardness Tester

Design and reliability of NGK type clay hardness tester used in this research were studied. From the results of the experiment, it was concluded that the factors affecting the hardness values of the clay sample measured with the different design hardness testers can be drawn as follows:

(1) The human error is one of the big factors affecting the deviation of the hardness number value and when a person is guided properly, the human error can be decreased easily.

(2) The design of the hardness tester, especially the figure of the cone, strongly affects the hardness number. When the figure of the cone is different, the testers can not be calibrated to give the similar hardness value even the spring is set at the same load. The hardness number values can be compared only when the testers have the same design.

(3) The hardness number values obtained are changed by the calibration. The hardness number values of each tester give a narrow distribution after the calibration.

5.1.2 Properties of Green Body

The terra cotta bodies incorporating sand and pottery stone in varying proportion and ratio of sand and pottery stone were made. The green properties of the clay bodies such as plasticity, drying shrinkage, green strength and drying sensitivity were evaluated and the following findings were found.

(1) Plasticity index of the clay body is strongly decreased in proportion to the amount of sand and pottery stone added. However, the ratio of sand/pottery stone does not affect the plasticity of the bodies. The suitable plasticity of the clay body for forming by hydraulic pressing machine is approximately 38 – 43 of Atterberg's plasticity index.

(2) By progressively adding sand and pottery stone to the clay body, it was found that the amount of working moisture required for the forming process decreases with increasing the total amount of sand and pottery stone.

(3) Green flexural strength of the clay body is decreased in proportion to the amount of sand and pottery stone added. In other words, green strength is strongly influenced by the clay content of the body. However, the ratio of sand/pottery stone does not affect the green strength of the body.

(4) Drying shrinkage decreases with increasing amount of sand and pottery stone. This behavior is also related to the different amount of working water used in the processing, since the more working moisture is required, the higher the drying shrinkage.

(5) Drying sensitivity index (both Bigot and Ratzenberger methods) of the clay body also decreases with increasing amount of sand and pottery stone. This would reduce the chance of cracking during drying process. Moreover, the linear correlation between Drying Sensitivity Index-Bigot (*DSI-B*) and –Ratzenberger (*DSI-R*) was found. The linear correlation coefficient is 0.92.

5.1.3 Properties of Fired Body

Properties of fired terra cotta bodies such as firing shrinkage, water absorption, bulk density and flexural strength were investigated and were concluded as the following.

(1) Firing shrinkage of the clay body decreases with increasing amount of sand and pottery stone. A decreasing of firing shrinkage is more affected at higher firing temperature (1100 °C). The linear firing shrinkage values of all clay bodies incorporating additives fired at 950 °C are in between 0.19 – 0.75 %.

(2) Water absorption of fired clay body increases with increasing sand and pottery stone, but starts to decrease when firing temperature is over 1000 °C. Water absorption values of all clay bodies incorporating additives fired at 950 °C are not so big different, the values are in between 13.5 – 14.7 %.

(3) Bulk density of fired clay body decreases with increasing sand and pottery stone, but starts to increase when firing temperature is over 1000 °C. Bulk densities of all clay bodies incorporating additives fired at 950 °C are 1.90 – 1.97 g/cm^3.

(4) Bending strength of the fired clay body is decreased by the addition of sand and pottery stone. The body having highest strength at 950 °C (23.8 MPa) is formula C (80 wt% clay + 8 wt% grog + 6 wt% sand + 6 wt% pottery stone). The lowest value (10.2 MPa) is formula I (60 wt% clay + 8 wt% grog + 24 wt% sand + 8 wt% pottery stone).

(5) Thermal expansion coefficient of fired clay bodies depends on the silica content in the body. Pure clay (formula M) has lowest thermal expansion coefficient of 8.95 × 10^{-6} /°C as it has lowest quartz content in the body.

In conclusion, the use of pottery stone in terracotta body is possible. The best formula obtained from this work is formula E (70 wt% clay + 8 wt% grog + 11 wt% sand + 11 wt% pottery stone) as the overall properties can be accepted and passed the standard requirement. In particular, the plasticity and the drying properties are very satisfactory. The green properties of the formula E are as follows: plasticity index 41.3, green flexural strength 3.82 MPa, linear drying shrinkage 6.78 %, drying sensitivity index-Bigot 0.73, The properties of formula E fired at 950 °C are as follows: linear firing shrinkage 0.5 %, bulk density 1.94 g/cm^3, water absorption 13.9 %, and modulus of rupture 17.1 MPa.

5.2 Recommendations

No research is an end itself. There is always avenue for future work. During the course of this research, the following topics were recommended for further study.

(1) Based on the above mentioned conclusion, the formula E would be applied to the real production of Siamese Merchandise Co., Ltd. Therefore, the

experiment on implementation of the formula E to the production of terra cotta pottery should be investigated.

(2) In this study, particle sizes of grog, sand and pottery stone were fixed to only one size (passed though 40 meshes sieve). Therefore, the effect of particle sizes of grog, sand and pottery stone on the properties of the terra cotta body should be studied.

(3) The experimental study on the effect of other non-plastic materials on the properties of terra cotta body is recommended for the future work.

(4) The effect of other low plasticity clays on green and fired properties of terra cotta body should also be studied.

(5) The plasticity and drying sensitivity are the important properties for the forming and drying processes of terracotta pottery. These properties are different depending on the resources of clay. There are many terracotta clay resources in Thailand such as Ayutthaya, Ang Thong, Rayong, Chanthaburi, Nakorn Sawan, Sukhothai, Nakhon Ratchasima and etc. Therefore, the plasticity, drying sensitivity and working moisture of those clays should be studied in the future.

References

[1] กรมวิทยาศาสตร์บริการ และคณะ, เอกสารในการสัมมนาเรื่อง เครื่องปั้นดินเผาราชบุรี ปี 2000 เสนอที่โรงแรมโกลเด้นท์ซิตี้ จ. ราชบุรี 17 ธันวาคม 2542. (เอกสารไม่ตีพิมพ์เผยแพร่)

[2] Prapun Aungatichart. Effeects of rice husk ash on the physical properties of terra cotta body. Master thesis. Department of Materials Science. Faculty of Science. Chulalongkorn University. (2004).

[3] Punyoot Huantanom. Development of frost resiatance property in terra-cotta pottery. Master thesis. Department of Materials Science. Faculty of Science. Chulalongkorn University. (2004).

[4] F. H. Norton. Elements of Ceramics. 2nd edition: Addison-Wesley, 1974.

[5] www.gardenvisit.com/glossary/glossary.htm

[6] www.mda.org.uk/bmmat/mathest.htm

[7] highered.mcgraw-hill.com/sites/007299634x/student_view0/glossary.html

[8] www.saterdesign.com/glossary/glossary2.asp

[9] W.E. Brownell, Structural clay products. New York : Springer-Verlag, (1976).

[10] American Society for Testing and Materials (ASTM). Standard Test Methods for Liquid Limit, Plastic Limit, and Plasticity Index of Soils. ASTM D4318-00. New York: ASTM, (2003).

[11] W. Ryan, and C. Radford. Whitewares production, testing and quality control. New York : Pergamon Press, (1987).

[12] D.A. Brosnan and G. C. Robinson. Introduction to drying of ceramics. Ohio: The American ceramic Society, (2003).

[13] R. Konig Ceramic drying. Krumbach: Publisher Novokeram, (1998).

[14] H. Ratzenberger. Causes and methods of determining the drying sensitivity of raw materials for structural ceramics and heavy clay products. ZI, 10 (1986): 535–540.

[15] H. Ratzenberger. Possibilities for reducing the drying sensitivity of ceramic raw materials. ZI, 11 (1986) 594–599.

[16] Ch. Schmidt-Reinholz. Natural drying sensitivity of clay ceramic materials and bodies-Causes and restriction through additives. Interbrick, 3 (1987): 23–27.

[17] H. Ratzenberger. An accelerated method for the determination of drying sensitivity. ZI, 6 (1990) 348–354.

[18] F. Saboya Jr. et al. The use of the powder marble by-product to enhance the properties of brick ceramic. Construction and Building Materials, 21 (2007): 1950-1960.

[19] E. A. El-Alfi et al. Effect of sand as non-plastic material on ceramic properties of clay bricks. Interceram, 53 (2004): 330 – 333.

[20] J. C. Knight. Influence of volcanic ash as flux on ceramic properties of low plasticity clay and high plasticity clay of Trinidad. British Ceramic Transaction. 98 (1999): 24 – 28.

[21] W. Russ et al. Application of spent grains to increase porosity in bricks. Construction and Building Materials, 19 (2005): 117–126.

[22] E. A. Dominguez and R. Ullmann. Ecological bricks made with clays and steel dust pollutants. Applied Clay Science. 11 (1996): 237 – 249.

[23] W. Acchar et al. Effect of marble and granite sludge in clay materials. Materials Science and Engineering, A 419 (2006): 306–309.

[24] I. Demir. Effect of organic residues addition on the technological properties of clay bricks. Waste Management, (2007) (In press).

[25] M. M. Elwan et al. Effect of solid waste sludge on the properties of clay bricks. International Ceramics Journal, 6 (2005): 33 – 37.

[26] T. Basegio et al. Environmental and technical aspects of the utilization of tannery sludge as a raw material for clay products. Journal of the European Ceramic Society, 22 (2002): 2251–2259.

[27] M. Dondi et al. Orimulsion fly ash in clay bricks—part 2: technological behavior of clay/ash mixtures. Journal of the European Ceramic Society, 22 (2002): 1737–1747.

[28] I. Demir and M. Orhan. Reuse of waste bricks in the production line. Building and Environment, 38 (2003): 1451 – 1455.

[29] X. Lingling et al. Study on fired bricks with replacing clay by fly ash in high volume ratio. Construction and Building Materials, 19 (2005): 243–247.

[30] S. N. Monteiro et al. Technological behavior of red ceramics incorporated with

brick waste. Revista Materia, 10 (2005): 537 – 542.

[31] I. B. Garcia et al. Technological characterization and ceramic application of gravel pit by-products from middle-course Jarama river deposits (central Spain). Applied Clay Science, 28 (2005): 283– 295.

[32] S. Kurama et al. The effect of boron waste in phase and microstructural development of a terracotta body during firing. Journal of the European Ceramic Society, 26 (2006): 755–760.

[33] E. Kalkan and S. Akbulut. The positive effects of silica fume on the permeability, swelling pressure and compressive strength of natural clay liners. Engineering Geology, 73 (2004): 145–156.

[34] M. Aineto et al. The role of a coal gasification fly ash as clay additive in building ceramic. Journal of the European Ceramic Society, (2006) (In press).

[35] Y. Pontikes et al. Thermal behaviour of clay mixtures with bauxite residue for the production of heavy-clay ceramics. Journal of the European Ceramic Society, (2006) (In press).

[36] S. A. El Sherbiny et al. Use of cement dust in the manufacture of vitrified sewer pipes. Waste Management, 24 (2004): 597–602.

[37] R. R. Menezes et al. Use of granite sawing wastes in the production of ceramic bricks and tiles. Journal of the European Ceramic Society, 25 (2005): 1149–1158.

[38] A. Acosta et al. Utilisation of IGCC slag and clay steriles in soft mud bricks (by pressing) for use in building bricks manufacturing. Waste Management, 22 (2002): 887–891.

[39] E. Kalkan. Utilization of red mud as a stabilization material for the preparation of clay liners. Engineering Geology, 87 (2006): 220–229.

[40] American Society for Testing and Materials (ASTM). Standard Test Methods for Drying and Firing Shrinkages of Ceramic Whiteware Clays. ASTM C326-82. New York: ASTM, (1997).

[41] American Society for Testing and Materials (ASTM). Standard Test Methods for Water Absorption, Bulk Density, Apparent Porosity, and Apparent Specific Gravity of Fired Whiteware Products. ASTM C373-88. New York : ASTM,

(1999).

[42] American Society for Testing and Materials (ASTM). Standard Test Methods for Flexural Properties of Ceramic Whiteware Materials. ASTM C674-88. New York : ASTM, (1999).

[43] Worrall, W.E. Clays and ceramic raw materials. London and New York: Elsevier applied science publishers, (1986).

[44] Von C. B. Investigation on drying sensitivity—a survey I. cfi/Ber. DKG. 7 (8) (1986): 410– 413.

[45] Von C. B. Investigation on drying sensitivity—a survey II. cfi/Ber. DKG. 9 (10) (1986): 482–486.

Appendices

Appendix A

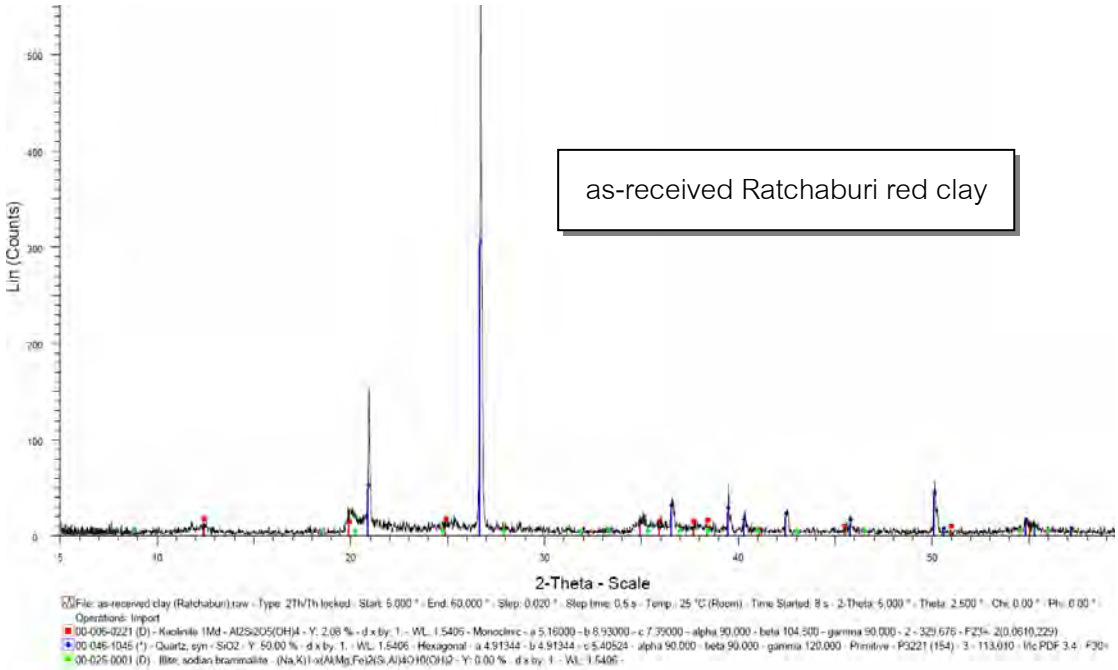
as-received Ratchaburi red clay
Lin (Counts)
2-Theta - Scale

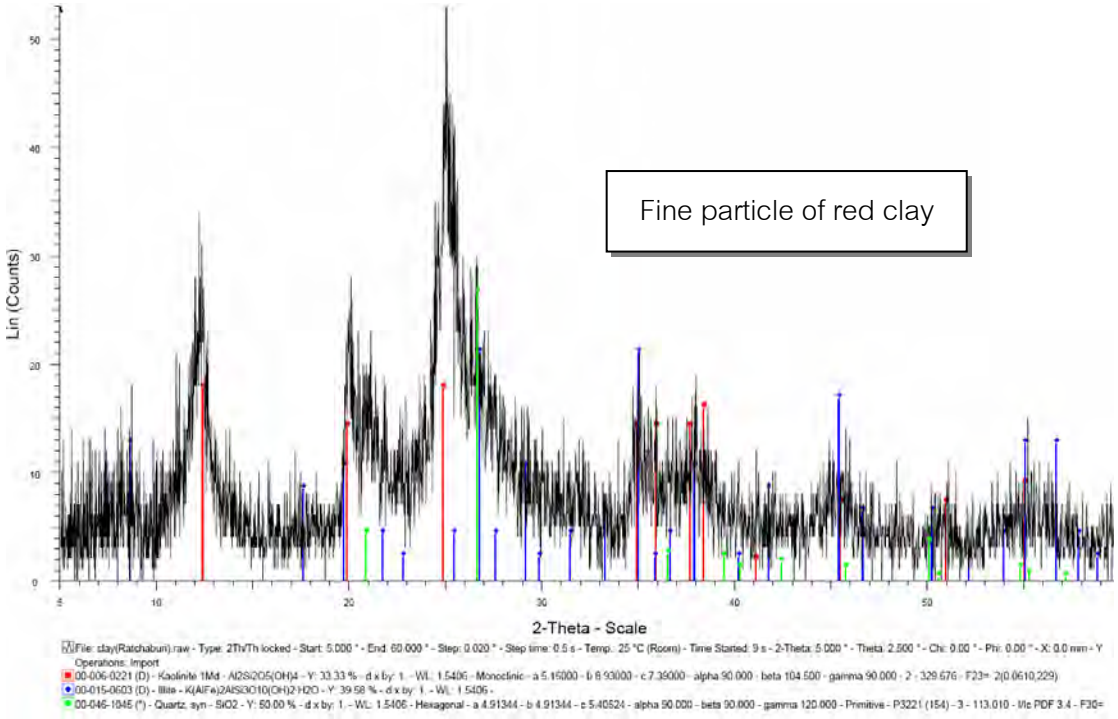
Fine particle of red clay
Lin (Counts)
2-Theta - Scale

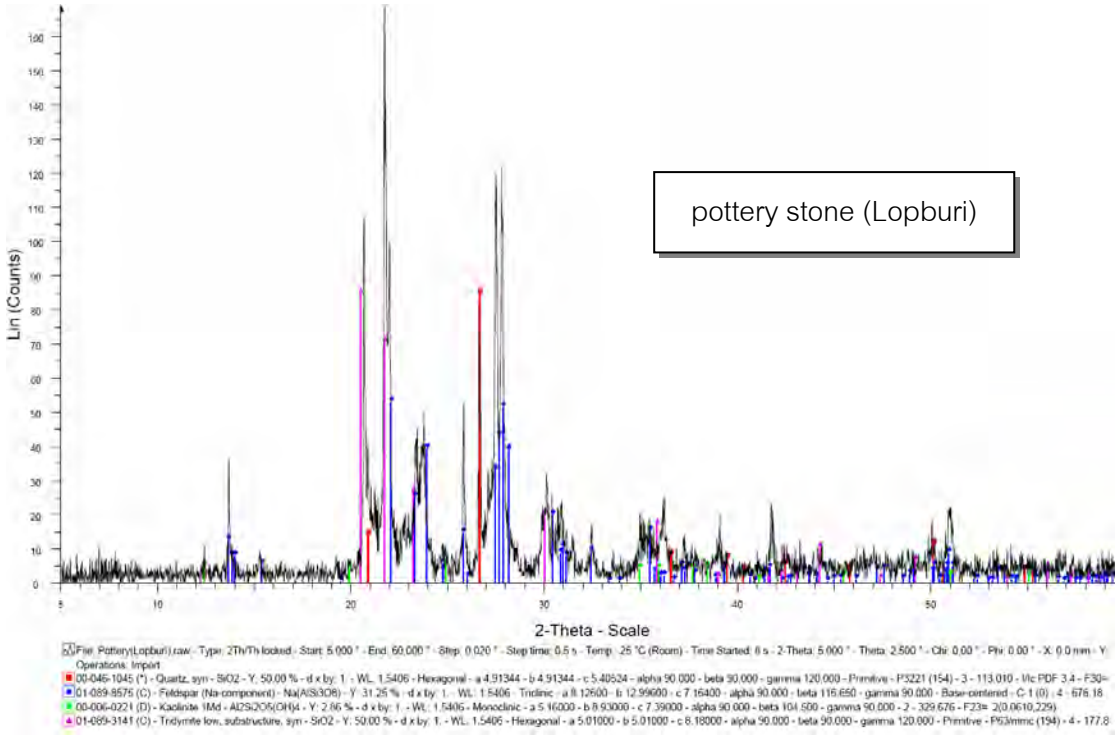
pottery stone (Lopburi)
Lin (Counts)
2-Theta - Scale

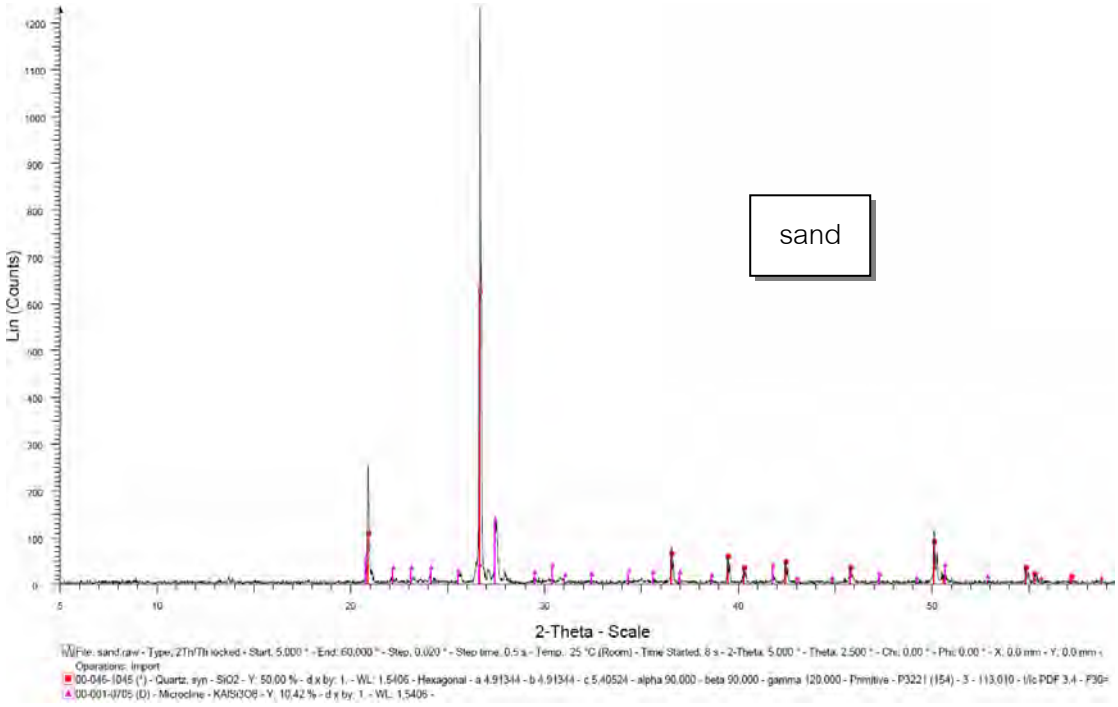
sand
Lin (Counts)
2-Theta - Scale

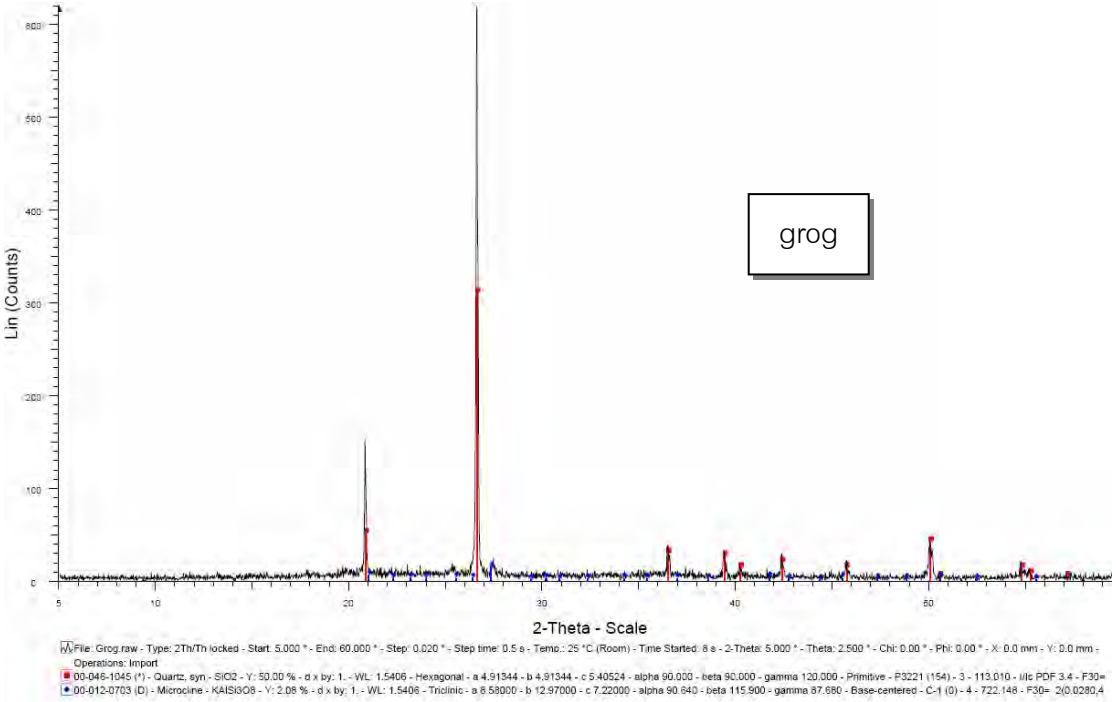
grog
Lin (Counts)
2-Theta - Scale
File: Grog.raw - Type: 2Th/Th locked - Start: 5.000 ° - End: 60.000 ° - Step: 0.020 ° - Step time: 0.5 s - Temp.: 25 °C (Room) - Time Started: 8 s - 2-Theta: 5.000 ° - Theta: 2.500 ° - Chi: 0.00 ° - Phi: 0.00 ° - X: 0.0 mm - Y: 0.0 mm - Operations: Import
00-046-1045 (*) - Quartz, syn - SiO2 - Y: 50.00 % - d x by: 1. - WL: 1.5406 - Hexagonal - a 4.91344 - b 4.91344 - c 5.40524 - alpha 90.000 - beta 90.000 - gamma 120.000 - Primitive - P3221 (154) - 3 - 113.010 - I/Ic PDF 3.4 - F30=
00-012-0703 (D) - Microcline - KAlSiO8 - Y: 2.08 % - d x by: 1. - WL: 1.5406 - Triclinic - a 8.58000 - b 12.97000 - c 7.22000 - alpha 90.640 - beta 115.900 - gamma 87.680 - Base-centered - C-1 (0) - 4 - 722.148 - F30= 2(0.0280,4

Appendix B

Table B-1 Experimental data of liquid limit (*LL*) of formula A

Formula	**A**				
container no.	1	2	3	4	5
container wt.(g)	10.45	10.71	10.38	10.39	10.23
container + wet wt.(g)	17.73	17.47	17.20	17.71	18.54
container + dry wt.(g)	15.30	15.04	14.71	14.99	15.36
wet wt. of clay (g)	7.28	6.76	6.82	7.32	8.31
wt. of water (g)	2.43	2.43	2.49	2.72	3.18
dry wt. of clay (g)	4.85	4.33	4.33	4.60	5.13
water content (%)	50.10	56.12	57.51	59.13	61.99
no. of blows	50	42	33	23	14

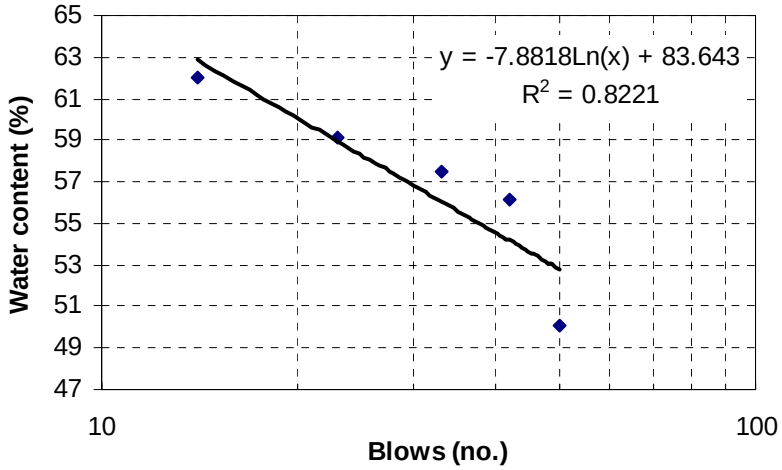

Table B-2 Experimental data of plastic limit (*PL*) of formula A

Formula	**A**		
container no.	1	2	3
container wt.(g)	10.45	10.69	10.36
container + wet wt.(g)	13.56	14.03	14.52
container + dry wt.(g)	13.20	13.66	14.06
wet wt. of clay (g)	3.11	3.34	4.16
wt. of water (g)	0.36	0.37	0.46
dry wt. of clay (g)	2.75	2.97	3.70
water content (%)	13.09	12.46	12.43
avg. water content (%)	12.66		

Table B-3 Experimental data of liquid limit (*LL*) of formula B

Formula	B				
container no.	1	2	3	4	5
container wt.(g)	11.07	10.91	11.22	10.3	9.84
container + wet wt.(g)	18.59	18.36	17.86	18.13	17.53
container + dry wt.(g)	15.85	15.66	15.38	15.11	14.45
wet wt. of clay (g)	7.52	7.45	6.64	7.83	7.69
wt. of water (g)	2.74	2.70	2.48	3.02	3.08
dry wt. of clay (g)	4.78	4.75	4.16	4.81	4.61
water content (%)	57.32	56.84	59.62	62.79	66.81
no. of blows	49	40	29	19	11

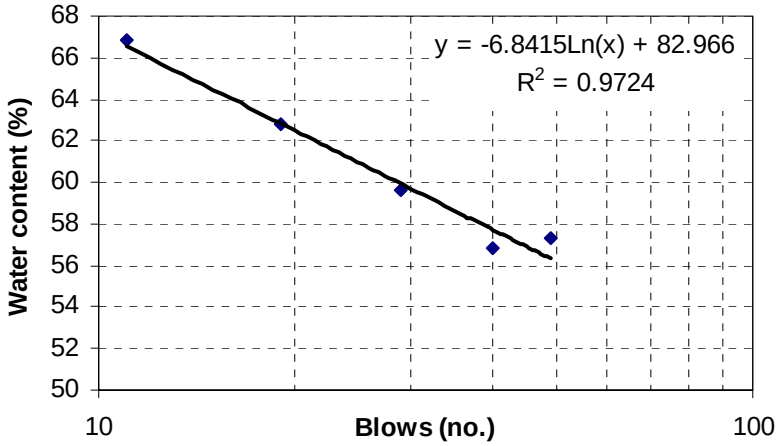

Table B-4 Experimental data of plastic limit (*PL*) of formula B

Formula	B		
container no.	1	2	3
container wt.(g)	11.07	10.92	11.22
container + wet wt.(g)	14.86	14.63	15.33
container + dry wt.(g)	14.41	14.14	14.82
wet wt. of clay (g)	3.79	3.71	4.11
wt. of water (g)	0.45	0.49	0.51
dry wt. of clay (g)	3.34	3.22	3.60
water content (%)	13.47	15.22	14.17
avg. water content (%)	14.29		

Table B-5 Experimental data of liquid limit (*LL*) of formula C

Formula	C				
container no.	1	2	3	4	5
container wt.(g)	9.31	10.20	10.41	10.76	11.00
container + wet wt.(g)	18.35	17.85	18.13	17.98	19.33
container + dry wt.(g)	15.18	15.12	15.32	15.26	16.10
wet wt. of clay (g)	9.04	7.65	7.72	7.22	8.33
wt. of water (g)	3.17	2.73	2.81	2.72	3.23
dry wt. of clay (g)	5.87	4.92	4.91	4.50	5.10
water content (%)	54.00	55.49	57.23	60.44	63.33
no. of blows	50	40	29	21	13

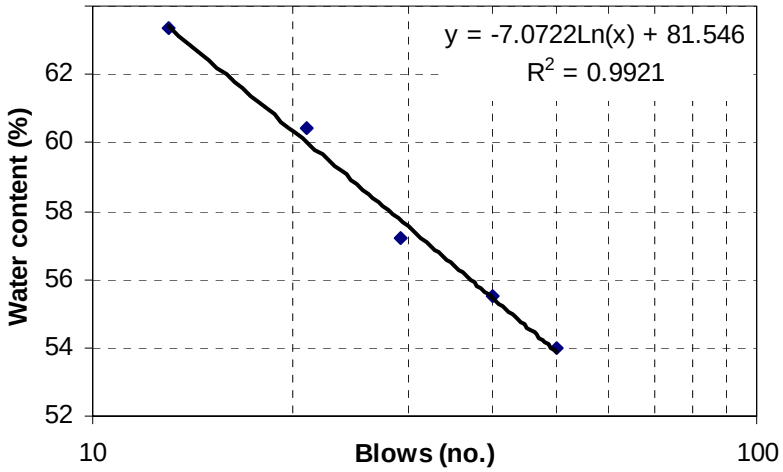

Table B-6 Experimental data of plastic limit (*PL*) of formula C

Formula	C		
container no.	1	2	3
container wt.(g)	9.31	10.21	10.43
container + wet wt.(g)	13.70	14.23	14.92
container + dry wt.(g)	13.16	13.75	14.37
wet wt. of clay (g)	4.39	4.02	4.49
wt. of water (g)	0.54	0.48	0.55
dry wt. of clay (g)	3.85	3.54	3.94
water content (%)	14.03	13.56	13.96
avg. water content (%)	13.85		

Table B-7 Experimental data of liquid limit (*LL*) of formula D

Formula	D				
container no.	1	2	3	4	5
container wt.(g)	10.97	11.04	10.73	10.67	11.78
container + wet wt.(g)	18.30	19.87	19.94	19.77	20.84
container + dry wt.(g)	15.77	16.75	16.57	16.38	17.37
wet wt. of clay (g)	7.33	8.83	9.21	9.10	9.06
wt. of water (g)	2.53	3.12	3.37	3.39	3.47
dry wt. of clay (g)	4.80	5.71	5.84	5.71	5.59
water content (%)	52.71	54.64	57.71	59.37	62.08
no. of blows	49	39	29	20	12

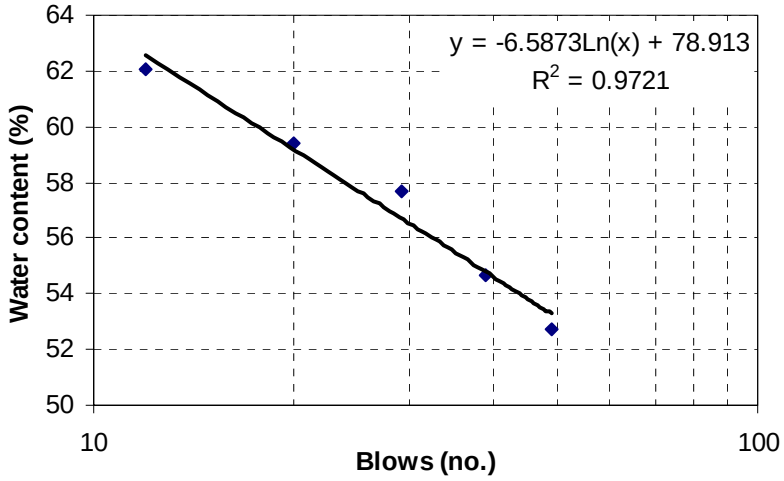

Table B-8 Experimental data of plastic limit (*PL*) of formula D

Formula	D		
container no.	1	2	3
container wt.(g)	10.92	11.04	10.71
container + wet wt.(g)	15.31	15.23	15.14
container + dry wt.(g)	14.78	14.71	14.57
wet wt. of clay (g)	4.39	4.19	4.43
wt. of water (g)	0.53	0.52	0.57
dry wt. of clay (g)	3.86	3.67	3.86
water content (%)	13.73	14.17	14.77
avg. water content (%)	14.22		

Table B-9 Experimental data of liquid limit (*LL*) of formula E

Formula	E				
container no.	1	2	3	4	5
container wt.(g)	10.47	10.52	11.46	9.97	12.65
container + wet wt.(g)	18.14	19.21	19.25	18.48	20.05
container + dry wt.(g)	15.67	16.26	16.53	15.43	17.26
wet wt. of clay (g)	7.67	8.69	7.79	8.51	7.40
wt. of water (g)	2.47	2.95	2.72	3.05	2.79
dry wt. of clay (g)	5.20	5.74	5.07	5.46	4.61
water content (%)	47.50	51.39	53.65	55.86	60.52
no. of blows	50	40	29	20	10

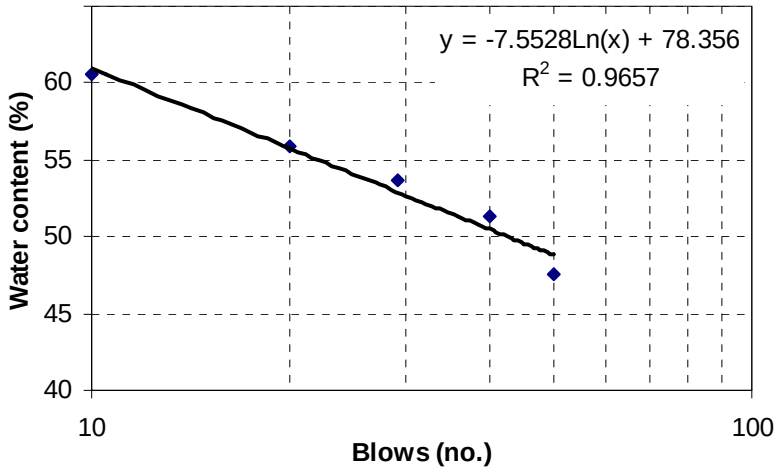

Table B-10 Experimental data of plastic limit (*PL*) of formula E

Formula	E		
container no.	1	2	3
container wt.(g)	10.48	10.52	11.47
container + wet wt.(g)	14.71	14.70	16.11
container + dry wt.(g)	14.23	14.23	15.58
wet wt. of clay (g)	4.23	4.18	4.64
wt. of water (g)	0.48	0.47	0.53
dry wt. of clay (g)	3.75	3.71	4.11
water content (%)	12.80	12.67	12.90
avg. water content (%)	12.79		

Table B-11 Experimental data of liquid limit (*LL*) of formula G

Formula	G				
container no.	1	2	3	4	5
container wt.(g)	11.93	10.83	10.09	12.78	12.76
container + wet wt.(g)	18.96	19.81	18.94	19.93	20.37
container + dry wt.(g)	16.73	16.89	15.95	17.43	17.61
wet wt. of clay (g)	7.03	8.98	8.85	7.15	7.61
wt. of water (g)	2.23	2.92	2.99	2.50	2.76
dry wt. of clay (g)	4.80	6.06	5.86	4.65	4.85
water content (%)	46.46	48.18	51.02	53.76	56.91
no. of blows	50	41	30	20	11

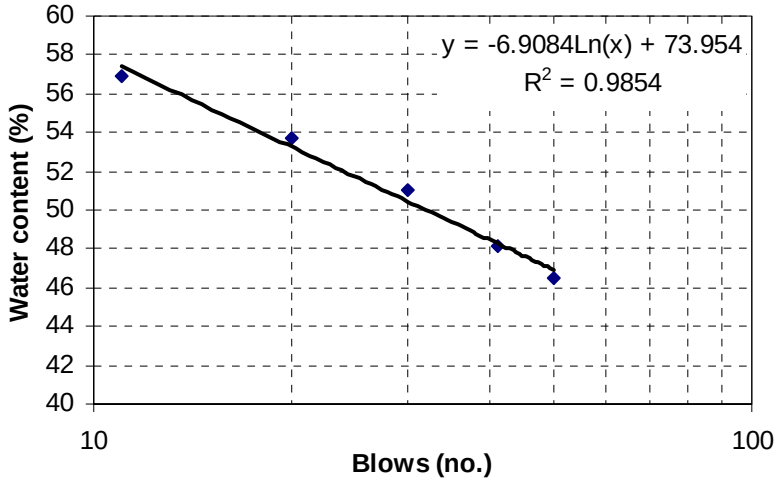

Table B-12 Experimental data of plastic limit (*PL*) of formula G

Formula	G		
container no.	1	2	3
container wt.(g)	11.94	10.84	10.10
container + wet wt.(g)	16.43	15.18	14.75
container + dry wt.(g)	15.95	14.70	14.26
wet wt. of clay (g)	4.49	4.34	4.65
wt. of water (g)	0.48	0.48	0.49
dry wt. of clay (g)	4.01	3.86	4.16
water content (%)	11.97	12.44	11.78
avg. water content (%)	12.06		

Table B-13 Experimental data of liquid limit (*LL*) of formula H

Formula	H				
container no.	1	2	3	4	5
container wt.(g)	11.87	11.17	10.36	12.99	12.99
container + wet wt.(g)	21.42	18.40	17.92	20.12	20.80
container + dry wt.(g)	18.25	15.93	15.27	17.56	17.84
wet wt. of clay (g)	9.55	7.23	7.56	7.13	7.81
wt. of water (g)	3.17	2.47	2.65	2.56	2.96
dry wt. of clay (g)	6.38	4.76	4.91	4.57	4.85
water content (%)	49.69	51.89	53.97	56.02	61.03
no. of blows	50	40	30	20	11

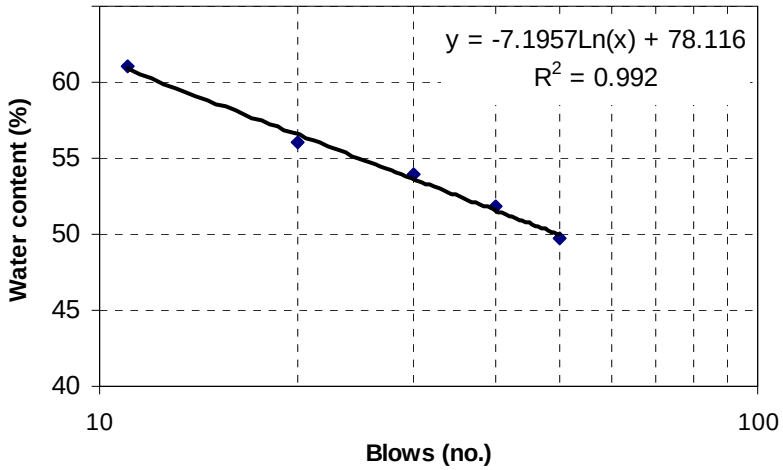

Table B-14 Experimental data of plastic limit (*PL*) of formula H

Formula	H		
container no.	1	2	3
container wt.(g)	11.87	11.16	10.35
container + wet wt.(g)	15.79	15.71	14.23
container + dry wt.(g)	15.34	15.16	13.77
wet wt. of clay (g)	3.92	4.55	3.88
wt. of water (g)	0.45	0.55	0.46
dry wt. of clay (g)	3.47	4.00	3.42
water content (%)	12.97	13.75	13.45
avg. water content (%)	13.39		

Table B-15 Experimental data of liquid limit (*LL*) of formula I

Formula	I				
container no.	1	2	3	4	5
container wt.(g)	11.41	10.91	10.68	10.88	10.20
container + wet wt.(g)	19.70	18.84	18.84	19.81	18.11
container + dry wt.(g)	17.31	16.41	16.28	16.93	15.44
wet wt. of clay (g)	8.29	7.93	8.16	8.93	7.91
wt. of water (g)	2.39	2.43	2.56	2.88	2.67
dry wt. of clay (g)	5.90	5.50	5.60	6.05	5.24
water content (%)	40.51	44.18	45.71	47.60	50.95
no. of blows	47	40	29	20	11

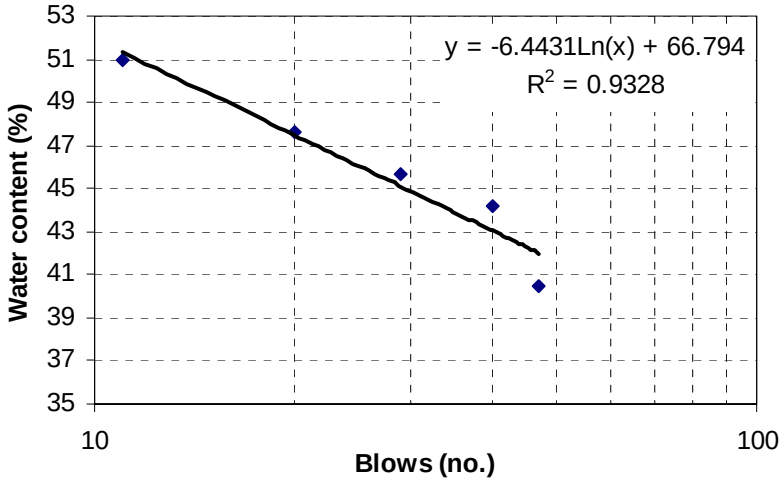

Table B-16 Experimental data of plastic limit (*PL*) of formula I

Formula	I		
container no.	1	2	3
container wt.(g)	11.30	10.91	10.63
container + wet wt.(g)	15.04	15.45	14.44
container + dry wt.(g)	14.70	15.05	14.08
wet wt. of clay (g)	3.74	4.54	3.81
wt. of water (g)	0.34	0.40	0.36
dry wt. of clay (g)	3.40	4.14	3.45
water content (%)	10.00	9.66	10.43
avg. water content (%)	10.03		

Table B-17 Experimental data of liquid limit (*LL*) of formula K

Formula	K				
container no.	1	2	3	4	5
container wt.(g)	11.14	10.36	12.25	11.20	11.04
container + wet wt.(g)	19.36	17.52	21.41	18.76	19.35
container + dry wt.(g)	16.82	15.23	18.41	16.21	16.38
wet wt. of clay (g)	8.22	7.16	9.16	7.56	8.31
wt. of water (g)	2.54	2.29	3.00	2.55	2.97
dry wt. of clay (g)	5.68	4.87	6.16	5.01	5.34
water content (%)	44.72	47.02	48.70	50.90	55.62
no. of blows	50	41	30	20	12

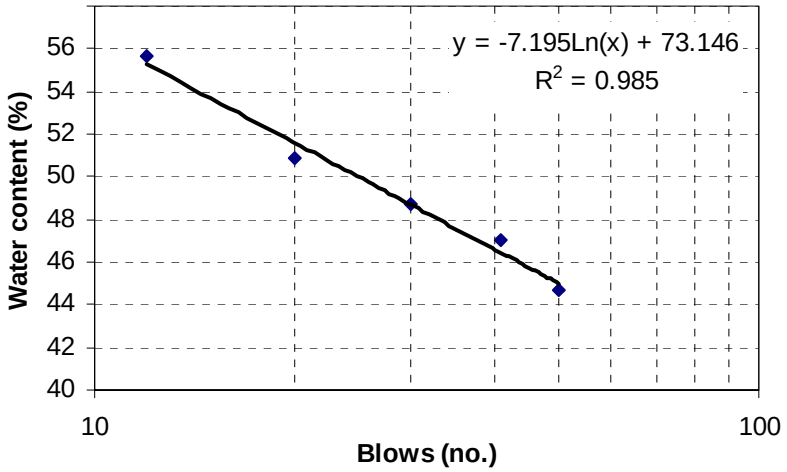

Table B-18 Experimental data of plastic limit (*PL*) of formula K

Formula	K		
container no.	1	2	3
container wt.(g)	11.14	10.36	12.26
container + wet wt.(g)	13.96	13.28	15.86
container + dry wt.(g)	13.64	12.94	15.44
wet wt. of clay (g)	2.82	2.92	3.60
wt. of water (g)	0.32	0.34	0.42
dry wt. of clay (g)	2.50	2.58	3.18
water content (%)	12.80	13.18	13.21
avg. water content (%)	13.06		

Table B-19 Experimental data of liquid limit (*LL*) of formula L

Formula	L				
container no.	1	2	3	4	5
container wt.(g)	10.51	11.73	10.77	11.35	10.52
container + wet wt.(g)	18.37	20.42	19.62	20.28	18.92
container + dry wt.(g)	15.95	17.7	16.78	17.31	15.99
wet wt. of clay (g)	7.86	8.69	8.85	8.93	8.40
wt. of water (g)	2.42	2.72	2.84	2.97	2.93
dry wt. of clay (g)	5.44	5.97	6.01	5.96	5.47
water content (%)	44.49	45.56	47.25	49.83	53.56
no. of blows	49	38	28	20	12

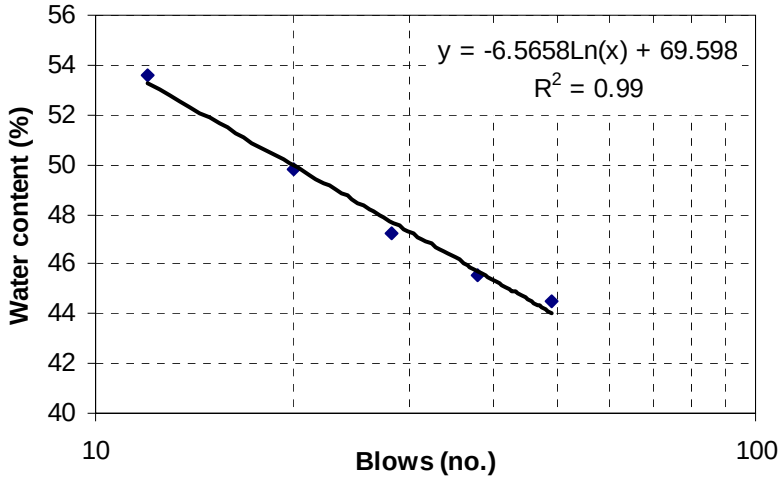

Table B-20 Experimental data of plastic limit (*PL*) of formula L

Formula	L		
container no.	1	2	3
container wt.(g)	10.50	11.75	10.77
container + wet wt.(g)	13.75	15.00	13.86
container + dry wt.(g)	13.40	14.64	13.53
wet wt. of clay (g)	3.25	3.25	3.09
wt. of water (g)	0.35	0.36	0.33
dry wt. of clay (g)	2.90	2.89	2.76
water Content (%)	12.07	12.46	11.96
avg. water content (%)	12.16		

Table B-21 Experimental data of liquid limit (*LL*) of formula M

Formula	M				
container no.	1	2	3	4	5
container wt.(g)	11.56	10.62	10.70	11.49	11.01
container + wet wt.(g)	19.97	18.29	18.49	19.64	19.09
container + dry wt.(g)	16.71	15.30	15.38	16.26	15.59
wet wt. of clay (g)	8.41	7.67	7.79	8.15	8.08
wt. of water (g)	3.26	2.99	3.11	3.38	3.50
dry wt. of clay (g)	5.15	4.68	4.68	4.77	4.58
water content (%)	63.30	63.89	66.45	70.86	76.42
no. of blows	50	40	30	21	12

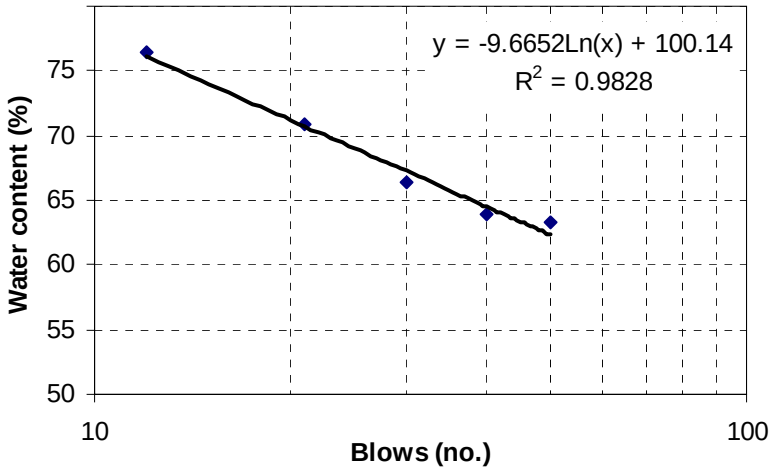

Table B-22 Experimental data of plastic limit (*PL*) of formula M

Formula	M		
container no.	1	2	3
container wt.(g)	11.55	10.60	10.72
container + wet wt.(g)	14.55	14.14	15.57
container + dry wt.(g)	14.15	13.68	14.93
wet wt. of clay (g)	3.00	3.54	4.85
wt. of water (g)	0.40	0.46	0.64
dry wt. of clay (g)	2.60	3.08	4.21
water content (%)	15.38	14.94	15.20
avg. water content (%)	15.17		

Appendix C

Table C Experimental data for moisture difference (*MD*) of clay formulae at various drying times

Drying time at 2.5 hours											
Formula	**Wt. of clay before drying (g)**				**Wt. of clay after drying (g)**				**Moisture content (%)**		**MD (%)**
	EW1	**EW2**	**EW(avg.)**	**IW**	**EW1**	**EW2**	**EW(avg.)**	**IW**	**EW(avg.)**	**IW**	
A	17.27	15.56	16.42	19.78	14.84	13.34	14.09	15.70	14.16	20.63	6.46
B	18.19	16.97	17.58	20.74	15.54	14.52	15.03	16.42	14.51	20.83	6.32
C	19.55	18.33	18.94	19.92	16.57	15.65	16.11	15.73	14.94	21.03	6.09
D	19.12	18.12	18.62	19.90	16.23	15.56	15.90	15.82	14.63	20.50	5.87
E	17.72	17.91	17.82	20.40	15.32	15.49	15.41	16.45	13.53	19.36	5.83
G	20.08	18.89	19.49	19.61	17.25	16.31	16.78	15.78	13.88	19.53	5.65
H	19.06	19.02	19.04	19.98	16.38	16.39	16.39	16.13	13.94	19.27	5.32
I	18.97	20.28	19.63	20.35	16.68	17.86	17.27	16.86	12.00	17.15	5.15
K	18.13	18.25	18.19	20.84	15.91	15.97	15.94	17.11	12.37	17.90	5.53
L	19.34	19.25	19.30	20.36	16.87	16.90	16.89	16.76	12.49	17.68	5.19
M	18.94	17.01	17.98	20.83	15.62	14.13	14.88	15.94	17.25	23.48	6.23
Drying time at 5 hours											
Formula	**Wt. of clay before drying (g)**				**Wt. of clay after drying (g)**				**Moisture content (%)**		**MD (%)**
	EW1	**EW2**	**EW(avg.)**	**IW**	**EW1**	**EW2**	**EW(avg.)**	**IW**	**EW(avg.)**	**IW**	
A	17.19	16.51	16.85	19.48	15.15	14.41	14.78	15.74	12.28	19.20	6.91
B	16.64	17.76	17.20	19.36	14.49	15.47	14.98	15.58	12.91	19.52	6.62
C	17.47	18.33	17.90	19.11	15.24	15.96	15.60	15.37	12.85	19.57	6.72
D	19.42	19.69	19.56	19.99	16.93	17.12	17.03	16.15	12.94	19.21	6.27
E	18.00	18.58	18.29	19.94	15.87	16.40	16.14	16.33	11.78	18.10	6.32
G	18.09	18.09	18.09	18.93	15.94	15.97	15.96	15.44	11.80	18.44	6.63
H	18.98	18.93	18.96	18.73	16.74	16.68	16.71	15.40	11.84	17.78	5.94
I	19.98	19.73	19.86	19.68	17.97	17.75	17.86	16.60	10.05	15.65	5.60
K	20.03	19.99	20.01	19.26	17.88	17.76	17.82	16.19	10.94	15.94	5.00
L	21.87	21.06	21.47	21.07	19.55	18.80	19.18	17.66	10.67	16.18	5.52
M	18.33	19.20	18.77	18.15	15.55	16.22	15.89	14.05	15.35	22.59	7.24

Table C Experimental data for moisture difference (*MD*) of clay formulae at various drying times (continued)

Drying time at 7.5 hours											
Formula	**Wt. of clay before drying (g)**				**Wt. of clay after drying (g)**				**Moisture content (%)**		**MD (%)**
	EW1	**EW2**	**EW(avg.)**	**IW**	**EW1**	**EW2**	**EW(avg.)**	**IW**	**EW(avg.)**	**IW**	
A	17.92	19.02	18.47	18.42	15.96	16.89	16.43	15.46	11.07	16.07	5.00
B	18.65	19.00	18.83	18.49	16.32	16.54	16.43	15.16	12.72	18.01	5.29
C	18.14	18.50	18.32	18.21	15.92	16.27	16.10	15.02	12.15	17.52	5.37
D	18.22	18.99	18.61	19.44	16.03	16.69	16.36	16.01	12.07	17.64	5.58
E	18.78	18.75	18.77	19.89	16.77	16.74	16.76	16.80	10.71	15.54	4.82
G	19.58	18.65	19.12	20.29	17.50	16.71	17.11	17.14	10.52	15.52	5.01
H	20.25	19.23	19.74	19.66	18.08	17.07	17.58	16.58	10.97	15.67	4.70
I	20.02	17.72	18.87	18.37	18.27	16.21	17.24	15.98	8.64	13.01	4.37
K	18.34	17.15	17.75	20.77	16.62	15.46	16.04	17.82	9.61	14.20	4.59
L	18.15	18.16	18.16	20.63	16.53	16.53	16.53	17.92	8.95	13.14	4.19
M	18.80	19.23	19.02	19.41	16.11	16.43	16.27	15.33	14.44	21.02	6.58
Drying time at 10 hours											
Formula	**Wt. of clay before drying (g)**				**Wt. of clay after drying (g)**				**Moisture content (%)**		**MD (%)**
	EW1	**EW2**	**EW(avg.)**	**IW**	**EW1**	**EW2**	**EW(avg.)**	**IW**	**EW(avg.)**	**IW**	
A	19.35	18.19	18.77	19.23	17.27	16.35	16.81	16.56	10.44	13.88	3.44
B	16.91	18.96	17.94	17.89	15.02	16.74	15.88	15.14	11.46	15.37	3.91
C	17.18	18.42	17.80	19.23	15.24	16.28	15.76	16.28	11.46	15.34	3.88
D	18.64	17.82	18.23	20.77	16.57	15.86	16.22	17.61	11.05	15.21	4.16
E	18.48	19.30	18.89	20.66	16.64	17.26	16.95	17.79	10.27	13.89	3.62
G	18.84	19.73	19.29	20.43	16.95	17.74	17.35	17.57	10.06	14.00	3.94
H	18.57	19.67	19.12	19.62	16.64	17.60	17.12	16.88	10.46	13.97	3.51
I	18.90	20.45	19.68	20.55	17.39	18.79	18.09	18.21	8.06	11.39	3.33
K	18.94	19.12	19.03	19.11	17.30	17.35	17.33	16.74	8.96	12.40	3.44
L	19.09	18.82	18.96	21.03	17.51	17.19	17.35	18.53	8.47	11.89	3.42
M	18.88	19.37	19.13	19.32	16.22	16.72	16.47	15.55	13.88	19.51	5.63

Table C Experimental data for moisture difference (*MD*) of clay formulae at various drying times (continued)

Drying time at 15 hours											
Formula	**Wt. of clay before drying (g)**				**Wt. of clay after drying (g)**				**Moisture content (%)**		**MD (%)**
	EW1	**EW2**	**EW(avg.)**	**IW**	**EW1**	**EW2**	**EW(avg.)**	**IW**	**EW(avg.)**	**IW**	
A	18.55	16.84	17.70	20.06	16.89	15.42	16.16	17.90	8.70	10.77	2.06
B	17.93	17.18	17.56	18.96	16.16	15.49	15.83	16.66	9.85	12.13	2.28
C	17.65	15.86	16.76	17.61	16.01	14.39	15.20	15.55	9.28	11.70	2.42
D	18.47	17.56	18.02	18.31	16.78	15.94	16.36	16.21	9.19	11.47	2.28
E	18.13	18.64	18.39	19.44	16.56	17.06	16.81	17.36	8.57	10.70	2.13
G	17.55	18.13	17.84	20.78	16.08	16.58	16.33	18.47	8.46	11.12	2.65
H	19.49	17.56	18.53	19.32	17.76	16.07	16.92	17.21	8.69	10.92	2.23
I	18.36	18.39	18.38	19.63	17.24	17.25	17.25	17.96	6.15	8.51	2.36
K	20.00	18.41	19.21	19.99	18.65	17.14	17.90	18.18	6.82	9.05	2.23
L	18.90	17.55	18.23	21.19	17.63	16.38	17.01	19.27	6.69	9.06	2.37
M	18.31	18.01	18.16	18.21	15.99	15.72	15.86	15.32	12.69	15.87	3.18
Drying time at 20 hours											
Formula	**Wt. of clay before drying (g)**				**Wt. of clay after drying (g)**				**Moisture content (%)**		**MD (%)**
	EW1	**EW2**	**EW(avg.)**	**IW**	**EW1**	**EW2**	**EW(avg.)**	**IW**	**EW(avg.)**	**IW**	
A	17.53	17.36	17.45	18.69	16.17	16.05	16.11	16.89	7.65	9.63	1.98
B	17.29	18.43	17.86	18.86	15.94	16.97	16.46	16.87	7.87	10.55	2.68
C	18.12	16.80	17.46	17.49	16.69	15.44	16.07	15.75	7.99	9.95	1.96
D	18.04	17.48	17.76	18.29	16.69	16.12	16.41	16.58	7.63	9.35	1.72
E	17.97	16.84	17.41	20.54	16.87	15.78	16.33	18.86	6.21	8.18	1.97
G	17.82	16.64	17.23	16.54	16.79	15.64	16.22	15.24	5.89	7.86	1.97
H	17.66	17.88	17.77	19.22	16.47	16.63	16.55	17.50	6.87	8.95	2.08
I	18.81	17.52	18.17	18.76	17.97	16.83	17.40	17.51	4.21	6.66	2.45
K	18.11	18.43	18.27	19.16	17.24	17.48	17.36	17.81	4.98	7.05	2.07
L	17.40	17.63	17.52	19.43	16.62	16.72	16.67	18.10	4.82	6.85	2.02
M	17.96	18.65	18.31	19.64	15.97	16.56	16.27	17.14	11.14	12.73	1.58

Table C Experimental data for moisture difference (*MD*) of clay formulae at various drying times (continued)

Drying time at 50 hours											
Formula	**Wt. of clay before drying (g)**				**Wt. of clay after drying (g)**				**Moisture content (%)**		**MD (%)**
	EW1	**EW2**	**EW(avg.)**	**IW**	**EW1**	**EW2**	**EW(avg.)**	**IW**	**EW(avg.)**	**IW**	
A	14.32	15.40	14.86	16.11	14.03	15.06	14.55	15.57	2.12	3.35	1.23
B	15.30	14.78	15.04	15.79	15.01	14.52	14.77	15.38	1.83	2.60	0.77
C	15.02	14.63	14.83	14.77	14.70	14.31	14.51	14.30	2.16	3.18	1.02
D	16.36	16.19	16.28	15.62	16.09	15.82	15.96	15.11	1.97	3.27	1.30
E	14.74	15.46	15.10	16.38	14.51	15.23	14.87	16.01	1.52	2.26	0.74
G	15.36	14.56	14.96	15.81	15.12	14.34	14.73	15.45	1.54	2.28	0.74
H	15.68	15.26	15.47	16.14	15.43	15.01	15.22	15.69	1.62	2.79	1.17
I	15.40	15.87	15.64	16.86	15.24	15.71	15.48	16.64	1.02	1.30	0.28
K	15.78	14.77	15.28	15.66	15.61	14.59	15.10	15.40	1.15	1.66	0.51
L	16.06	16.61	16.34	16.64	15.86	16.39	16.13	16.36	1.29	1.68	0.40
M	14.97	14.99	14.98	15.43	14.44	14.45	14.45	14.61	3.57	5.31	1.74

Appendix D

Table D Bending strength of green bodies of all clay formulae

Formula	No.	Maximum load (N)	MOR (MPa)	Average (MPa)	SD
A	1	20.83	4.31		
	2	20.07	4.15		
	3	20.13	4.16		
	4	18.63	3.85		
	5	18.24	3.77		
	6	18.98	3.93	4.13	0.24
	7	20.20	4.18		
	8	19.30	3.99		
	9	21.53	4.45		
	10	21.67	4.48		
B	1	21.01	4.28		
	2	25.33	5.16		
	3	20.29	4.13		
	4	20.82	4.24		
	5	25.15	5.12		
	6	23.20	4.73	4.74	0.44
	7	23.78	4.84		
	8	23.74	4.84		
	9	26.80	5.46		
	10	22.38	4.56		
C	1	25.80	5.26		
	2	22.69	4.62		
	3	23.98	4.89		
	4	25.22	5.14		
	5	24.72	5.04		
	6	24.73	5.04	5.02	0.27
	7	24.99	5.09		
	8	27.09	5.52		
	9	24.26	4.94		
	10	22.73	4.63		
D	1	22.23	4.53		
	2	22.37	4.56		
	3	22.21	4.52		
	4	21.35	4.35		
	5	23.84	4.86		
	6	23.89	4.87	4.68	0.20
	7	22.73	4.63		
	8	23.44	4.78		
	9	23.13	4.71		
	10	24.62	5.02		

Table D Bending strength of green bodies of all clay formulae (continued)

Formula	No.	Maximum load (N)	MOR (MPa)	Average (MPa)	SD
E	1	18.98	3.64		
	2	20.57	3.95		
	3	18.66	3.58		
	4	18.81	3.61		
	5	20.66	3.97		
	6	19.99	3.84	3.82	0.18
	7	19.40	3.72		
	8	21.37	4.10		
	9	19.78	3.80		
	10	20.65	3.96		
G	1	20.83	4.31		
	2	20.07	4.15		
	3	20.13	4.16		
	4	18.63	3.85		
	5	18.24	3.77		
	6	18.98	3.93	4.13	0.24
	7	20.20	4.18		
	8	19.30	3.99		
	9	21.53	4.45		
	10	21.67	4.48		
H	1	21.01	4.28		
	2	25.33	5.16		
	3	20.29	4.13		
	4	20.82	4.24		
	5	25.15	5.12		
	6	23.20	4.73	4.74	0.44
	7	23.78	4.84		
	8	23.74	4.84		
	9	26.80	5.46		
	10	22.38	4.56		
I	1	25.80	5.26		
	2	22.69	4.62		
	3	23.98	4.89		
	4	25.22	5.14		
	5	24.72	5.04		
	6	24.73	5.04	5.02	0.27
	7	24.99	5.09		
	8	27.09	5.52		
	9	24.26	4.94		
	10	22.73	4.63		

Table D Bending strength of green bodies of all clay formulae (continued)

Formula	No.	Maximum load (N)	MOR (MPa)	Average (MPa)	SD
K	1	22.23	4.53		
	2	22.37	4.56		
	3	22.21	4.52		
	4	21.35	4.35		
	5	23.84	4.86		
	6	23.89	4.87	4.68	0.20
	7	22.73	4.63		
	8	23.44	4.78		
	9	23.13	4.71		
	10	24.62	5.02		
L	1	18.98	3.64		
	2	20.57	3.95		
	3	18.66	3.58		
	4	18.81	3.61		
	5	20.66	3.97		
	6	19.99	3.84	3.82	0.18
	7	19.40	3.72		
	8	21.37	4.10		
	9	19.78	3.80		
	10	20.65	3.96		
M	1	37.57	7.89		
	2	34.00	7.14		
	3	37.10	7.79		
	4	39.19	8.23		
	5	40.23	8.45		
	6	37.82	7.94	7.70	0.54
	7	38.87	8.16		
	8	35.03	7.36		
	9	34.92	7.33		
	10	32.13	6.75		

Appendix E

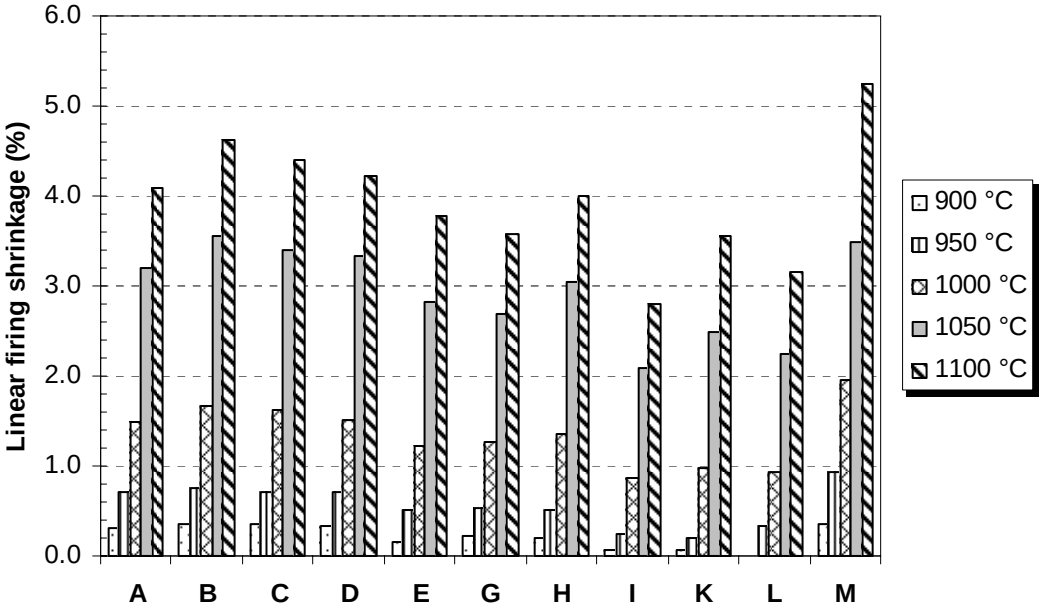

Linear firing shrinkage of fired mixed clay bodies at various temperatures

Table E-1 Experimental data of firing shrinkage of fired bodies at 900 °C

900 °C						
Formula	#	Length before drying (mm)	Length after firing (mm)	Linear firing shrinkage (%)	Avg.	S.D.
A	1	94.45	94.30	0.16	0.32	0.15
	2	94.75	94.60	0.16		
	3	94.55	94.40	0.16		
	4	94.65	94.50	0.16		
	5	94.90	94.60	0.32		
	6	94.45	94.10	0.37		
	7	94.25	93.85	0.42		
	8	94.25	93.85	0.42		
	9	94.40	93.90	0.53		
	10	94.55	94.10	0.48		
B	1	94.35	94.15	0.21	0.35	0.13
	2	94.40	94.30	0.11		
	3	94.30	94.00	0.32		
	4	94.10	93.85	0.27		
	5	94.50	94.10	0.42		
	6	94.50	94.20	0.32		
	7	94.20	93.75	0.48		
	8	94.25	93.85	0.42		
	9	94.45	94.00	0.48		
	10	94.15	93.70	0.48		
C	1	94.45	94.25	0.21	0.36	0.11
	2	94.50	94.30	0.21		
	3	94.75	94.45	0.32		
	4	94.90	94.60	0.32		
	5	94.60	94.25	0.37		
	6	94.65	94.35	0.32		
	7	94.65	94.25	0.42		
	8	94.65	94.25	0.42		
	9	94.40	93.90	0.53		
	10	94.60	94.15	0.48		
D	1	94.40	94.20	0.21	0.34	0.10
	2	94.30	94.15	0.16		
	3	94.65	94.25	0.42		
	4	94.55	94.25	0.32		
	5	94.15	93.85	0.32		
	6	94.40	94.10	0.32		
	7	94.75	94.30	0.47		
	8	94.30	93.95	0.37		
	9	94.70	94.30	0.42		
	10	94.35	93.95	0.42		

Table E-1 Experimental data of firing shrinkage of fired bodies at 900 °C (continued)

900 °C						
Formula	#	Length before drying (mm)	Length after firing (mm)	Linear firing shrinkage (%)	Avg.	S.D.
E	1	94.60	94.60	0.00	0.16	0.12
	2	94.95	94.95	0.00		
	3	94.70	94.65	0.05		
	4	94.95	94.85	0.11		
	5	94.90	94.80	0.11		
	6	94.80	94.55	0.26		
	7	94.85	94.60	0.26		
	8	94.80	94.55	0.26		
	9	94.90	94.65	0.26		
	10	94.65	94.35	0.32		
G	1	94.85	94.75	0.11	0.22	0.07
	2	94.80	94.70	0.11		
	3	94.90	94.65	0.26		
	4	94.55	94.40	0.16		
	5	94.70	94.45	0.26		
	6	94.80	94.60	0.21		
	7	94.80	94.55	0.26		
	8	94.80	94.55	0.26		
	9	94.80	94.55	0.26		
	10	94.85	94.55	0.32		
H	1	94.80	94.75	0.05	0.20	0.10
	2	94.80	94.75	0.05		
	3	94.55	94.40	0.16		
	4	94.85	94.65	0.21		
	5	94.75	94.55	0.21		
	6	94.70	94.55	0.16		
	7	94.85	94.60	0.26		
	8	94.80	94.50	0.32		
	9	94.80	94.50	0.32		
	10	94.85	94.60	0.26		
I	1	95.00	95.00	0.00	0.06	0.06
	2	94.65	94.65	0.00		
	3	95.15	95.15	0.00		
	4	94.90	94.80	0.11		
	5	94.90	94.85	0.05		
	6	95.00	95.00	0.00		
	7	95.05	95.00	0.05		
	8	94.95	94.80	0.16		
	9	95.00	94.90	0.11		
	10	94.95	94.80	0.16		

Table E-1 Experimental data of firing shrinkage of fired bodies at 900 °C (continued)

900 °C						
Formula	#	Length before drying (mm)	Length after firing (mm)	Linear firing shrinkage (%)	Avg.	S.D.
K	1	94.90	94.90	0.00	0.06	0.09
	2	94.65	94.65	0.00		
	3	94.95	94.95	0.00		
	4	94.80	94.80	0.00		
	5	94.80	94.70	0.11		
	6	94.90	94.90	0.00		
	7	94.85	94.80	0.05		
	8	94.70	94.65	0.05		
	9	94.90	94.70	0.21		
	10	94.60	94.40	0.21		
L	1	95.20	95.20	0.00	0.01	0.02
	2	95.15	95.15	0.00		
	3	95.10	95.10	0.00		
	4	95.05	95.05	0.00		
	5	95.10	95.10	0.00		
	6	95.05	95.05	0.00		
	7	95.00	95.00	0.00		
	8	94.90	94.90	0.00		
	9	95.00	95.00	0.00		
	10	95.15	95.10	0.05		
M	1	94.25	94.15	0.11	0.25	0.22
	2	94.35	94.20	0.16		
	3	94.40	94.00	0.42		
	4	94.35	94.00	0.37		
	5	94.30	93.90	0.42		
	6	94.40	93.95	0.48		
	7	94.60	94.10	0.53		

Table E-2 Experimental data of firing shrinkage of fired bodies at 950 °C

950 °C						
Formula	#	Length before drying (mm)	Length after firing (mm)	Linear firing shrinkage (%)	Avg.	S.D.
A	1	94.70	94.25	0.48	0.72	0.16
	2	94.35	93.85	0.53		
	3	94.45	93.80	0.69		
	4	94.55	94.00	0.58		
	5	94.70	93.95	0.79		
	6	94.35	93.75	0.64		
	7	94.50	93.65	0.90		
	8	94.75	93.95	0.84		
	9	94.60	93.80	0.85		
	10	94.55	93.70	0.90		
B	1	93.95	93.45	0.53	0.75	0.17
	2	94.50	94.00	0.53		
	3	94.50	93.95	0.58		
	4	94.55	93.85	0.74		
	5	94.25	93.55	0.74		
	6	94.20	93.55	0.69		
	7	94.60	93.75	0.90		
	8	94.00	93.20	0.85		
	9	93.95	93.00	1.01		
	10	94.45	93.55	0.95		
C	1	94.65	94.15	0.53	0.71	0.15
	2	94.65	94.15	0.53		
	3	94.60	94.00	0.63		
	4	94.80	94.25	0.58		
	5	94.70	94.05	0.69		
	6	94.80	94.15	0.69		
	7	94.70	93.90	0.84		
	8	94.70	93.90	0.84		
	9	94.65	93.90	0.79		
	10	94.75	93.85	0.95		
D	1	94.80	94.35	0.47	0.71	0.18
	2	94.40	94.00	0.42		
	3	94.55	94.00	0.58		
	4	94.60	94.00	0.63		
	5	94.50	93.80	0.74		
	6	94.50	93.80	0.74		
	7	94.50	93.70	0.85		
	8	94.55	93.70	0.90		
	9	94.50	93.65	0.90		
	10	94.45	93.60	0.90		

Table E-2 Experimental data of firing shrinkage of fired bodies at 950 °C (continued)

950 °C						
Formula	#	Length before drying (mm)	Length after firing (mm)	Linear firing shrinkage (%)	Avg.	S.D.
E	1	94.70	94.40	0.32	0.52	0.15
	2	94.65	94.40	0.26		
	3	94.80	94.40	0.42		
	4	94.70	94.25	0.48		
	5	94.85	94.40	0.47		
	6	94.85	94.35	0.53		
	7	95.05	94.45	0.63		
	8	94.75	94.10	0.69		
	9	94.90	94.25	0.68		
	10	94.70	94.05	0.69		
G	1	94.80	94.45	0.37	0.54	0.10
	2	94.80	94.40	0.42		
	3	94.75	94.25	0.53		
	4	94.75	94.35	0.42		
	5	94.65	94.15	0.53		
	6	94.60	94.05	0.58		
	7	94.80	94.20	0.63		
	8	94.75	94.15	0.63		
	9	94.80	94.20	0.63		
	10	94.80	94.20	0.63		
H	1	94.70	94.45	0.26	0.51	0.14
	2	94.50	94.20	0.32		
	3	94.75	94.35	0.42		
	4	94.50	94.10	0.42		
	5	94.70	94.15	0.58		
	6	94.75	94.25	0.53		
	7	94.70	94.15	0.58		
	8	94.65	94.05	0.63		
	9	94.55	93.95	0.63		
	10	94.55	93.90	0.69		
I	1	95.10	95.00	0.11	0.24	0.12
	2	94.90	94.85	0.05		
	3	94.90	94.80	0.11		
	4	94.95	94.75	0.21		
	5	95.30	95.10	0.21		
	6	95.10	94.80	0.32		
	7	94.90	94.60	0.32		
	8	94.95	94.65	0.32		
	9	94.90	94.60	0.32		
	10	94.95	94.55	0.42		

Table E-2 Experimental data of firing shrinkage of fired bodies at 950 °C (continued)

950 °C						
Formula	#	Length before drying (mm)	Length after firing (mm)	Linear firing shrinkage (%)	Avg.	S.D.
K	1	95.05	95.05	0.00	0.19	0.16
	2	95.00	95.00	0.00		
	3	95.20	95.15	0.05		
	4	95.20	95.20	0.00		
	5	94.85	94.65	0.21		
	6	94.95	94.70	0.26		
	7	95.00	94.75	0.26		
	8	95.00	94.70	0.32		
	9	95.20	94.85	0.37		
	10	95.00	94.60	0.42		
L	1	94.75	94.55	0.21	0.33	0.09
	2	94.95	94.75	0.21		
	3	94.95	94.65	0.32		
	4	94.70	94.45	0.26		
	5	94.75	94.50	0.26		
	6	94.90	94.55	0.37		
	7	95.00	94.65	0.37		
	8	95.15	94.75	0.42		
	9	95.00	94.55	0.47		
	10	95.05	94.65	0.42		
M	1	94.55	93.90	0.69	0.93	0.22
	2	94.45	93.85	0.64		
	3	94.35	93.60	0.79		
	4	94.00	93.15	0.90		
	5	94.35	93.45	0.95		
	6	94.40	93.35	1.11		
	7	94.30	93.20	1.17		
	8	94.05	92.90	1.22		

Table E-3 Experimental data of firing shrinkage of fired bodies at 1000 °C

1000 °C						
Formula	#	Length before drying (mm)	Length after firing (mm)	Linear firing shrinkage (%)	Avg.	S.D.
A	1	95.05	94.05	1.05	1.50	0.34
	2	94.65	93.80	0.90		
	3	94.45	93.20	1.32		
	4	94.60	93.35	1.32		
	5	94.30	92.85	1.54		
	6	94.60	93.15	1.53		
	7	94.60	92.95	1.74		
	8	94.65	92.90	1.85		
	9	94.70	92.95	1.85		
	10	94.50	92.75	1.85		
B	1	94.40	93.25	1.22	1.66	0.41
	2	94.35	93.45	0.95		
	3	94.50	93.20	1.38		
	4	94.30	93.00	1.38		
	5	94.30	92.65	1.75		
	6	94.50	92.85	1.75		
	7	94.45	92.60	1.96		
	8	94.45	92.60	1.96		
	9	94.50	92.45	2.17		
	10	94.70	92.70	2.11		
C	1	94.55	93.55	1.06	1.63	0.39
	2	94.85	93.80	1.11		
	3	94.75	93.50	1.32		
	4	94.55	93.20	1.43		
	5	94.90	93.30	1.69		
	6	94.85	93.20	1.74		
	7	94.65	92.95	1.80		
	8	94.70	92.85	1.95		
	9	94.60	92.60	2.11		
	10	94.75	92.75	2.11		
D	1	94.50	93.60	0.95	1.52	0.40
	2	94.70	93.75	1.00		
	3	94.75	93.55	1.27		
	4	94.35	93.20	1.22		
	5	94.45	93.05	1.48		
	6	94.60	93.10	1.59		
	7	94.65	92.90	1.85		
	8	94.50	92.70	1.90		
	9	94.80	93.00	1.90		
	10	94.65	92.70	2.06		

Table E-3 Experimental data of firing shrinkage of fired bodies at 1000 °C (continued)

1000 °C						
Formula	#	Length before drying (mm)	Length after firing (mm)	Linear firing shrinkage (%)	Avg.	S.D.
E	1	94.85	94.20	0.69	1.23	0.36
	2	94.95	94.20	0.79		
	3	95.00	94.10	0.95		
	4	94.80	93.85	1.00		
	5	94.85	93.65	1.27		
	6	94.80	93.60	1.27		
	7	94.95	93.50	1.53		
	8	94.80	93.30	1.58		
	9	94.90	93.35	1.63		
	10	95.05	93.50	1.63		
G	1	94.65	93.90	0.79	1.26	0.33
	2	94.75	94.00	0.79		
	3	94.80	93.90	0.95		
	4	94.95	93.95	1.05		
	5	94.90	93.65	1.32		
	6	94.65	93.30	1.43		
	7	94.80	93.35	1.53		
	8	94.80	93.35	1.53		
	9	95.10	93.60	1.58		
	10	94.95	93.40	1.63		
H	1	94.85	94.00	0.90	1.36	0.33
	2	94.95	94.10	0.90		
	3	94.75	93.60	1.21		
	4	94.95	93.95	1.05		
	5	94.75	93.40	1.42		
	6	94.95	93.65	1.37		
	7	94.75	93.10	1.74		
	8	95.00	93.50	1.58		
	9	94.60	93.00	1.69		
	10	94.60	92.95	1.74		
I	1	95.35	94.85	0.52	0.87	0.26
	2	95.00	94.55	0.47		
	3	95.10	94.40	0.74		
	4	95.35	94.70	0.68		
	5	95.10	94.30	0.84		
	6	94.80	93.90	0.95		
	7	95.20	94.15	1.10		
	8	95.05	94.05	1.05		
	9	95.30	94.25	1.10		
	10	95.10	93.95	1.21		

Table E-3 Experimental data of firing shrinkage of fired bodies at 1000 °C (continued)

1000 °C						
Formula	#	Length before drying (mm)	Length after firing (mm)	Linear firing shrinkage (%)	Avg.	S.D.
K	1	95.10	94.60	0.53	0.98	0.30
	2	95.00	94.50	0.53		
	3	95.00	94.25	0.79		
	4	94.95	94.15	0.84		
	5	95.25	94.25	1.05		
	6	94.80	93.85	1.00		
	7	95.10	93.95	1.21		
	8	95.10	93.90	1.26		
	9	95.10	93.85	1.31		
	10	95.10	93.85	1.31		
L	1	95.00	94.60	0.42	0.91	0.30
	2	95.00	94.55	0.47		
	3	95.15	94.50	0.68		
	4	94.95	94.15	0.84		
	5	94.95	94.05	0.95		
	6	94.95	94.05	0.95		
	7	95.05	93.90	1.21		
	8	94.95	94.00	1.00		
	9	94.95	93.75	1.26		
	10	95.00	93.80	1.26		
M	1	94.30	92.95	1.43	1.95	0.43
	2	94.65	93.40	1.32		
	3	94.30	92.70	1.70		
	4	94.40	92.90	1.59		
	5	94.30	92.50	1.91		
	6	94.40	92.55	1.96		
	7	94.60	92.40	2.33		
	8	94.45	92.25	2.33		
	9	94.45	92.05	2.54		
	10	94.60	92.35	2.38		

Table E-4 Experimental data of firing shrinkage of fired bodies at 1050 °C

1050 °C						
Formula	#	Length before drying (mm)	Length after firing (mm)	Linear firing shrinkage (%)	Avg.	S.D.
A	1	94.75	91.85	3.06	3.19	0.20
	2	94.65	92.10	2.69		
	3	94.95	92.00	3.11		
	4	94.45	91.45	3.18		
	5	94.85	91.75	3.27		
	6	94.65	91.60	3.22		
	7	94.70	91.55	3.33		
	8	94.60	91.45	3.33		
	9	94.75	91.60	3.32		
	10	94.50	91.30	3.39		
B	1	94.65	91.75	3.06	3.55	0.30
	2	94.35	91.50	3.02		
	3	94.30	91.05	3.45		
	4	94.25	90.95	3.50		
	5	94.60	91.10	3.70		
	6	94.25	90.85	3.61		
	7	94.55	91.00	3.75		
	8	94.20	90.70	3.72		
	9	94.25	90.65	3.82		
	10	94.60	90.95	3.86		
C	1	95.00	92.05	3.11	3.39	0.22
	2	95.10	92.30	2.94		
	3	94.65	91.50	3.33		
	4	94.55	91.45	3.28		
	5	94.90	91.60	3.48		
	6	94.85	91.55	3.48		
	7	94.60	91.25	3.54		
	8	94.85	91.45	3.58		
	9	94.35	90.95	3.60		
	10	94.70	91.35	3.54		
D	1	94.75	92.05	2.85	3.33	0.22
	2	94.45	91.40	3.23		
	3	94.75	91.70	3.22		
	4	94.65	91.55	3.28		
	5	95.05	91.85	3.37		
	6	94.60	91.30	3.49		
	7	94.50	91.25	3.44		
	8	94.55	91.25	3.49		
	9	94.65	91.25	3.59		

Table E-4 Experimental data of firing shrinkage of fired bodies at 1050 °C (continued)

1050 °C						
Formula	#	Length before drying (mm)	Length after firing (mm)	Linear firing shrinkage (%)	Avg.	S.D.
E	1	94.75	92.45	2.43	2.83	0.23
	2	94.75	92.40	2.48		
	3	95.05	92.50	2.68		
	4	94.65	92.00	2.80		
	5	94.65	91.95	2.85		
	6	94.65	91.85	2.96		
	7	94.65	91.80	3.01		
	8	94.40	91.55	3.02		
	9	94.30	91.40	3.08		
	10	94.50	91.65	3.02		
G	1	94.70	92.40	2.43	2.68	0.18
	2	94.65	92.40	2.38		
	3	94.80	92.40	2.53		
	4	94.65	92.10	2.69		
	5	94.70	91.95	2.90		
	6	94.80	92.15	2.80		
	7	94.85	92.15	2.85		
	8	94.85	92.20	2.79		
	9	94.90	92.30	2.74		
	10	94.95	92.35	2.74		
H	1	94.90	92.30	2.74	3.05	0.18
	2	94.75	92.15	2.74		
	3	94.90	92.00	3.06		
	4	94.55	91.75	2.96		
	5	94.80	91.75	3.22		
	6	94.70	91.75	3.12		
	7	94.70	91.65	3.22		
	8	94.75	91.75	3.17		
	9	95.00	92.05	3.11		
	10	94.75	91.75	3.17		
I	1	95.00	93.15	1.95	2.09	0.16
	2	95.15	93.50	1.73		
	3	94.85	92.85	2.11		
	4	95.20	93.30	2.00		
	5	95.20	93.20	2.10		
	6	94.75	92.80	2.06		
	7	94.75	92.65	2.22		
	8	94.75	92.65	2.22		
	9	95.05	92.95	2.21		
	10	94.95	92.80	2.26		

Table E-4 Experimental data of firing shrinkage of fired bodies at 1050 °C (continued)

1050 °C						
Formula	#	Length before drying (mm)	Length after firing (mm)	Linear firing shrinkage (%)	Avg.	S.D.
K	1	95.10	93.10	2.10	2.49	0.23
	2	95.00	93.00	2.11		
	3	94.90	92.60	2.42		
	4	94.95	92.65	2.42		
	5	94.75	92.25	2.64		
	6	94.95	92.45	2.63		
	7	94.90	92.30	2.74		
	8	95.20	92.70	2.63		
	9	95.15	92.65	2.63		
	10	95.15	92.65	2.63		
L	1	94.95	92.95	2.11	2.24	0.15
	2	94.90	93.00	2.00		
	3	95.00	92.90	2.21		
	4	94.90	92.85	2.16		
	5	95.05	92.85	2.31		
	6	94.95	92.95	2.11		
	7	95.15	92.90	2.36		
	8	95.15	92.85	2.42		
	9	94.90	92.70	2.32		
	10	95.05	92.75	2.42		
M	1	94.60	91.35	3.44	3.48	0.59
	2	94.65	91.45	3.38		
	3	94.45	91.80	2.81		
	4	94.45	91.80	2.81		
	5	94.55	91.70	3.01		
	6	94.90	91.00	4.11		
	7	94.60	90.65	4.18		
	8	94.65	90.75	4.12		

Table E-5 Experimental data of firing shrinkage of fired bodies at 1100 °C

1100 °C						
Formula	#	Length before drying (mm)	Length after firing (mm)	Linear firing shrinkage (%)	Avg.	S.D.
A	1	94.30	90.55	3.98	4.09	0.08
	2	94.45	90.70	3.97		
	3	94.55	90.75	4.02		
	4	94.20	90.35	4.09		
	5	94.40	90.50	4.13		
	6	94.40	90.50	4.13		
	7	94.55	90.65	4.12		
	8	94.80	90.85	4.17		
	9	94.60	90.65	4.18		
	10	94.50	90.60	4.13		
B	1	94.20	90.00	4.46	4.63	0.08
	2	94.25	89.95	4.56		
	3	94.45	90.05	4.66		
	4	94.55	90.20	4.60		
	5	94.65	90.25	4.65		
	6	94.25	89.85	4.67		
	7	94.50	90.00	4.76		
	8	94.25	89.90	4.62		
	9	94.35	89.95	4.66		
	10	94.35	89.95	4.66		
C	1	94.55	90.55	4.23	4.39	0.12
	2	94.50	90.55	4.18		
	3	94.30	90.25	4.29		
	4	94.65	90.45	4.44		
	5	94.65	90.40	4.49		
	6	94.50	90.35	4.39		
	7	94.60	90.35	4.49		
	8	94.75	90.50	4.49		
	9	94.30	90.10	4.45		
	10	94.60	90.35	4.49		
D	1	94.70	90.85	4.07	4.23	0.12
	2	94.50	90.70	4.02		
	3	94.30	90.25	4.29		
	4	94.50	90.45	4.29		
	5	94.35	90.40	4.19		
	6	94.50	90.50	4.23		
	7	94.35	90.35	4.24		
	8	94.35	90.25	4.35		
	9	94.60	90.45	4.39		
	10	94.60	90.55	4.28		

Table E-5 Experimental data of firing shrinkage of fired bodies at 1100 °C (continued)

1100 °C						
Formula	#	Length before drying (mm)	Length after firing (mm)	Linear firing shrinkage (%)	Avg.	S.D.
E	1	94.85	91.35	3.69	3.77	0.08
	2	94.50	91.10	3.60		
	3	94.95	91.40	3.74		
	4	94.95	91.35	3.79		
	5	94.90	91.35	3.74		
	6	94.60	90.95	3.86		
	7	94.80	91.15	3.85		
	8	94.65	91.05	3.80		
	9	94.65	91.00	3.86		
	10	95.00	91.40	3.79		
G	1	94.70	91.35	3.54	3.57	0.08
	2	94.65	91.45	3.38		
	3	94.95	91.60	3.53		
	4	94.85	91.40	3.64		
	5	94.65	91.20	3.65		
	6	94.60	91.20	3.59		
	7	94.65	91.25	3.59		
	8	94.65	91.25	3.59		
	9	94.85	91.45	3.58		
	10	94.80	91.40	3.59		
H	1	94.70	91.05	3.85	4.00	0.10
	2	94.80	91.10	3.90		
	3	94.70	90.95	3.96		
	4	94.70	91.00	3.91		
	5	94.80	91.00	4.01		
	6	94.60	90.70	4.12		
	7	94.70	90.75	4.17		
	8	94.50	90.65	4.07		
	9	94.85	91.05	4.01		
	10	94.65	90.85	4.01		
I	1	95.20	92.65	2.68	2.80	0.07
	2	94.85	92.30	2.69		
	3	94.95	92.25	2.84		
	4	94.95	92.35	2.74		
	5	95.10	92.45	2.79		
	6	95.10	92.40	2.84		
	7	95.00	92.30	2.84		
	8	95.10	92.35	2.89		
	9	95.05	92.35	2.84		
	10	94.95	92.25	2.84		

Table E-5 Experimental data of firing shrinkage of fired bodies at 1100 °C (continued)

1100 °C						
Formula	#	Length before drying (mm)	Length after firing (mm)	Linear firing shrinkage (%)	Avg.	S.D.
K	1	94.85	91.50	3.53	3.56	0.08
	2	94.95	91.65	3.48		
	3	94.90	91.65	3.42		
	4	95.00	91.55	3.63		
	5	95.00	91.50	3.68		
	6	95.00	91.60	3.58		
	7	94.75	91.35	3.59		
	8	94.85	91.40	3.64		
	9	95.00	91.65	3.53		
	10	95.00	91.65	3.53		
L	1	95.15	92.35	2.94	3.16	0.14
	2	94.80	91.90	3.06		
	3	95.20	92.20	3.15		
	4	95.00	92.10	3.05		
	5	95.20	92.15	3.20		
	6	95.25	92.15	3.25		
	7	95.10	91.85	3.42		
	8	94.90	92.00	3.06		
	9	95.05	92.00	3.21		
	10	95.10	92.00	3.26		
M	1	94.50	89.75	5.03	5.24	0.17
	2	94.55	89.65	5.18		
	3	94.85	89.95	5.17		
	4	94.50	89.35	5.45		
	5	94.80	89.80	5.27		
	6	94.65	89.90	5.02		
	7	94.90	89.65	5.53		
	8	94.85	89.80	5.32		
	9	94.65	89.70	5.23		

Appendix F

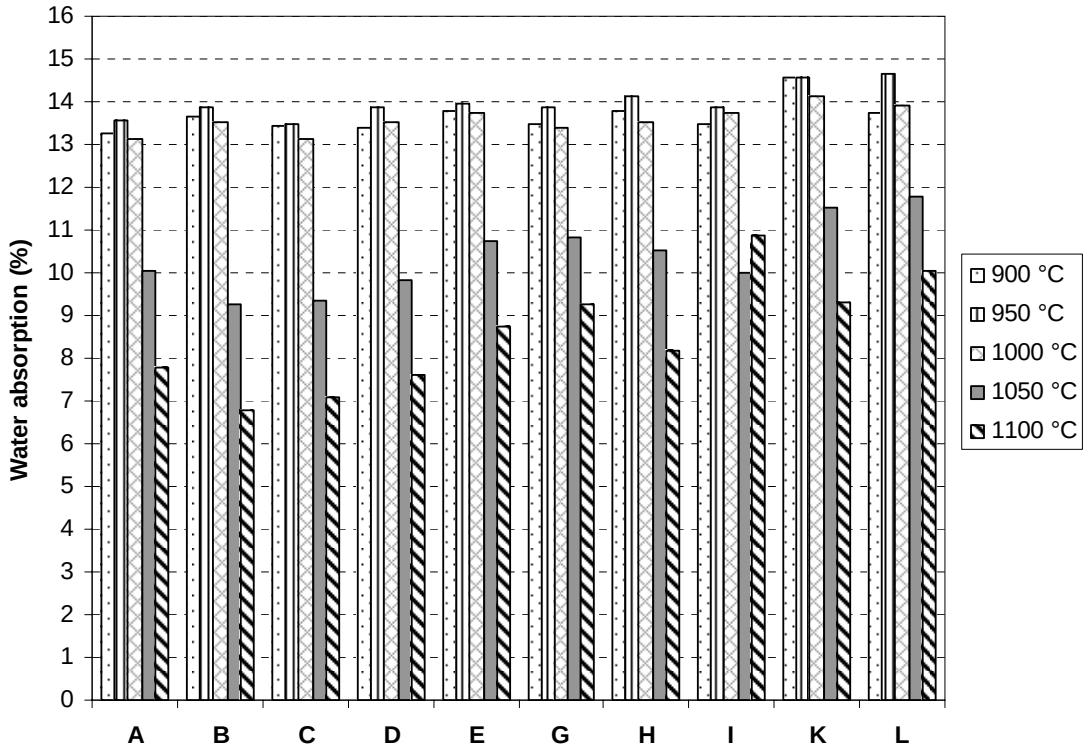

Water absorption of fired mixed clay bodies at various temperatures

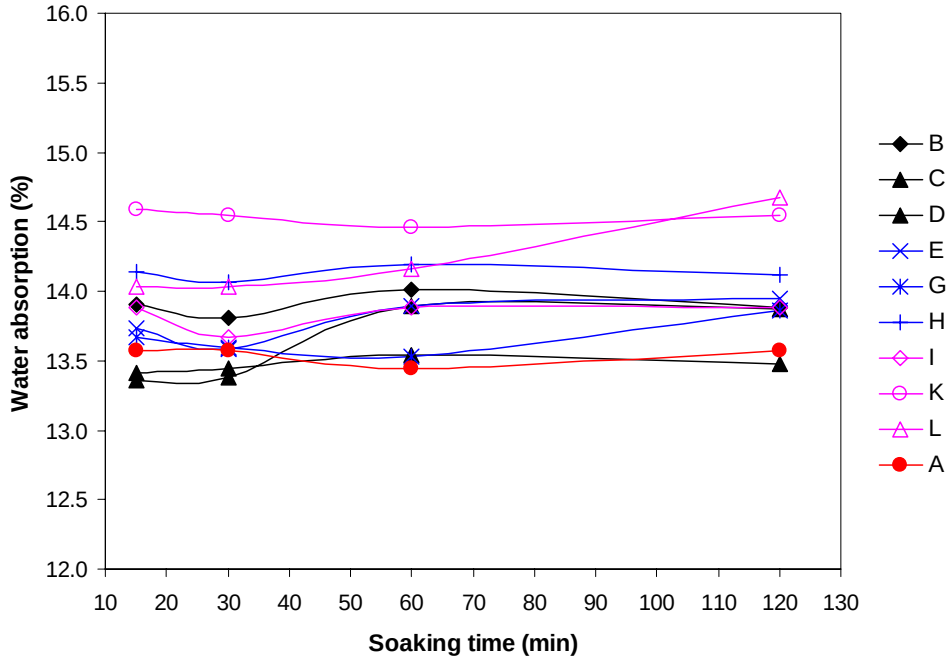

Effect of soaking times on water absorption of the bodies fired at 950 °C

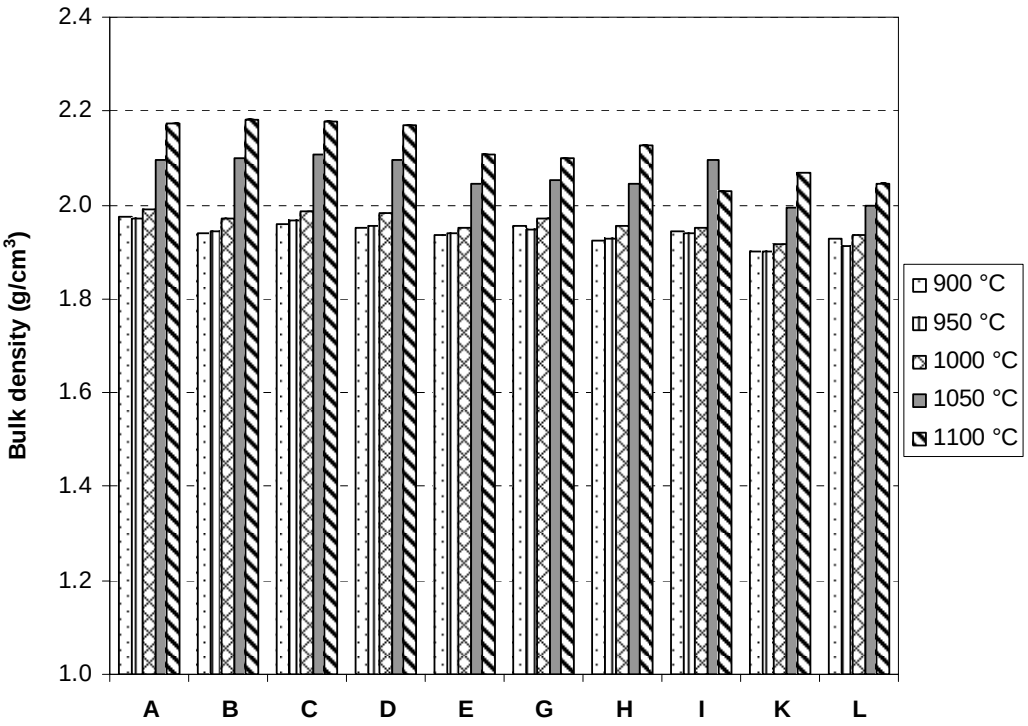

Bulk density of fired mixed clay bodies at various temperatures

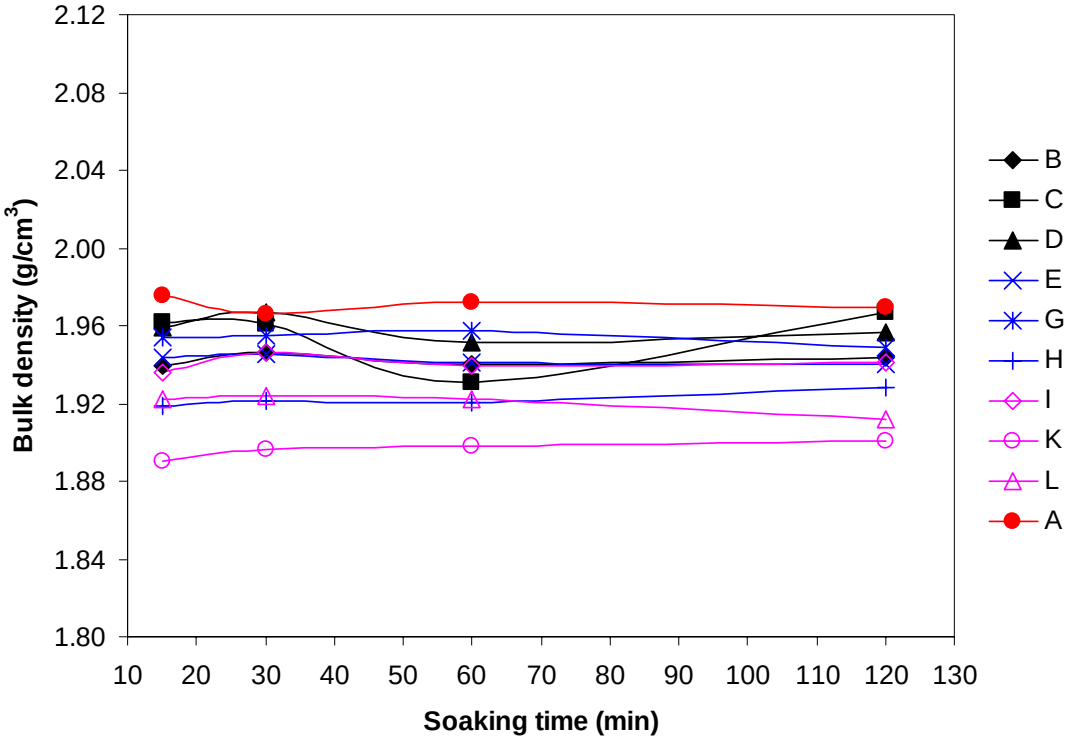

Effect of soaking times on bulk density of the bodies fired at 950 °C

Table F-1 Experimental data of bulk density and water absorption of fired bodies at 900°C

900 °C								
Formula	#	D (g)	W (g)	S (g)	A.P. (%)	W.A (%)	A.D.(g/cm^3)	B.D.(g/cm^3)
A	1	8.47	9.57	5.29	25.70	12.99	2.65	1.97
	2	8.22	9.32	5.18	26.57	13.38	2.70	1.98
	3	8.37	9.40	5.20	24.52	12.31	2.63	1.99
	4	8.07	9.51	5.28	34.04	17.84	2.88	1.90
	5	8.29	9.11	5.05	20.20	9.89	2.55	2.04
Avg.					***26.21***	***13.28***	***2.68***	***1.98***
S.D.					***5.02***	***2.89***	***0.12***	***0.05***
B	1	8.68	9.87	5.40	26.62	13.71	2.64	1.94
	2	8.54	9.73	5.31	26.92	13.93	2.64	1.93
	3	8.04	9.11	5.03	26.23	13.31	2.66	1.96
	4	8.79	9.98	5.49	26.50	13.54	2.66	1.95
	5	8.29	9.44	5.15	26.81	13.87	2.63	1.93
Avg.					***26.62***	***13.67***	***2.64***	***1.94***
S.D.					***0.27***	***0.26***	***0.01***	***0.02***
C	1	8.90	10.07	5.56	25.94	13.15	2.66	1.97
	2	8.42	9.55	5.28	26.46	13.42	2.67	1.97
	3	8.58	9.74	5.36	26.48	13.52	2.66	1.95
	4	8.96	10.19	5.61	26.86	13.73	2.67	1.95
	5	9.12	10.34	5.71	26.35	13.38	2.67	1.96
Avg.					***26.42***	***13.44***	***2.66***	***1.96***
S.D.					***0.33***	***0.21***	***0.01***	***0.01***
D	1	7.72	8.77	4.79	26.38	13.60	2.63	1.93
	2	8.07	9.14	5.05	26.16	13.26	2.66	1.97
	3	8.29	9.39	5.14	25.88	13.27	2.62	1.94
	4	9.55	10.81	5.94	25.87	13.19	2.64	1.95
	5	8.30	9.44	5.21	26.95	13.73	2.68	1.96
Avg.					***26.25***	***13.41***	***2.65***	***1.95***
S.D.					***0.45***	***0.24***	***0.02***	***0.01***
E	1	8.32	9.45	5.18	26.46	13.58	2.64	1.94
	2	9.21	10.47	5.72	26.53	13.68	2.63	1.93
	3	7.65	8.72	4.78	27.16	13.99	2.66	1.94
	4	8.19	9.32	5.09	26.71	13.80	2.63	1.93
	5	8.85	10.08	5.55	27.15	13.90	2.67	1.95
Avg.					***26.80***	***13.79***	***2.65***	***1.94***
S.D.					***0.33***	***0.16***	***0.02***	***0.01***
G	1	8.32	9.43	5.20	26.24	13.34	2.66	1.96
	2	8.25	9.35	5.15	26.19	13.33	2.65	1.96
	3	8.70	9.89	5.44	26.74	13.68	2.66	1.95
	4	9.33	10.57	5.84	26.22	13.29	2.66	1.97
	5	8.75	9.96	5.48	27.01	13.83	2.67	1.95
Avg.					***26.48***	***13.49***	***2.66***	***1.96***
S.D.					***0.37***	***0.24***	***0.01***	***0.01***

Table F-1 Experimental data of bulk density and water absorption of fired bodies at 900°C (continued)

900 °C								
Formula	#	D (g)	W (g)	S (g)	A.P. (%)	W.A (%)	A.D.(g/cm^3)	B.D.(g/cm^3)
H	1	8.74	9.92	5.40	26.11	13.50	2.61	1.93
	2	8.09	9.18	4.99	26.01	13.47	2.60	1.92
	3	9.28	10.58	5.78	27.08	14.01	2.64	1.93
	4	8.64	9.86	5.37	27.17	14.12	2.63	1.92
	5	8.33	9.48	5.18	26.74	13.81	2.64	1.93
Avg.					***26.62***	***13.78***	***2.62***	***1.93***
S.D.					***0.54***	***0.29***	***0.02***	***0.00***
I	1	10.02	11.39	6.21	26.45	13.67	2.62	1.93
	2	9.05	10.29	5.65	26.72	13.70	2.65	1.94
	3	8.84	10.03	5.49	26.21	13.46	2.63	1.94
	4	8.66	9.82	5.40	26.24	13.39	2.65	1.95
	5	9.93	11.24	6.17	25.84	13.19	2.63	1.95
Avg.					***26.29***	***13.48***	***2.64***	***1.94***
S.D.					***0.33***	***0.21***	***0.01***	***0.01***
K	1	8.56	9.81	5.31	27.78	14.60	2.63	1.90
	2	8.11	9.29	5.01	27.57	14.55	2.61	1.89
	3	8.68	9.95	5.41	27.97	14.63	2.65	1.91
	4	8.52	9.77	5.30	27.96	14.67	2.64	1.90
	5	8.71	9.97	5.41	27.63	14.47	2.63	1.90
Avg.					***27.78***	***14.58***	***2.63***	***1.90***
S.D.					***0.19***	***0.08***	***0.01***	***0.01***
L	1	8.23	9.35	5.10	26.35	13.61	2.62	1.93
	2	9.22	10.46	5.71	26.11	13.45	2.62	1.93
	3	8.77	10.01	5.45	27.19	14.14	2.63	1.92
	4	8.84	10.05	5.48	26.48	13.69	2.62	1.93
	5	9.18	10.44	5.70	26.58	13.73	2.63	1.93
Avg.					***26.54***	***13.72***	***2.62***	***1.93***
S.D.					***0.41***	***0.26***	***0.01***	***0.01***
M	1	8.12	9.19	5.11	26.23	13.18	2.69	1.98
	2	7.82	8.86	4.90	26.26	13.30	2.67	1.97
	3	10.15	11.52	6.40	26.76	13.50	2.70	1.98
	4	9.76	11.06	6.16	26.53	13.32	2.70	1.99
	5	8.82	10.00	5.58	26.70	13.38	2.71	1.99
Avg.					***26.49***	***13.33***	***2.69***	***1.98***
S.D.					***0.24***	***0.12***	***0.02***	***0.01***

Table F-2 Experimental data of bulk density and water absorption of fired bodies at 950°C

950 °C								
Formula	#	D (g)	W (g)	S (g)	A.P. (%)	W.A (%)	A.D.(g/cm^3)	B.D.(g/cm^3)
A	1	8.25	9.41	5.22	27.68	14.06	2.71	1.96
	2	9.14	10.35	5.73	26.19	13.24	2.67	1.97
	3	9.03	10.27	5.69	27.07	13.73	2.69	1.97
	4	8.77	9.97	5.53	27.03	13.68	2.70	1.97
	5	8.81	9.97	5.53	26.13	13.17	2.68	1.98
Avg.					***26.82***	***13.58***	***2.69***	***1.97***
S.D.					***0.66***	***0.37***	***0.02***	***0.01***
B	1	8.65	9.83	5.39	26.58	13.64	2.64	1.94
	2	9.27	10.55	5.79	26.89	13.81	2.66	1.94
	3	8.90	10.16	5.57	27.45	14.16	2.66	1.93
	4	8.74	9.96	5.49	27.29	13.96	2.68	1.95
	5	8.95	10.19	5.62	27.13	13.85	2.68	1.95
Avg.					***27.07***	***13.88***	***2.66***	***1.94***
S.D.					***0.34***	***0.19***	***0.02***	***0.01***
C	1	9.05	10.27	5.68	26.58	13.48	2.68	1.97
	2	8.62	9.80	5.42	26.94	13.69	2.69	1.96
	3	8.93	10.13	5.61	26.55	13.44	2.68	1.97
	4	9.31	10.57	5.85	26.69	13.53	2.68	1.97
	5	9.50	10.76	5.96	26.25	13.26	2.67	1.97
Avg.					***26.60***	***13.48***	***2.68***	***1.97***
S.D.					***0.25***	***0.15***	***0.00***	***0.00***
D	1	8.96	10.22	5.64	27.51	14.06	2.69	1.95
	2	9.39	10.67	5.89	26.78	13.63	2.67	1.96
	3	8.68	9.87	5.45	26.92	13.71	2.68	1.96
	4	8.40	9.55	5.30	27.06	13.69	2.70	1.97
	5	8.70	9.94	5.49	27.87	14.25	2.70	1.95
Avg.					***27.23***	***13.87***	***2.69***	***1.96***
S.D.					***0.45***	***0.27***	***0.01***	***0.01***
E	1	9.12	10.38	5.71	26.98	13.82	2.67	1.95
	2	8.82	10.07	5.51	27.41	14.17	2.66	1.93
	3	8.66	9.88	5.43	27.42	14.09	2.67	1.94
	4	9.56	10.90	5.99	27.29	14.02	2.67	1.94
	5	8.80	10.00	5.49	26.61	13.64	2.65	1.94
Avg.					***27.14***	***13.95***	***2.66***	***1.94***
S.D.					***0.35***	***0.22***	***0.01***	***0.01***
G	1	9.50	10.80	5.96	26.86	13.68	2.67	1.96
	2	9.55	10.87	5.99	27.05	13.82	2.67	1.95
	3	9.08	10.35	5.70	27.31	13.99	2.68	1.95
	4	9.32	10.59	5.85	26.79	13.63	2.68	1.96
	5	9.36	10.69	5.86	27.54	14.21	2.67	1.93
Avg.					***27.11***	***13.87***	***2.67***	***1.95***
S.D.					***0.31***	***0.24***	***0.00***	***0.01***

Table F-2 Experimental data of bulk density and water absorption of fired bodies at 950°C (continued)

950 °C								
Formula	#	D (g)	W (g)	S (g)	A.P. (%)	W.A (%)	A.D.(g/cm^3)	B.D.(g/cm^3)
H	1	9.51	10.86	5.92	27.33	14.20	2.64	1.92
	2	8.88	10.14	5.54	27.39	14.19	2.65	1.92
	3	8.92	10.17	5.57	27.17	14.01	2.65	1.93
	4	8.69	9.93	5.41	27.43	14.27	2.64	1.92
	5	9.41	10.72	5.91	27.23	13.92	2.68	1.95
Avg.					***27.31***	***14.12***	***2.65***	***1.93***
S.D.					***0.11***	***0.14***	***0.02***	***0.01***
I	1	9.11	10.36	5.69	26.77	13.72	2.66	1.94
	2	9.86	11.23	6.16	27.02	13.89	2.66	1.94
	3	9.62	10.93	6.03	26.73	13.62	2.67	1.96
	4	9.29	10.58	5.80	26.99	13.89	2.65	1.94
	5	9.46	10.81	5.92	27.61	14.27	2.66	1.93
Avg.					***27.02***	***13.88***	***2.66***	***1.94***
S.D.					***0.35***	***0.25***	***0.01***	***0.01***
K	1	8.48	9.71	5.29	27.83	14.50	2.65	1.91
	2	9.02	10.34	5.61	27.91	14.63	2.64	1.90
	3	9.61	11.02	5.95	27.81	14.67	2.62	1.89
	4	9.52	10.90	5.91	27.66	14.50	2.63	1.90
	5	9.35	10.70	5.79	27.49	14.44	2.62	1.90
Avg.					***27.74***	***14.55***	***2.63***	***1.90***
S.D.					***0.16***	***0.10***	***0.01***	***0.01***
L	1	9.11	10.44	5.67	27.88	14.60	2.64	1.90
	2	9.46	10.83	5.90	27.79	14.48	2.65	1.91
	3	9.20	10.54	5.75	27.97	14.57	2.66	1.91
	4	9.68	11.09	6.07	28.09	14.57	2.67	1.92
	5	8.59	9.89	5.40	28.95	15.13	2.68	1.91
Avg.					***28.14***	***14.67***	***2.66***	***1.91***
S.D.					***0.47***	***0.26***	***0.02***	***0.01***
M	1	10.58	12.00	6.64	26.49	13.42	2.68	1.97
	2	8.12	9.21	5.13	26.72	13.42	2.71	1.98
	3	6.15	6.91	3.82	24.60	12.36	2.63	1.98
	4	9.25	10.45	5.84	26.03	12.97	2.70	2.00
	5	8.97	10.14	5.69	26.29	13.04	2.73	2.01
Avg.					***26.03***	***13.04***	***2.69***	***1.99***
S.D.					***0.84***	***0.44***	***0.04***	***0.02***

Table F-3 Experimental data of bulk density and water absorption of fired bodies at 1000°C

1000 °C								
Formula	#	D (g)	W (g)	S (g)	A.P. (%)	W.A (%)	A.D.(g/cm^3)	B.D.(g/cm^3)
A	1	7.94	8.97	4.99	25.88	12.97	2.68	1.99
	2	9.34	10.60	5.88	26.69	13.49	2.69	1.97
	3	9.02	10.22	5.70	26.55	13.30	2.71	1.99
	4	9.06	10.24	5.72	26.11	13.02	2.70	2.00
	5	8.98	10.14	5.67	25.95	12.92	2.70	2.00
Avg.					***26.24***	***13.14***	***2.70***	***1.99***
S.D.					***0.37***	***0.25***	***0.01***	***0.01***
B	1	8.56	9.73	5.37	26.83	13.67	2.67	1.96
	2	8.61	9.80	5.42	27.17	13.82	2.69	1.96
	3	8.61	9.79	5.43	27.06	13.70	2.70	1.97
	4	9.09	10.29	5.72	26.26	13.20	2.69	1.98
	5	8.85	10.01	5.55	26.01	13.11	2.67	1.98
Avg.					***26.67***	***13.50***	***2.69***	***1.97***
S.D.					***0.51***	***0.32***	***0.01***	***0.01***
C	1	8.55	9.68	5.39	26.34	13.22	2.70	1.99
	2	8.69	9.88	5.48	27.05	13.69	2.70	1.97
	3	8.96	10.10	5.62	25.45	12.72	2.67	1.99
	4	8.25	9.31	5.18	25.67	12.85	2.68	1.99
	5	8.50	9.62	5.35	26.23	13.18	2.69	1.98
Avg.					***26.15***	***13.13***	***2.69***	***1.98***
S.D.					***0.63***	***0.38***	***0.01***	***0.01***
D	1	9.04	10.26	5.71	26.81	13.50	2.71	1.98
	2	9.01	10.26	5.71	27.47	13.87	2.72	1.97
	3	8.61	9.78	5.46	27.08	13.59	2.72	1.99
	4	8.68	9.85	5.47	26.71	13.48	2.70	1.98
	5	8.80	9.95	5.57	26.26	13.07	2.72	2.00
Avg.					***26.87***	***13.50***	***2.71***	***1.98***
S.D.					***0.45***	***0.29***	***0.01***	***0.01***
E	1	8.99	10.25	5.62	27.21	14.02	2.66	1.94
	2	9.40	10.69	5.86	26.71	13.72	2.65	1.94
	3	9.51	10.85	5.97	27.46	14.09	2.68	1.94
	4	8.80	10.05	5.56	27.84	14.20	2.71	1.95
	5	9.03	10.17	5.66	25.28	12.62	2.67	2.00
Avg.					***26.90***	***13.73***	***2.67***	***1.95***
S.D.					***1.00***	***0.64***	***0.02***	***0.02***
G	1	9.45	10.74	5.94	26.88	13.65	2.68	1.96
	2	9.85	11.20	6.19	26.95	13.71	2.68	1.96
	3	9.41	10.65	5.92	26.22	13.18	2.69	1.98
	4	9.53	10.81	5.98	26.50	13.43	2.68	1.97
	5	9.49	10.73	5.94	25.89	13.07	2.66	1.97
Avg.					***26.49***	***13.41***	***2.68***	***1.97***
S.D.					***0.45***	***0.28***	***0.01***	***0.01***

Table F-3 Experimental data of bulk density and water absorption of fired bodies at 1000 °C (continued)

1000 °C								
Formula	#	D (g)	W (g)	S (g)	A.P. (%)	W.A (%)	A.D.(g/cm^3)	B.D.(g/cm^3)
H	1	8.96	10.17	5.60	26.48	13.50	2.66	1.95
	2	8.71	9.89	5.42	26.40	13.55	2.64	1.94
	3	9.03	10.26	5.67	26.80	13.62	2.68	1.96
	4	9.47	10.75	5.93	26.56	13.52	2.67	1.96
	5	8.56	9.70	5.36	26.27	13.32	2.67	1.97
Avg.					***26.50***	***13.50***	***2.66***	***1.96***
S.D.					***0.20***	***0.11***	***0.01***	***0.01***
I	1	10.09	11.49	6.32	27.08	13.88	2.67	1.95
	2	9.65	11.01	6.05	27.42	14.09	2.67	1.94
	3	9.12	10.37	5.72	26.88	13.71	2.67	1.95
	4	9.13	10.37	5.72	26.67	13.58	2.67	1.96
	5	9.45	10.73	5.92	26.61	13.54	2.67	1.96
Avg.					***26.93***	***13.76***	***2.67***	***1.95***
S.D.					***0.33***	***0.23***	***0.00***	***0.01***
K	1	8.90	10.18	5.52	27.47	14.38	2.62	1.90
	2	9.14	10.45	5.67	27.41	14.33	2.63	1.91
	3	8.97	10.24	5.58	27.25	14.16	2.64	1.92
	4	8.70	9.93	5.41	27.21	14.14	2.64	1.92
	5	8.40	9.55	5.21	26.50	13.69	2.62	1.93
Avg.					***27.17***	***14.14***	***2.63***	***1.92***
S.D.					***0.39***	***0.27***	***0.01***	***0.01***
L	1	8.81	10.06	5.49	27.35	14.19	2.65	1.92
	2	8.67	9.90	5.41	27.39	14.19	2.65	1.92
	3	8.77	10.01	5.49	27.43	14.14	2.67	1.93
	4	9.92	11.28	6.19	26.72	13.71	2.65	1.94
	5	8.50	9.64	5.29	26.21	13.41	2.64	1.95
Avg.					***27.02***	***13.93***	***2.65***	***1.93***
S.D.					***0.54***	***0.35***	***0.01***	***0.01***
M	1	7.34	8.26	4.64	25.41	12.53	2.71	2.02
	2	8.44	9.51	5.33	25.60	12.68	2.71	2.01
	3	8.30	9.31	5.24	24.82	12.17	2.70	2.03
	4	7.57	8.48	4.78	24.59	12.02	2.70	2.04
	5	8.27	9.20	5.20	23.25	11.25	2.69	2.06
Avg.					***24.73***	***12.13***	***2.70***	***2.03***
S.D.					***0.93***	***0.56***	***0.01***	***0.02***

Table F-4 Experimental data of bulk density and water absorption of fired bodies at 1050 °C

1050 °C								
Formula	#	D (g)	W (g)	S (g)	A.P. (%)	W.A (%)	A.D.(g/cm^3)	B.D.(g/cm^3)
A	1	8.07	8.89	5.05	21.35	10.16	2.66	2.09
	2	8.08	8.92	5.06	21.76	10.40	2.67	2.09
	3	8.35	9.18	5.21	20.91	9.94	2.65	2.10
	4	8.27	9.12	5.15	21.41	10.28	2.64	2.08
	5	8.15	8.92	5.08	20.05	9.45	2.65	2.12
Avg.					***21.10***	***10.04***	***2.65***	***2.09***
S.D.					***0.66***	***0.37***	***0.01***	***0.01***
B	1	8.67	9.53	5.35	20.57	9.92	2.60	2.07
	2	8.92	9.79	5.55	20.52	9.75	2.64	2.10
	3	8.04	8.76	4.97	19.00	8.96	2.61	2.11
	4	8.73	9.51	5.38	18.89	8.93	2.60	2.11
	5	8.07	8.77	4.97	18.42	8.67	2.59	2.12
Avg.					***19.48***	***9.25***	***2.61***	***2.10***
S.D.					***1.00***	***0.55***	***0.02***	***0.02***
C	1	8.76	9.62	5.45	20.62	9.82	2.64	2.09
	2	8.14	8.92	5.05	20.16	9.58	2.63	2.10
	3	8.16	8.89	5.05	19.01	8.95	2.62	2.12
	4	8.10	8.87	5.05	20.16	9.51	2.65	2.11
	5	8.57	9.34	5.32	19.15	8.98	2.63	2.12
Avg.					***19.82***	***9.37***	***2.63***	***2.11***
S.D.					***0.70***	***0.38***	***0.01***	***0.01***
D	1	8.39	9.20	5.23	20.40	9.65	2.65	2.11
	2	8.22	9.06	5.09	21.16	10.22	2.62	2.06
	3	8.35	9.20	5.22	21.36	10.18	2.66	2.09
	4	7.66	8.38	4.77	19.94	9.40	2.64	2.12
	5	9.22	10.11	5.75	20.41	9.65	2.65	2.11
Avg.					***20.66***	***9.82***	***2.64***	***2.10***
S.D.					***0.59***	***0.36***	***0.02***	***0.02***
E	1	8.39	9.33	5.22	22.87	11.20	2.64	2.03
	2	8.48	9.41	5.27	22.46	10.97	2.63	2.04
	3	8.22	9.08	5.09	21.55	10.46	2.62	2.05
	4	8.31	9.22	5.15	22.36	10.95	2.62	2.04
	5	8.68	9.56	5.36	20.95	10.14	2.61	2.06
Avg.					***22.04***	***10.74***	***2.62***	***2.05***
S.D.					***0.77***	***0.43***	***0.01***	***0.01***
G	1	7.81	8.67	4.87	22.63	11.01	2.65	2.05
	2	9.24	10.25	5.74	22.39	10.93	2.63	2.04
	3	8.57	9.51	5.35	22.60	10.97	2.65	2.05
	4	8.93	9.89	5.56	22.17	10.75	2.64	2.06
	5	9.07	10.01	5.62	21.41	10.36	2.62	2.06
Avg.					***22.24***	***10.80***	***2.64***	***2.05***
S.D.					***0.50***	***0.27***	***0.01***	***0.01***

Table F-4 Experimental data of bulk density and water absorption of fired bodies at 1050 °C (continued)

1050 °C								
Formula	#	D (g)	W (g)	S (g)	A.P. (%)	W.A (%)	A.D.(g/cm^3)	B.D.(g/cm^3)
H	1	8.20	9.12	5.10	22.89	11.22	2.64	2.03
	2	8.73	9.64	5.39	21.41	10.42	2.61	2.05
	3	8.65	9.58	5.36	22.04	10.75	2.62	2.04
	4	8.25	9.08	5.09	20.80	10.06	2.60	2.06
	5	8.39	9.25	5.16	21.03	10.25	2.59	2.04
Avg.					***21.63***	***10.54***	***2.61***	***2.05***
S.D.					***0.84***	***0.46***	***0.02***	***0.01***
I	1	8.88	9.06	5.51	5.07	2.03	2.63	2.49
	2	8.49	9.53	5.27	24.41	12.25	2.63	1.99
	3	9.24	10.34	5.72	23.81	11.90	2.62	1.99
	4	8.40	9.41	5.22	24.11	12.02	2.63	2.00
	5	9.14	10.22	5.69	23.84	11.82	2.64	2.01
Avg.					***20.25***	***10.00***	***2.63***	***2.10***
S.D.					***8.49***	***4.46***	***0.01***	***0.22***
K	1	9.47	10.57	5.85	23.31	11.62	2.61	2.00
	2	8.96	10.02	5.52	23.56	11.83	2.60	1.98
	3	8.98	10.02	5.54	23.21	11.58	2.60	2.00
	4	9.03	10.05	5.57	22.77	11.30	2.60	2.01
	5	8.62	9.60	5.28	22.69	11.37	2.57	1.99
Avg.					***23.11***	***11.54***	***2.60***	***2.00***
S.D.					***0.37***	***0.21***	***0.01***	***0.01***
L	1	9.37	10.47	5.80	23.55	11.74	2.62	2.00
	2	9.37	10.52	5.82	24.47	12.27	2.63	1.99
	3	8.81	9.86	5.45	23.81	11.92	2.61	1.99
	4	9.30	10.40	5.77	23.76	11.83	2.63	2.00
	5	8.93	9.93	5.51	22.62	11.20	2.60	2.01
Avg.					***23.64***	***11.79***	***2.62***	***2.00***
S.D.					***0.66***	***0.39***	***0.01***	***0.01***
M	1	8.64	9.37	5.39	18.34	8.45	2.65	2.16
	2	11.41	12.25	7.08	16.25	7.36	2.63	2.20
	3	8.73	9.41	5.43	17.09	7.79	2.64	2.19
	4	8.96	9.62	5.55	16.22	7.37	2.62	2.19
	5	8.11	8.70	5.05	16.16	7.27	2.64	2.21
Avg.					***16.81***	***7.65***	***2.63***	***2.19***
S.D.					***0.94***	***0.49***	***0.01***	***0.02***

Table F-5 Experimental data of bulk density and water absorption of fired bodies at 1100 °C

1100 °C								
Formula	#	D (g)	W (g)	S (g)	A.P. (%)	W.A (%)	A.D.(g/cm^3)	B.D.(g/cm^3)
A	1	8.84	9.52	5.46	16.75	7.69	2.61	2.17
	2	8.83	9.55	5.49	17.73	8.15	2.64	2.17
	3	8.96	9.66	5.59	17.20	7.81	2.65	2.19
	4	8.40	9.04	5.19	16.62	7.62	2.61	2.17
	5	8.21	8.83	5.06	16.45	7.55	2.60	2.17
Avg.					***16.95***	***7.77***	***2.62***	***2.18***
S.D.					***0.52***	***0.24***	***0.02***	***0.01***
B	1	8.18	8.80	5.02	16.40	7.58	2.58	2.16
	2	8.08	8.63	4.98	15.07	6.81	2.60	2.21
	3	8.62	9.19	5.25	14.47	6.61	2.55	2.18
	4	8.23	8.75	4.97	13.76	6.32	2.52	2.17
	5	9.00	9.60	5.51	14.67	6.67	2.57	2.19
Avg.					***14.87***	***6.80***	***2.56***	***2.18***
S.D.					***0.98***	***0.47***	***0.03***	***0.02***
C	1	8.84	9.49	5.42	15.97	7.35	2.58	2.17
	2	8.63	9.25	5.28	15.62	7.18	2.57	2.17
	3	8.25	8.84	5.07	15.65	7.15	2.59	2.18
	4	8.86	9.52	5.47	16.30	7.45	2.61	2.18
	5	9.33	9.92	5.70	13.98	6.32	2.56	2.20
Avg.					***15.50***	***7.09***	***2.58***	***2.18***
S.D.					***0.89***	***0.45***	***0.02***	***0.02***
D	1	9.16	9.90	5.64	17.37	8.08	2.59	2.14
	2	9.30	10.05	5.76	17.48	8.06	2.62	2.16
	3	9.20	9.89	5.70	16.47	7.50	2.62	2.19
	4	8.07	8.65	4.96	15.72	7.19	2.59	2.18
	5	8.99	9.64	5.52	15.78	7.23	2.58	2.18
Avg.					***16.56***	***7.61***	***2.60***	***2.17***
S.D.					***0.84***	***0.44***	***0.02***	***0.02***
E	1	8.95	9.77	5.49	19.16	9.16	2.58	2.08
	2	8.92	9.73	5.51	19.19	9.08	2.61	2.11
	3	8.83	9.58	5.41	17.99	8.49	2.57	2.11
	4	9.02	9.76	5.51	17.41	8.20	2.56	2.12
	5	8.92	9.71	5.50	18.76	8.86	2.60	2.11
Avg.					***18.50***	***8.76***	***2.58***	***2.11***
S.D.					***0.78***	***0.40***	***0.02***	***0.01***
G	1	9.56	10.50	5.94	20.61	9.83	2.63	2.09
	2	8.99	9.89	5.58	20.88	10.01	2.63	2.08
	3	9.12	9.92	5.65	18.74	8.77	2.62	2.13
	4	9.56	10.42	5.89	18.98	9.00	2.60	2.10
	5	9.30	10.10	5.70	18.18	8.60	2.58	2.11
Avg.					***19.48***	***9.24***	***2.61***	***2.10***
S.D.					***1.20***	***0.64***	***0.02***	***0.02***

Table F-5 Experimental data of bulk density and water absorption of fired bodies at 1100 °C (continued)

1100 °C								
Formula	#	D (g)	W (g)	S (g)	A.P. (%)	W.A (%)	A.D.(g/cm^3)	B.D.(g/cm^3)
H	1	9.14	9.90	5.58	17.59	8.32	2.56	2.11
	2	8.92	9.69	5.47	18.25	8.63	2.58	2.11
	3	9.13	9.88	5.61	17.56	8.21	2.59	2.13
	4	9.19	9.92	5.65	17.10	7.94	2.59	2.15
	5	8.19	8.83	5.01	16.75	7.81	2.57	2.14
Avg.					***17.45***	***8.18***	***2.58***	***2.13***
S.D.					***0.57***	***0.32***	***0.01***	***0.02***
I	1	8.80	9.77	5.45	22.45	11.02	2.62	2.03
	2	9.45	10.49	5.83	22.32	11.01	2.60	2.02
	3	10.04	11.13	6.19	22.06	10.86	2.60	2.03
	4	9.21	10.19	5.68	21.73	10.64	2.60	2.04
	5	9.75	10.80	6.01	21.92	10.77	2.60	2.03
Avg.					***22.10***	***10.86***	***2.60***	***2.03***
S.D.					***0.29***	***0.16***	***0.01***	***0.01***
K	1	8.71	9.54	5.35	19.81	9.53	2.58	2.07
	2	10.23	11.22	6.25	19.92	9.68	2.56	2.05
	3	9.61	10.47	5.84	18.57	8.95	2.54	2.07
	4	10.43	11.39	6.35	19.05	9.20	2.55	2.06
	5	9.66	10.55	5.92	19.22	9.21	2.57	2.08
Avg.					***19.31***	***9.31***	***2.56***	***2.07***
S.D.					***0.56***	***0.29***	***0.02***	***0.01***
L	1	8.93	9.82	5.48	20.51	9.97	2.58	2.05
	2	8.72	9.63	5.37	21.36	10.44	2.59	2.04
	3	10.22	11.22	6.26	20.16	9.78	2.57	2.05
	4	9.37	10.32	5.71	20.61	10.14	2.55	2.03
	5	9.43	10.36	5.80	20.39	9.86	2.59	2.06
Avg.					***20.61***	***10.04***	***2.58***	***2.05***
S.D.					***0.45***	***0.26***	***0.02***	***0.01***

Appendix G

Table G-1 Bending strength of fired clay bodies at 900 °C

900 °C					
Formula	No.	Maximum load (N)	MOR (MPa)	Average (MPa)	SD
A	1	92.92	19.22		
	2	76.15	15.75		
	3	79.56	16.45		
	4	84.53	17.48		
	5	84.71	17.52	18.14	1.40
	6	92.59	19.15		
	7	95.80	19.81		
	8	92.13	19.05		
	9	91.25	18.87		
B	1	83.10	16.93		
	2	82.17	16.74		
	3	94.60	19.27		
	4	96.76	19.71		
	5	92.77	18.90		
	6	104.59	21.31	20.43	2.58
	7	102.32	20.84		
	8	114.80	23.39		
	9	117.37	23.91		
	10	114.39	23.30		
C	1	82.92	16.89		
	2	74.20	15.12		
	3	85.14	17.34		
	4	87.99	17.92		
	5	99.98	20.37		
	6	95.46	19.45	19.17	2.30
	7	96.75	19.71		
	8	103.16	21.02		
	9	109.19	22.24		
	10	106.35	21.67		
D	1	77.79	15.85		
	2	81.38	16.58		
	3	84.94	17.30		
	4	91.18	18.57		
	5	89.95	18.33		
	6	90.82	18.50	18.53	1.92
	7	108.61	22.13		
	8	85.53	17.42		
	9	100.55	20.48		
	10	98.72	20.11		

Table G-1 Bending strength of fired clay bodies at 900 °C (continued)

900 °C					
Formula	No.	Maximum load (N)	MOR (MPa)	Average (MPa)	SD
E	1	60.77	11.67		
	2	66.69	12.80		
	3	73.83	14.17		
	4	74.87	14.37		
	5	73.49	14.11		
	6	79.15	15.19	14.47	1.40
	7	78.49	15.07		
	8	78.85	15.14		
	9	82.51	15.84		
	10	85.33	16.38		
G	1	68.30	13.11		
	2	65.26	12.53		
	3	74.55	14.31		
	4	72.91	14.00		
	5	74.06	14.22		
	6	65.33	12.54	13.97	0.95
	7	76.78	14.74		
	8	74.30	14.26		
	9	76.59	14.70		
	10	79.88	15.33		
H	1	71.53	13.73		
	2	73.16	14.04		
	3	78.72	15.11		
	4	72.59	13.93		
	5	83.52	16.03		
	6	83.92	16.11	15.76	1.54
	7	91.95	17.65		
	8	94.09	18.06		
	9	87.92	16.88		
	10	83.42	16.01		
I	1	45.69	8.52		
	2	41.18	7.68		
	3	50.32	9.38		
	4	47.48	8.85		
	5	55.62	10.37		
	6	55.34	10.32	9.45	1.02
	7	52.43	9.77		
	8	48.54	9.05		
	9	49.97	9.32		
	10	60.19	11.22		

Table G-1 Bending strength of fired clay bodies at 900 °C (continued)

900 °C					
Formula	No.	Maximum load (N)	MOR (MPa)	Average (MPa)	SD
K	1	57.82	10.78		
	2	51.20	9.55		
	3	61.32	11.43		
	4	61.06	11.38		
	5	67.06	12.50		
	6	60.47	11.27	11.57	0.97
	7	68.02	12.68		
	8	60.65	11.31		
	9	66.39	12.38		
	10	66.86	12.46		
L	1	53.46	9.97		
	2	51.47	9.59		
	3	55.21	10.29		
	4	61.24	11.42		
	5	55.49	10.35		
	6	62.47	11.65	10.93	0.80
	7	62.75	11.70		
	8	59.84	11.16		
	9	61.35	11.44		
	10	62.65	11.68		
M	1	80.83	18.04		
	2	42.97	9.59		
	3	105.17	23.47		
	4	82.34	18.38	19.04	4.89
	5	85.54	19.09		
	6	110.82	24.74		
	7	89.52	19.98		

Table G-2 Bending strength of fired clay bodies at 950 °C

950 °C					
Formula	No.	Maximum load (N)	MOR (MPa)	Average (MPa)	SD
A	1	100.18	21.03		
	2	100.14	21.02		
	3	108.17	22.71		
	4	109.23	22.93		
	5	99.13	20.81		
	6	88.14	18.51	20.92	1.35
	7	99.69	20.93		
	8	98.59	20.70		
	9	101.70	21.35		
	10	91.24	19.16		
B	1	114.43	23.31		
	2	111.64	22.74		
	3	113.76	23.17		
	4	114.62	23.35		
	5	120.87	24.62		
	6	116.92	23.82	23.51	0.88
	7	110.90	22.59		
	8	109.68	22.34		
	9	123.01	25.06		
	10	118.04	24.05		
C	1	119.38	24.69		
	2	105.31	21.78		
	3	107.03	22.13		
	4	119.05	24.62		
	5	109.84	22.72		
	6	119.57	24.73	23.80	1.50
	7	124.65	25.78		
	8	123.29	25.50		
	9	106.79	22.08		
	10	115.78	23.94		
D	1	104.43	21.60		
	2	103.10	21.32		
	3	98.88	20.45		
	4	99.40	20.56		
	5	103.36	21.37		
	6	94.89	19.62	21.71	1.79
	7	98.68	20.41		
	8	122.87	25.41		
	9	107.96	22.33		
	10	116.17	24.03		

Table G-2 Bending strength of fired clay bodies at 950 °C (continued)

950 °C					
Formula	No.	Maximum load (N)	MOR (MPa)	Average (MPa)	SD
E	1	82.71	16.35		
	2	80.21	15.86		
	3	87.17	17.23		
	4	90.81	17.95		
	5	90.04	17.80		
	6	80.54	15.92	17.06	0.89
	7	85.01	16.81		
	8	84.37	16.68		
	9	93.70	18.53		
	10	88.28	17.46		
G	1	76.16	14.84		
	2	75.74	14.75		
	3	79.82	15.55		
	4	78.96	15.38		
	5	81.56	15.89		
	6	82.40	16.05	15.62	0.52
	7	81.83	15.94		
	8	81.14	15.81		
	9	84.29	16.42		
	10	79.72	15.53		
H	1	90.09	17.30		
	2	84.20	16.16		
	3	96.30	18.49		
	4	96.54	18.53		
	5	95.41	18.32		
	6	87.62	16.82	17.33	0.89
	7	88.92	17.07		
	8	91.60	17.59		
	9	84.50	16.22		
	10	87.27	16.75		
I	1	52.27	9.75		
	2	53.51	9.98		
	3	55.11	10.27		
	4	55.62	10.37		
	5	58.70	10.94		
	6	54.39	10.14	10.22	0.38
	7	51.61	9.62		
	8	55.16	10.28		
	9	55.17	10.29		
	10	56.63	10.56		

Table G-2 Bending strength of fired clay bodies at 950 °C (continued)

950 °C					
Formula	No.	Maximum load (N)	MOR (MPa)	Average (MPa)	SD
K	1	65.57	12.22		
	2	63.37	11.81		
	3	71.67	13.36		
	4	68.07	12.69		
	5	70.84	13.21		
	6	71.87	13.40	12.94	0.59
	7	68.58	12.78		
	8	68.93	12.85		
	9	71.47	13.32		
	10	73.77	13.75		
L	1	61.91	11.54		
	2	64.58	12.04		
	3	63.70	11.88		
	4	66.90	12.47		
	5	67.29	12.54		
	6	68.64	12.80	12.13	0.56
	7	65.19	12.15		
	8	63.09	11.76		
	9	69.49	12.95		
	10	50.18	11.20		
M	1	64.38	14.37		
	2	49.09	10.96		
	3	101.03	22.55		
	4	81.15	18.11	21.30	7.38
	5	102.25	22.82		
	6	139.16	31.06		
	7	130.96	29.23		

Table G-3 Bending strength of fired clay bodies at 1000 °C

1000 °C					
Formula	No.	Maximum load (N)	MOR (MPa)	Average (MPa)	SD
A	1	96.38	20.86		
	2	96.95	20.99		
	3	96.22	20.83		
	4	101.32	21.93		
	5	100.13	21.67		
	6	92.55	20.03	20.43	1.04
	7	92.52	20.03		
	8	89.54	19.38		
	9	93.06	20.14		
	10	85.39	18.48		
B	1	121.67	25.55		
	2	118.51	24.88		
	3	123.52	25.93		
	4	124.42	26.12		
	5	130.34	27.37		
	6	124.28	26.09	25.77	1.57
	7	107.09	22.48		
	8	135.62	28.47		
	9	119.52	25.09		
	10	122.68	25.76		
C	1	113.57	24.58		
	2	113.72	24.61		
	3	115.32	24.96		
	4	127.85	27.67		
	5	114.19	24.72		
	6	115.22	24.94	25.21	1.15
	7	112.01	24.24		
	8	124.62	26.97		
	9	112.97	24.45		
	10	115.47	24.99		
D	1	101.29	21.92		
	2	103.62	22.43		
	3	101.71	22.01		
	4	111.59	24.15		
	5	105.82	22.90		
	6	109.49	23.70	23.28	0.98
	7	106.16	22.98		
	8	114.52	24.79		
	9	109.23	23.64		
	10	111.96	24.23		

Table G-3 Bending strength of fired clay bodies at 1000 °C (continued)

1000 °C					
Formula	No.	Maximum load (N)	MOR (MPa)	Average (MPa)	SD
E	1	87.59	17.84		
	2	75.09	15.30		
	3	80.08	16.31		
	4	85.31	17.38		
	5	89.82	18.30		
	6	86.46	17.61	17.29	0.94
	7	81.36	16.57		
	8	88.27	17.98		
	9	86.49	17.62		
	10	88.32	17.99		
G	1	78.67	15.56		
	2	84.34	16.68		
	3	80.16	15.85		
	4	77.93	15.41		
	5	83.36	16.48		
	6	77.66	15.36	15.53	0.65
	7	75.54	14.94		
	8	77.77	15.38		
	9	73.94	14.62		
	10	75.90	15.01		
H	1	86.92	17.19		
	2	95.96	18.97		
	3	98.33	19.44		
	4	98.84	19.54		
	5	97.29	19.24		
	6	106.18	20.99	19.52	1.16
	7	100.69	19.91		
	8	97.35	19.25		
	9	108.48	21.45		
	10	97.08	19.20		
I	1	53.68	10.01		
	2	52.68	9.82		
	3	54.60	10.18		
	4	52.92	9.87		
	5	53.97	10.06		
	6	54.75	10.21	10.25	0.34
	7	54.77	10.21		
	8	56.99	10.62		
	9	58.02	10.82		
	10	57.14	10.65		

Table G-3 Bending strength of fired clay bodies at 1000 °C (continued)

1000 °C					
Formula	No.	Maximum load (N)	MOR (MPa)	Average (MPa)	SD
K	1	70.05	13.06		
	2	71.66	13.36		
	3	73.07	13.62		
	4	73.50	13.70		
	5	75.19	14.02		
	6	72.26	13.47	14.00	0.71
	7	74.90	13.96		
	8	80.12	14.94		
	9	80.51	15.01		
	10	79.84	14.89		
L	1	67.05	12.50		
	2	65.07	12.13		
	3	58.95	10.99		
	4	61.23	11.41		
	5	68.72	12.81		
	6	60.14	11.21	12.13	0.75
	7	66.45	12.39		
	8	63.56	11.85		
	9	68.78	12.82		
	10	70.92	13.22		
M	1	76.37	17.58		
	2	156.08	35.94		
	3	66.58	15.33		
	4	100.42	23.12		
	5	68.83	15.85	24.08	8.97
	6	130.95	30.15		
	7	60.71	13.98		
	8	159.85	36.81		
	9	121.27	27.92		

Table G-4 Bending strength of fired clay bodies at 1050 °C

1050 °C					
Formula	No.	Maximum load (N)	MOR (MPa)	Average (MPa)	SD
A	1	82.14	18.33		
	2	91.32	20.38		
	3	88.39	19.73		
	4	90.51	20.20		
	5	91.10	20.34		
	6	91.72	20.47	19.93	0.65
	7	90.06	20.10		
	8	87.97	19.64		
	9	91.74	20.48		
	10	87.88	19.62		
B	1	142.08	31.23		
	2	125.72	27.63		
	3	117.02	25.72		
	4	132.78	29.18		
	5	138.32	30.40		
	6	126.56	27.82	28.52	1.54
	7	125.52	27.59		
	8	130.98	28.79		
	9	129.80	28.53		
	10	128.95	28.34		
C	1	109.23	24.38		
	2	111.14	24.81		
	3	121.63	27.15		
	4	110.27	24.61		
	5	113.57	25.35		
	6	119.03	26.57	25.26	1.28
	7	106.13	23.69		
	8	120.96	27.00		
	9	106.08	23.68		
	10	113.47	25.33		
D	1	99.45	21.86		
	2	101.58	22.33		
	3	115.63	25.41		
	4	93.55	20.56		
	5	104.42	22.95	22.24	1.67
	6	103.10	22.66		
	7	107.07	23.53		
	8	95.43	20.97		
	9	90.57	19.91		

Table G-4 Bending strength of fired clay bodies at 1050 °C (continued)

1050 °C					
Formula	No.	Maximum load (N)	MOR (MPa)	Average (MPa)	SD
E	1	83.19	16.95		
	2	90.85	18.51		
	3	100.49	20.47		
	4	82.77	16.86		
	5	97.20	19.80		
	6	92.54	18.85	18.29	1.31
	7	83.47	17.00		
	8	94.10	19.17		
	9	89.65	18.26		
	10	83.40	16.99		
G	1	81.53	16.61		
	2	77.20	15.73		
	3	75.99	15.48		
	4	73.06	14.88		
	5	71.52	14.57		
	6	79.33	16.16	15.51	0.69
	7	72.27	14.72		
	8	74.11	15.10		
	9	79.88	16.27		
	10	76.38	15.56		
H	1	93.66	19.08		
	2	108.21	22.04		
	3	106.50	21.70		
	4	113.92	23.21		
	5	102.54	20.89	21.24	1.17
	6	102.60	20.90		
	7	102.17	20.81		
	8	108.15	22.03		
	9	100.48	20.47		
I	1	51.45	9.59		
	2	57.19	10.66		
	3	52.62	9.81		
	4	53.66	10.00		
	5	54.69	10.20		
	6	58.60	10.93	10.33	0.44
	7	56.12	10.46		
	8	56.09	10.46		
	9	58.34	10.88		
	10	55.14	10.28		

Table G-4 Bending strength of fired clay bodies at 1050 °C (continued)

1050 °C					
Formula	No.	Maximum load (N)	MOR (MPa)	Average (MPa)	SD
K	1	81.86	15.71		
	2	82.21	15.78		
	3	75.18	14.43		
	4	89.40	17.16		
	5	85.23	16.36	16.02	1.01
	6	89.43	17.17		
	7	88.39	16.97		
	8	82.90	15.92		
	9	76.38	14.66		
L	1	71.71	13.77		
	2	68.06	13.07		
	3	62.92	12.08		
	4	70.09	13.46		
	5	71.49	13.72	13.51	0.69
	6	76.54	14.69		
	7	70.06	13.45		
	8	71.79	13.78		
	9	70.51	13.54		
M	1	142.82	35.03		
	3	119.83	29.39		
	4	176.45	43.28		
	5	150.68	36.96	36.02	6.09
	6	145.10	35.59		
	7	178.65	43.82		
	8	114.53	28.09		

Table G-5 Bending strength of fired clay bodies at 1100 °C

1100 °C					
Formula	No.	Maximum load (N)	MOR (MPa)	Average (MPa)	SD
A	1	95.47	21.98		
	2	92.83	21.37		
	3	86.19	19.85		
	4	98.70	22.73		
	5	99.45	22.90		
	6	101.49	23.37	22.29	1.02
	7	99.99	23.02		
	8	98.64	22.71		
	9	97.70	22.50		
	10	97.52	22.46		
B	1	128.40	29.57		
	2	121.05	27.87		
	3	125.89	28.99		
	4	139.34	32.09		
	5	126.12	29.04	30.70	2.72
	6	142.48	32.81		
	7	152.45	35.10		
	8	118.81	27.36		
	9	145.17	33.43		
C	1	118.56	26.88		
	2	124.83	28.30		
	3	124.32	28.18		
	4	115.41	26.16		
	5	122.64	27.80		
	6	126.89	28.77	28.71	1.80
	7	137.24	31.11		
	8	128.94	29.23		
	9	125.82	28.52		
	10	141.88	32.16		
D	1	100.91	22.88		
	2	99.32	22.52		
	3	109.16	24.75		
	4	108.93	24.69		
	5	103.74	23.52		
	6	98.70	22.38	24.07	1.58
	7	110.27	25.00		
	8	121.66	27.58		
	9	101.32	22.97		
	10	107.74	24.43		

Table G-5 Bending strength of fired clay bodies at 1100 °C (continued)

1100 °C					
Formula	No.	Maximum load (N)	MOR (MPa)	Average (MPa)	SD
E	1	95.03	19.95		
	2	97.81	20.53		
	3	98.45	20.67		
	4	103.15	21.66		
	5	96.80	20.32		
	6	108.36	22.75	20.91	1.01
	7	97.48	20.47		
	8	106.88	22.44		
	9	95.67	20.09		
	10	96.24	20.21		
G	1	86.36	17.59		
	2	82.70	16.85		
	3	88.96	18.12		
	4	89.19	18.17		
	5	76.25	15.53	17.10	0.82
	6	85.34	17.39		
	7	82.00	16.71		
	8	82.48	16.80		
	9	82.00	16.70		
H	1	108.33	22.74		
	2	121.83	25.58		
	3	121.24	25.45		
	4	121.82	25.58		
	5	124.12	26.06		
	6	125.46	26.34	25.52	1.18
	7	125.41	26.33		
	8	116.54	24.47		
	9	128.35	26.95		
	10	122.56	25.73		
I	1	57.85	11.11		
	2	57.19	10.98		
	3	66.24	12.72		
	4	59.60	11.44		
	5	59.55	11.43	11.57	0.85
	6	53.07	10.19		
	7	66.76	12.82		
	8	63.27	12.15		
	9	58.72	11.27		

Table G-5 Bending strength of fired clay bodies at 1100 °C (continued)

1100 °C					
Formula	No.	Maximum load (N)	MOR (MPa)	Average (MPa)	SD
K	1	98.68	19.51		
	2	91.77	18.15		
	3	100.80	19.93		
	4	103.94	20.55		
	5	94.15	18.62		
	6	106.41	21.04	20.10	1.12
	7	110.48	21.84		
	8	102.46	20.26		
	9	101.97	20.16		
	10	105.99	20.96		
L	1	73.35	14.50		
	2	72.62	14.36		
	3	83.52	16.51		
	4	83.57	16.52		
	5	83.05	16.42		
	6	82.01	16.22	15.88	0.80
	7	80.63	15.94		
	8	80.26	15.87		
	9	81.95	16.20		
	10	82.32	16.28		

List of Publications

Paper I: Prapun Aungatichart, Sirithan Jiemsirilers and Shigetaka Wada. Design and Reliability of Clay Hardness Tester, *Published in J. Ceram. Soc. Japan. 114[10], (2006) 829-832.*

Paper II: Prapun Aungatichart and Shigetaka Wada. Correlation between Drying Sensitivity Index-Bigot and -Ratzenberger of Red Clay from Ratchaburi Province (Thailand), *Submitted for publication to Appl. Clay. Sci.*

Paper III: Prapun Aungatichart and Shigetaka Wada. Correlation between Drying Sensitivity Index-Bigot and Plasticity Index of Terra Cotta Bodies Made of Red Clay from Ratchaburi Province (Thailand), *to be submitted for publication.*

VITA

Mr. Prapun Aungatichart was born in 1961, Ratchaburi, Thailand. He received his Bachelor's degree of Engineering in Industrial Engineering from Chulalongkorn University in 1985 and received his Master's degree of Science in Industrial Technology from Eastern Michigan University, USA, in 1987. He also received his Master's degree of Science in Ceramic Technology from Chulalongkorn University in April 2005. He began to study for his doctorate in Materials Science (Ceramics) at the Department of Materials Science, Faculty of Science, Chulalongkorn University in June 2005 and completed his Ph.D. study in April 2008. Now he is the president of the Siamese Merchandise Co., Ltd. that produces terracotta pottery products for export.